Title
WNT signaling in pancreas development and disease

Permalink
https://escholarship.org/uc/item/1xx1n75j

Author
Heiser, Patrick William

Publication Date
2007-05-29

Peer reviewed|Thesis/dissertation

WNT signaling in pancreas development and disease

by

Patrick W. Heiser

DISSERTATION

Submitted in partial satisfaction of the requirements for the degree of

DOCTOR OF PHILOSOPHY

in

Biomedical Sciences

in the

for Heather…

…without whom,
the journey would not
have been much fun.

Acknowledgments

According to an African proverb that was made famous by Hillary Clinton, it "takes a village to raise a child." In the case of raising this graduate student, it has actually required far more than a village. In fact, it can be argued that a booming metropolis was needed. I would like to recognize a few of the many citizens of this fair city to whom I owe an enormous debt for my growth as a person and as a scientist.

First, I would like to thank my mentor, Matthias Hebrok. His enthusiasm for science, and life in general, is infectious. I could not have asked for a better teacher. Upon joining the lab, I was immediately struck by how deeply Matthias cared about both my academic success and my personal well-being. He provided an environment where I was able to thrive, and I thank him for that. I will sorely miss our discussions. But more importantly, I will miss having the opportunity to use my now vast library of jokes about German people.

The other members of my thesis committee, Michael German and Gail Martin have also given freely of their time during the course of my doctoral work. Given how extraordinarily busy these two individuals are, I have a deep sense of appreciation for the hours they spent discussing my data with me and for the many excellent suggestions they both provided.

I would also like to acknowledge the many individuals that have passed through the hallowed corridors of the Hebrok lab on the 11th floor of Health Sciences West. Pooja Agarwal, Geraldine Bienvenu, Regina Burris, Sara Cervantes, David Cano, Pedro Gutierrez, Hiroshi Kawahira, Janet Lau, Susan Levin, Jennifer Lilla, Travis Merrigan, John Morris, Marina Pasca, Sabina Perez, Sapna Puri, Shigeki Sekine, and Grace Wei

have all played a significant role in enriching my life and digging me out of various crises. I will forever treasure their friendship and miss our time spent together…making fun of Matthias. Many terrifying tales and hilarious antidotes of our times together could be spilled across these pages. However, my respect for these individuals and my desire to protect the innocent prevent me from delving deeper. Plus, despite numerous 12 step programs, hypnotherapy, and even an intervention or two, I still suffer from chronic procrastination. This document is due at the registrar in a few hours…so I must <u>try</u> to keep it brief. I will, however, make two exceptions:

David Cano began a post-doc in the lab during my second year in graduate school. His arrival in the lab was preceded by one of the most engaging seminars I have ever attended. David presented his graduate work on a bacterial virulence regulatory gene called <u>PhoQ</u>. This unfortunate combination of letters, spoken in David's Spanish accent sounded uncannily similar to a very vulgar phrase. Seated at the back of the conference room, I was able to watch as 30 distinguished scientists struggled to suppress the adolescent side of their brains while the many fascinating properties of "PhoQ" were described again and again. David maintained his composure throughout the talk, despite his confusion about why everyone in attendance appeared to be unusually amused.

David is a careful, methodical, and highly ethical scientist. I have learned a great about science (and even more about movies) through my interactions with him. Moreover, he displays an encyclopedic knowledge of the current literature. I must admit that I have become lazy about using PubMed to search through articles. It is more efficient to ask David if he knows whether anyone has published a certain piece of data. Pubmed can't tell you the author, date, AND figure panel where the information you seek

is located…but more often than not, David can. I am also grateful to David for his assistance with the last few experiments described in Chapter 4 of this thesis. He has been a calming presence in the maelstrom of my final weeks in lab. I'd also like to extend my gratitude to David's wife, Anabel and their son Alejandro. Our time in San Francisco has been greatly enhanced by their friendship.

Janet Lau is the second member of the Hebrok lab that I would like to take a moment to personally acknowledge. Her arrival in the lab meant that I had a fellow Biomedical Science graduate student to commiserate with. Given her extensive background in pancreas research from time spent in Mike German's lab, she also brought expertise that made my life much easier. Janet showed me how to find my first e10.5 pancreas and taught me how to isolate pancreatic islets (the trick is sliding the needle into the common bile duct, just like "sliding your foot into a stocking.") In my life, I have only met one other person who is as generous and kind as Janet is. His name is Fred Fermin, and Janet married him. They have become our dear friends. I thank them for their help throughout the years with emergency child care, their encouraging words, and their infectious smiles. Their special brand of "sunshine" brightened even the foggiest of San Francisco days.

When we first moved to San Francisco, we were extraordinarily lucky to have been given a spot in the UCSF student housing complex, high atop fog draped Mt. Sutro. However, scoring an affordable apartment at the peak of the ".com" boom was only a small part of our good fortune. Instead, I am most grateful that by happenstance our apartment lay just down the hall from the amazing Dr. Richard Knight, his wife Laurie, and their children Aidan and Peyton. One of my teachers in elementary school was fond of saying that "your friends are what determine your world." I would like to thank the

after twenty five years, I'm still enrolled. This lesson was not conveyed in words, but through example. I remember Dad patiently explaining the same algebra concept ten different ways, despite my very vocal frustration about the uselessness of it all. I will also never forget Mom staying up with me into the wee hours of the night to help make posters for my first science fair. Because of countless similar examples, the message was clear and taken to heart: school is important. In addition, they indulged my many interests, fed me books as fast as I could read them, and gave me the confidence to follow my dreams wherever they led. I hope that I can live up to their example as I raise my own children.

Speaking of my children, it is only just that I recognize my sons, James and Eric for the chaos, excitement, and joy that they have brought into my life. I want to thank them for the time that they have given up with me so that I could finish work on this dissertation. I would also like to thank them both for making me forget all of my woes about work the minute I arrive home each night. They are easily my most successful experiment in human genetics.

Last, and most importantly, I would like thank my beautiful wife Heather. The work described in this thesis would not have been possible without her support and encouragement. During my time in graduate school, she completed her business degree at San Francisco State University while working a part-time job, raising our kids, and doing far more than her fair share to keep our household running. If I had attempted to juggle a fraction of the tasks Heather manages each day, I would have long ago lost all sanity. Simply put: Heather is the most remarkable woman I have ever known. I am fortunate to have her by my side.

Nearly seven years have passed since I strolled across Parnassus Ave to begin my first day of graduate school. During that time, I have witnessed the birth of my children, experienced many humbling failures at the benchtop (along with an occasional triumph here and there), forged amazing new friendships, said farewell to loved ones, reveled in the beauty and energy of San Francisco, learned volumes about the many different varieties of fog, and acquired a new alma mater. On balance, these have been some of the happiest years of my life.

Gratias vobis ago.

Contributions of Co-Authors to the Presented Work

Chapter 1 contains text published in the review article: "Development and cancer: lessons learned in the pancreas."

Cell Cycle. 2004 Mar;3(3):270-2.

Heiser, PW., Hebrok M.

Chapter 2 contains text and figures that were originally published in the article: "Stabilization of β-catenin impacts pancreas growth." I am first author on this manuscript and conducted the majority of experiments described. Janet Lau contributed data describing the expression pattern of Cre-recombinase in the different mouse strains described and analyzed the insulin and glucagon content of pancreatic lysates. Pedro Herrera and Makoto Taketo both provided mouse strains that were used in this paper.

Development. 2006 May;133(10):2023-32.

Heiser, PW, Lau J, Taketo MM, Herrera PL, Hebrok M

Chapter 3 is a reprint of text and figures that were published in the article "Wnt signaling regulates pancreatic beta cell proliferation." I am a co-first author on this paper along with Ingrid Rulifson and Satyajit Karnik. I designed and conducted experimentation utilizing the β-catenin^{active} mouse to assess the affect of Wnt-signaling hyperactivation on islet formation and adult function. Ingrid Rulifson is responsible for assaying the affect of gain and loss of function in the Wnt signaling pathway on β-cell development. Satyajit Karnik assisted with the completion of the experimentation that was begun by

Ingrid Rulifson, including assaying the affect of Wnt ligand on cultured cells and cadaveric islets. Hainan Chen and Xueying Gu conducted the insulin secretion assays described in the paper. Makoto Taketo provided mice used in this study. Roel Nusse provided soluble Wnt ligand used in the in vitro experiments described. Seung Kim played a role in the supervision and direction of the work described.

Proc Natl Acad Sci U S A. 2007 Apr 10;104(15):6247-52.

Rulifson IC, Karnik SK, Heiser PW, Ten Berge D, Chen H, Gu X, Taketo MM, Nusse R, Hebrok M, Kim SK.

Chapter 4 is currently in preparation. The work is entitled: "Stabilization of Beta-catenin Induces Pancreas Tumor Formation." I am first author on this manuscript and conducted the majority of experiments described. David Cano assisted in the characterization of Wnt target gene expression and the analysis of the pattern of Cre expression in the various mouse strains used. James Kench and Andrew Biankin provided the human solid pseudopapillary tumor tissue and conducted the histological comparison of the murine and human lesions. Makoto Taketo provided mice used in this study.

Heiser, PW, Cano D, Kench, J, Biankin, A, Taketo, MM, Hebrok M.

Matthias Hebrok is listed as a co-author in each of the publications described above. He directed and supervised the research that forms the basis for this dissertation.

Wnt Signaling in Pancreas Development and Disease

By Patrick W. Heiser

ABSTRACT

β-catenin, a cellular adhesion protein, plays a central role in the canonical Wnt-signaling pathway. Wnt ligand binding enables β-catenin to enter the nucleus where it interacts with TCF/Lef transcriptional coactivators to drive expression of Wnt-responsive target genes. However, in the absence of Wnt ligand, free cytoplasmic β-catenin is targeted for degradation via ubiquitylation sites encoded by the third exon of the β-catenin gene.

Previous studies utilizing Wnt-responsive reporter mice have demonstrated that the canonical Wnt pathway is active within the early pancreatic epithelium. Moreover, deletion of β-catenin within the murine pancreas results in a variety of phenotypes, including organ hypoplasia and a reduction in endocrine mass. In this study, we have used the β-cat^{active} mouse to activate pancreatic Wnt signaling in a variety of biological contexts.

The third exon of the β-catenin gene is flanked by lox P sites in these β-cat^{active} mice. Therefore, Cre-recombinase mediated excision of this exon results in a constituitive activation of the β-catenin signaling pathway, since the protein can no longer be targeted for degradation.

Strong activation of β-catenin by e10.5 within the pancreatic epithelium results in near complete pancreas ablation and neonatal lethality in PdxCre^{early} β-cat^{active} mice. This

is preceded by a cell autonomous loss of Pdx1, a decrease in FGF10 signaling, and an increase in Hedgehog (Hh) Hh signaling. Conversely, PdxCre^{late} β-cat^{active} mice exhibit a nearly five fold increase in pancreas mass due to acinar cell proliferation. This dramatic difference in phenotype is the result of a delay in the onset of Cre expression in the PdxCre^{late} mouse.

Increased pancreatic mass is also seen in p48 Cre β-cat^{active} mice. However, unlike the PdxCre^{late} β-cat^{active} mouse strain, these animals develop large pancreatic lesions that resemble human pseudopapillary tumors. These lesions may originate in the pancreatic ducts, a cell type that is targeted efficiently by the p48 Cre, but not the PdxCre^{late} strain.

Finally, we show that activation of β-catenin is sufficient to induce β-cell proliferation and expansion of β-cell mass. This finding may be of therapeutic importance in the development of cell based therapies for Type I diabetes.

Table of Contents   page

List of Tables   page

List of Figures   page

List of Figures   page

Chapter 1

Introduction

Pancreatic development is initiated at embryonic day 8 post coitum (e8) in mice and 28 post coitum in humans when evaginations of the endodermal layer give rise to distinct ventral and dorsal pancreatic buds. A treelike ductal system develops within these enlarging epithelial buds that eventually gives rise to endocrine and exocrine compartments, both of which play vital roles in vertebrates. The exocrine pancreas, which constitutes the vast majority of the organ, generates and secretes digestive enzymes into the gastrointestinal tract via pancreatic ducts. The endocrine pancreas is composed of four distinct cell types, including insulin producing β cells and glucagon producing α-cells, which are intimately involved in regulating glucose homeostasis. These cells are nestled within the exocrine matrix in discrete structures known as islets of Langerhans.

Expression of the gene encoding Pdx1 (also known as IPF1), a homeobox transcription factor, has been shown to be critically important in instructing endodermal differentiation during pancreatic and duodenal organogenesis. *Pdx1* is broadly expressed throughout the pancreatic epithelium at detectable levels beginning at e8.5 (Ahlgren et al., 1996; Jonsson et al., 1994). Pdx-1^{+} precursor cells have been shown to give rise to all three pancreatic lineages: endocrine, exocrine, and duct. Deletion of the *Pdx1* gene in mice blocks normal pancreas development, resulting in organ ablation and neonatal lethality(Jonsson et al., 1994; Offield et al., 1996). Similarly, expression of *p48* (also known as *PTF-1*), a basic helix-loop-helix (bHLH) transcription factor is also critical for normal pancreas development. Deletion of the gene encoding p48 has been shown to result in a complete loss of pancreatic exocrine tissue and neonatal lethality(Krapp et al., 1998). Expression of p48 is detectable at e9.5, which is perhaps one day behind the onset

of Pdx1 expression (Krapp et al., 1998). While p48^{+} precursor cells have also been shown to give rise to islet, exocrine, and ductal cells, its expression domain within the early pancreatic epithelium is much more limited than that of Pdx1 (Kawaguchi et al., 2002). In addition, the FGF, Hedgehog (Hh), Notch, TGF-β/Activin, and other embryonic signaling pathways have also been clearly implicated in pancreatic development (reviewed in (Kim and Hebrok, 2001)).

Further dissection of these embryonic signaling pathways involved in normal formation of the pancreas is critically important for two reasons. First, Type I diabetes is an insidious autoimmune disease that results in the destruction of insulin producing β-cells. Transplantation of human islet cells from cadaveric sources has proven successful in restoring normal blood glucose homeostasis in individuals with severe type I diabetes (Shapiro et al., 2000). However, the amount of transplantable islet material is extremely limited. Therefore, it is hoped that knowledge of the molecular mechanisms involved in the normal differentiation of cells from the early endoderm into the mature β-cells of the pancreas might prove instructive in coaxing isolated stem cells into following a similar path of differentiation, in vitro. In this manner, we might someday generate a safe, effective, and plentiful source of transplantable β-cells for use in reversing Type I diabetes in affected patients.

Second, cancer progression and organ development are similar phenomena. Both involve rapid bursts of proliferation, angiogenesis, tissue remodeling, and cell migration. Therefore, it is not surprising that both processes utilize similar signaling machinery. In fact, many recent studies have suggested that cancer is a disease triggered by the erroneous re-activation of signaling pathways that are typically down-regulated after the

completion of embryonic development. This link between embryonic development and cancer is particularly exciting because it suggests that we might be able to exploit the knowledge gained in studies of developmental biology to obtain novel insights into tumor biology. Our evolving understanding of pancreatic adenocarcinoma is an excellent example of this relationship between development and cancer. Recent studies have indicated important roles for two major developmental signaling pathways in pancreatic cancer: Notch and Hedgehog (Hh).

Several elegant studies have indicated that Notch signaling plays an important role in cell fate determination within the developing pancreas. There are four Notch genes in vertebrates, each of which encodes a single pass transmembrane receptor. Binding of ligands, including Delta-like 1 (Dll1) and Serrate 1 and 2, leads to intracellular cleavage of the Notch receptor. The resultant activation of the intracellular domain of the notch receptor allows for interaction with the DNA-binding protein RBP-Jκ This interaction induces expression of the basic helix-loop-helix (bHLH) *HES* genes, which act to down-regulate expression of downstream target genes.

In mice, Notch 1 and Hes1 expression can be detected in the pancreatic epithelium at e9.5, an early stage of pancreas development. By e11.5, Notch2 also becomes expressed at high levels within the branching epithelium, the structure thought to be the source of endocrine and exocrine stem cells(Lammert et al., 2000). Mice deficient for either the DNA binding protein RBP-Jκ or the notch ligand, Dll1, exhibit an accelerated differentiation of endocrine cells and a depletion of epithelial progenitors(Apelqvist et al., 1999). Moreover, mice lacking the HES1 gene, an important target of Notch signaling, also display precocious endocrine differentiation concomitant with exocrine

hypoplasia(Jensen et al., 2000). Conversely, ectopic activation of Notch in murine

pancreas explants results in an expansion of an undifferentiated population of precursor

cells(Miyamoto et al., 2003). Taken together, it appears that the primary role of Notch

signaling during normal pancreas organogenesis is to regulate the differentiation of

epithelial precursors. It is also possible that Notch signaling may continue to play a role

in the adult by maintaining the undifferentiated state of the putative pool of pancreatic

stem cells that is thought to mediate islet cell turn over and organ repair.

Because Notch signaling appears to allow cells to remain in a non-differentiated,

proliferative state, it is not surprising that a new study has implicated aberrant re-

activation of this developmental pathway in some pancreatic adenocarcinomas.

Miyamoto, et al propose a model in which EGF receptor activity represents an initiating

event in pancreatic adenocarcinoma leading to Notch activation, and subsequent

expansion of a population of undifferentiated cells. They performed Affymetrix chip

analysis of cRNA prepared from human pancreatic adenocarcinoma and detected

upregulated levels of Notch signaling components in the majority of samples evaluated.

Further, not only is Notch present in some tumors, but studies using pancreas explants

demonstrate a causative role for the pathway in tumor formation. Transfection of adult

pancreas explants with an adenoviral encoded, activated form of the intracellular domain

of Notch resulted in a metaplastic conversion of the exocrine cell epithelium to

epithelium more characteristic of ductal cells and expansion of a precursor cell

population(Miyamoto et al., 2003).

Similarly, recent studies suggest a previously unappreciated role for developmentally

critical Hh signaling pathway in pancreatic cancer. There are three mammalian Hh

genes: Shh, Ihh, and Dhh which encode for secreted proteins. The current model of Hh

signaling proposes that binding of a Hh ligand to its cognate transmembrane receptor,

Patched, results in activation of another transmembrane protein, Smoothened, which in

turn leads to stabilization of Gli transcription factors that act on Hh responsive genes.

During normal pancreas organogenesis, Shh is excluded from the developing

pancreas, but remains expressed in the surrounding stomach and duodenal epithelium. In

this manner, Shh expression establishes a sharp molecular boundary, which allows for the

proper patterning of the duodenal and pancreatic epithelium. Chemical inhibition of the

Hh signaling pathway in embryonic chicks results in expansion of the pancreas and an

increase in endocrine cell number(Kim and Melton, 1998). Conversely, ectopic

expression of *Shh* within the developing pancreas of transgenic mice has been show to

result in a dramatic loss of both exocrine and endocrine tissue(Apelqvist et al., 1997).

Therefore, it is possible that Hh signaling, like Notch, plays a role in regulating the

differentiation of pancreatic precursor cells. Surprisingly, Ihh, Dhh, and Ptc are each

expressed within the developing pancreas, indicating that some level of Hh pathway

activity does occur during pancreas organogenesis(Hebrok et al., 2000). Furthermore, the

Hh receptor, Ptch, remains expressed in the islets and ductal epithelium of the adult

pancreas, indicating that these pancreatic compartments also retain the ability to respond

to Hh ligands(Hebrok et al., 2000).

These developmental insights, namely the putative role for Hh signaling in cell fate

commitment and the expression of a Hh receptor within the ductal epithelium where

pancreatic adenocarcinoma is thought to arise, paved the way for two recent efforts

focused on identifying a link between pancreatic cancer and Hh signaling. Thayer, et al

and Berman, et al found significant Hh pathway upregulation in a number of primary human pancreatic tumors(Berman et al., 2003; Thayer et al., 2003). Moreover, transgenic overexpression of Shh within the pancreas results in lesions reminiscent of PanIN, a precursor of pancreatic adenocarcinoma(Thayer et al., 2003). Interestingly, this Shh over expression also resulted in the accumulation of genetic alterations that resemble published descriptions of the progression of human pancreatic adenocarcinoma. Her2/neu is upregulated in the epithelium and k-ras mutations were also detected in a subset of the lesions(Thayer et al., 2003). Taken together, it appears likely that Hh signaling is an early mediator of pancreatic cancer tumorigenesis. Moreover, it also appears that a subset of cell lines established from both primary and metastatic adenocarcinomas continue to require active hedgehog signaling. Chemical inhibition of the pathway with cyclopamine induces apoptosis and blocks proliferation in these cell lines both *in vitro* and *in vivo*(Thayer et al., 2003). Hh signaling may therefore also play a role in later tumor progression and survival.

Surprisingly, most signaling events during development are initiated by a small axis of signaling pathways, including the Notch and Hh pathways discussed above, as well as Wnt, Fibroblast growth factor (FGF), and Transforming growth factor-β (TGF-β). The outcome depends on the strength, duration, and order in which these pathways are activated or repressed. The roles that these pathways might play in pancreatic cancer certainly deserve scrutiny. However, just as embryonic development involves a milieu of intracellular signaling, so too does tumor establishment and progression. Therefore, examination of one pathway at a time cannot provide a clear picture of the complex biology of the tumor. Examination of how multiple developmental pathways are

hijacked during tumorigenesis may become an important avenue of investigation. Fortunately, embryological studies have already provided a road map as to how one might proceed.

For example, Hh signaling plays a part in activation of the EGF receptor pathway during Drosophila head formation(Amin et al., 1999). Because the work by Miyamoto, *et al* suggests that EGF receptor activation leading to Notch signaling is an important early step in pancreas tumor formation(Miyamoto et al., 2003), it would also be interesting to examine the relationship between these two pathways in the context of the tumor. Close analysis should allow us to build a functional hierarchy of how developmental pathways interact during tumor initiation and progression and lead to improved models of adenocarcinoma.

Another example of how developmental pathway interactions might instruct pancreatic cancer is provided by work suggesting that molecular studies in *Drosophila* indicate that Wingless (the Wnt homolog) is required for expression of Hh(Lee et al., 1992; Tabata and Kornberg, 1994). Additionally, Wnt7a appears to provide the signal for Shh expression in the anteroposterior patterning of the limb in mice(Yang and Niswander, 1995). Therefore, it is possible that cross talk between these pathways may play a role in pancreatic adenocarcinoma. Interestingly, misexpression of Wnt signaling components has been observed in some human pancreatic cancers.(Koesters and von Knebel Doeberitz, 2003; Kolligs et al., 2002; Tanaka et al., 2001).

Therefore, the studies described in this dissertation have explored how manipulation of the canonical Wnt signaling pathway, through constituitive activation of β-catenin, impacts pancreas development, adult organ function, and tumorigenic potential.

When this study was initiated, little was known about the role that Wnt signaling might play in pancreas development. However, in recent years a more complete story has emerged. In the absence of Wnt ligand, levels of the cellular adhesion protein, β-catenin, within the cytoplasm are suppressed by active phosphorylation of β-catenin by a large complex that includes GSK and Axin. This phosphorylation targets β-catenin for degradation by cellular ubiquitylation machinery, which in term keeps the concentration of free β-catenin within the cytoplasm low. However, upon Wnt ligand binding, the GSK/Axin complex is inhibited. As a result, unphosphorylated β-catenin accumulates in the cytoplasm and begins to enter the nucleus where it interacts with Tcf/Lef transcriptional coactivators, thereby driving the expression of Wnt-responsive target genes (reviewed in (Bienz, 2005; Nelson and Nusse, 2004; Pandur and Kuhl, 2001). Based upon studies of Wnt reporter mice, in which Tcf/Lef responsive elements are coupled to the β-galactosidase reporter, and by careful analysis of the pattern of unphosphorylated β-catenin in the developing murine pancreas, the canonical Wnt pathway is active during early pancreatic formation and is down regulated once development of the organ is complete (Dessimoz et al., 2005; Murtaugh et al., 2005). Loss of Wnt pathway activity within the developing pancreas results in pancreas exocrine hypoplasia(Dessimoz et al., 2005; Murtaugh et al., 2005; Papadopoulou and Edlund, 2005), pancreatitis, and loss of endocrine mass (Dessimoz et al., 2005; Rulifson et al., 2007) depending on the context and method used to perturb the pathway.

The studies presented in this dissertation utilize a mouse generated by Makoto Taketo's group in which the third exon of β-catenin was flanked by lox-P sites(Harada et al., 1999). This exon contains the phosphorylation sites that target the protein for

degradation. Therefore, Cre-recombinase mediated excision of this exon results in a constitutively active form of the protein. By crossing these mice to a variety of pancreatic-Cre transgenic mice, we were able to assess the effect of erroneous activation of the Wnt signaling pathway on distinct time points during early pancreatic development, as well as its impact on the three adult pancreatic cell types: exocrine, endocrine, and duct.

Taken together with the other published studies, it is clear that Wnt signaling is essential for normal pancreas development. Moreover, the level of Wnt signaling pathway activity is dynamic during organogenesis. Its timing, dosage, and cellular domain must be tightly regulated to prevent developmental defect or tumorigenesis.

References

Ahlgren, U., Jonsson, J. and Edlund, H. (1996). The morphogenesis of the pancreatic mesenchyme is uncoupled from that of the pancreatic epithelium in IPF1/PDX1-deficient mice. *Development* 122, 1409-16.

Amin, A., Li, Y. and Finkelstein, R. (1999). Hedgehog activates the EGF receptor pathway during Drosophila head development. *Development* 126, 2623-30.

Apelqvist, A., Ahlgren, U. and Edlund, H. (1997). Sonic hedgehog directs specialised mesoderm differentiation in the intestine and pancreas [published erratum appears in Curr Biol 1997 Dec 1;7(12):R809]. *Curr Biol* 7, 801-4.

Apelqvist, A., Li, H., Sommer, L., Beatus, P., Anderson, D. J., Honjo, T., Hrabe de Angelis, M., Lendahl, U. and Edlund, H. (1999). Notch signalling controls pancreatic cell differentiation. *Nature* 400, 877-81.

Berman, D. M., Karhadkar, S. S., Maitra, A., Montes De Oca, R., Gerstenblith, M. R., Briggs, K., Parker, A. R., Shimada, Y., Eshleman, J. R., Watkins, D. N. et al. (2003). Widespread requirement for Hedgehog ligand stimulation in growth of digestive tract tumours. *Nature* 425, 846-51.

Bienz, M. (2005). beta-Catenin: a pivot between cell adhesion and Wnt signalling. *Curr Biol* 15, R64-7.

Dessimoz, J., Bonnard, C., Huelsken, J. and Grapin-Botton, A. (2005). Pancreas-specific deletion of beta-catenin reveals Wnt-dependent and Wnt-independent functions during development. *Curr Biol* 15, 1677-83.

Harada, N., Tamai, Y., Ishikawa, T., Sauer, B., Takaku, K., Oshima, M. and Taketo, M. M. (1999). Intestinal polyposis in mice with a dominant stable mutation of the beta-catenin gene. *Embo J* 18, 5931-42.

Hebrok, M., Kim, S. K., St.Jacques, B., McMahon, A. P. and Melton, D. A. (2000). Regulation of pancreas development by Hedgehog signaling. *Development* 127, 4905-4913.

Jensen, J., Pedersen, E. E., Galante, P., Hald, J., Heller, R. S., Ishibashi, M., Kageyama, R., Guillemot, F., Serup, P. and Madsen, O. D. (2000). Control of endodermal endocrine development by Hes-1. *Nat Genet* 24, 36-44.

Jonsson, J., Carlsson, L., Edlund, T. and Edlund, H. (1994). Insulin-promoter-factor 1 is required for pancreas development in mice. *Nature* 371, 606-9.

Kawaguchi, Y., Cooper, B., Gannon, M., Ray, M., MacDonald, R. J. and Wright, C. V. (2002). The role of the transcriptional regulator Ptf1a in converting intestinal to pancreatic progenitors. *Nat Genet* 32, 128-34.

Kim, S. K. and Hebrok, M. (2001). Intercellular signals regulating pancreas development and function. *Genes Dev* 15, 111-27.

Kim, S. K. and Melton, D. A. (1998). Pancreas development is promoted by cyclopamine, a hedgehog signaling inhibitor. *Proc Natl Acad Sci U S A* 95, 13036-41. Koesters, R. and von Knebel Doeberitz, M. (2003). The Wnt signaling pathway in solid childhood tumors. *Cancer Lett* 198, 123-38.

Kolligs, F. T., Bommer, G. and Goke, B. (2002). Wnt/beta-catenin/tcf signaling: a critical pathway in gastrointestinal tumorigenesis. *Digestion* 66, 131-44.

Krapp, A., Knofler, M., Ledermann, B., Burki, K., Berney, C., Zoerkler, N., Hagenbuchle, O. and Wellauer, P. K. (1998). The bHLH protein PTF1-p48 is essential for the formation of the exocrine and the correct spatial organization of the endocrine pancreas. *Genes Dev* 12, 3752-63.

Lammert, E., Brown, J. and Melton, D. A. (2000). Notch gene expression during pancreatic organogenesis. *Mech Dev* 94, 199-203.

Lee, J. J., von Kessler, D. P., Parks, S. and Beachy, P. A. (1992). Secretion and localized transcription suggest a role in positional signaling for products of the segmentation gene hedgehog. *Cell* 71, 33-50.

Miyamoto, Y., Maitra, A., Ghosh, B., Zechner, U., Argani, P., Iacobuzio-Donahue, C. A., Sriuranpong, V., Iso, T., Meszoely, I. M., Wolfe, M. S. et al. (2003). Notch mediates TGF alpha-induced changes in epithelial differentiation during pancreatic tumorigenesis. *Cancer Cell* 3, 565-76.

Murtaugh, L. C., Law, A. C., Dor, Y. and Melton, D. A. (2005). Beta-catenin is essential for pancreatic acinar but not islet development. *Development* 132, 4663-74. Nelson, W. J. and Nusse, R. (2004). Convergence of Wnt, beta-catenin, and cadherin pathways. *Science* 303, 1483-7.

Offield, M. F., Jetton, T. L., Labosky, P. A., Ray, M., Stein, R. W., Magnuson, M. A., Hogan, B. L. and Wright, C. V. (1996). PDX-1 is required for pancreatic outgrowth and differentiation of the rostral duodenum. *Development* 122, 983-95. Pandur, P. and Kuhl, M. (2001). An arrow for wingless to take-off. *Bioessays* 23, 207-10.

Papadopoulou, S. and Edlund, H. (2005). Attenuated Wnt signaling perturbs pancreatic growth but not pancreatic function. *Diabetes* 54, 2844-51.

Rulifson, I. C., Karnik, S. K., Heiser, P. W., ten Berge, D., Chen, H., Gu, X., Taketo, M. M., Nusse, R., Hebrok, M. and Kim, S. K. (2007). Wnt signaling regulates pancreatic beta cell proliferation. *Proc Natl Acad Sci U S A* 104, 6247-52.

Shapiro, A. M., Lakey, J. R., Ryan, E. A., Korbutt, G. S., Toth, E., Warnock, G. L., Kneteman, N. M. and Rajotte, R. V. (2000). Islet transplantation in seven patients with type 1 diabetes mellitus using a glucocorticoid-free immunosuppressive regimen [see comments]. *N Engl J Med* 343, 230-8.

Tabata, T. and Kornberg, T. B. (1994). Hedgehog is a signaling protein with a key role in patterning Drosophila imaginal discs. *Cell* 76, 89-102.

Tanaka, Y., Kato, K., Notohara, K., Hojo, H., Ijiri, R., Miyake, T., Nagahara, N., Sasaki, F., Kitagawa, N., Nakatani, Y. et al. (2001). Frequent beta-catenin mutation and cytoplasmic/nuclear accumulation in pancreatic solid-pseudopapillary neoplasm. *Cancer Res* 61, 8401-4.

Thayer, S. P., di Magliano, M. P., Heiser, P. W., Nielsen, C. M., Roberts, D. J., Lauwers, G. Y., Qi, Y. P., Gysin, S., Fernandez-del Castillo, C., Yajnik, V. et al. (2003). Hedgehog is an early and late mediator of pancreatic cancer tumorigenesis. *Nature* 425, 851-6.

Yang, Y. and Niswander, L. (1995). Interaction between the signaling molecules WNT7a and SHH during vertebrate limb development: dorsal signals regulate anteroposterior patterning. *Cell* 80, 939-47.

Chapter 2

Stabilization of β-catenin impacts pancreas growth

Abstract

A recent study has shown that deletion of β-catenin within the pancreatic epithelium results in a loss of pancreas mass (Murtaugh et al., 2005). Here, we show that ectopic stabilization of β-catenin within mouse pancreatic epithelium can have divergent effects on both organ formation and growth. Robust stabilization of β-catenin during early organogenesis drives changes in Hedgehog and FGF10 signaling, and induces a loss of Pdx1 expression in early pancreatic progenitor cells. Together, these perturbations in early pancreatic specification culminate in a severe reduction of pancreas mass and postnatal lethality. In contrast, inducing the stabilized form of β-catenin at a later time point in pancreas development causes enhanced proliferation that results in a dramatic increase in pancreas organ size. Taken together, these data suggest a previously unappreciated temporal/spatial role for β-catenin signaling in the regulation of pancreas organ growth.

Introduction

β-catenin function is essential for the canonical arm of the Wnt signaling pathway

(reviewed in (Willert and Nusse, 1998)). In the absence of Wnt ligand, cytoplasmic

pools of β-catenin are highly unstable because of multiple phosphorylations in the

protein's amino terminus that target the protein for degradation. However, when the Wnt

co-receptors LRP and Frizzled are engaged by ligand, the assembly of proteins

responsible for this phosphorylation state is inhibited. Consequently, the

unphosphorylated form of β-catenin accumulates in the cytoplasm, making it available

for entry into the nucleus. Once in the nucleus, β-catenin interacts with TCF/LEF

transcriptional co-activators to promote the expression of target genes (Nelson and Nusse,

2004).

Previous work has established that the third exon of the β-catenin gene encodes the

amino terminal phosphorylation sites necessary for degradation of the protein via

ubiquitylation (Harada et al., 1999). Therefore, the removal of this exon in transgenic

mice using Cre/loxP technology results in a constitutively stabilized, or activated, form of

the β-catenin protein (Harada et al., 1999). These *β-cat^{active}* mice have proven to be

useful in probing the effects of β-catenin signaling on embryonic stem cell

differentiation, progenitor cell expansion in the nervous system, epithelial-mesenchymal

transition in the epiblast, and other phenomena (Kemler et al., 2004; Kielman et al., 2002;

Zechner et al., 2003).

Previous studies have demonstrated that Wnt signaling components are dynamically

expressed within the developing pancreas, suggesting that canonical Wnt signaling may

be involved in pancreas organogenesis (Dessimoz et al., 2005; Heller et al., 2003;

Murtaugh et al., 2005; Papadopoulou and Edlund, 2005) . Two independent labs recently reported divergent phenotypes resulting from the conditional deletion of β-catenin within the pancreatic epithelium. In one instance, loss of β-catenin resulted in a reduction in pancreatic endocrine cell numbers, whereas the gross morphology of the organ appeared normal at birth (Dessimoz et al., 2005). However, a separate report demonstrated that loss of β-catenin did not affect pancreatic endocrine cell mass, despite the almost complete loss of the exocrine compartment. Here, we have used the $\beta\text{-}cat^{active}$ mouse to help clarify how β-catenin stability affects pancreas development and organ maturation.

In mice, pancreas morphogenesis begins by 9.5 days post coitum (e9.5) when epithelial tissue fated to become the dorsal pancreas buds from the gut endoderm within a mesenchymal cap (Kim and Hebrok, 2001). Emergence of two distinct ventral pancreatic buds occurs slightly later, by e10.25-10.5. Signaling by the mesenchyme is essential for epithelial proliferation and branching. The epithelium eventually gives rise to two distinct tissue compartments: exocrine cells that produce digestive enzymes and endocrine cells that produce hormones essential for regulating blood glucose levels.

Pdx1, a homeobox transcription factor, is one of the earliest genes to be expressed within the developing pancreatic epithelium and is essential for normal organ formation. Moreover, Pdx1 expressing pancreatic progenitor cells have been shown to give rise to all three types of pancreatic tissue: endocrine, exocrine, and duct (Gu et al., 2002). A number of independent lines of transgenic mice that express Cre recombinase under the control of *Pdx1* promoter fragments have been generated (Gannon et al., 2000; Gu et al., 2002; Herrera, 2000). Our characterization of two of these strains indicated that the temporal and spatial activity of Cre-recombinase differed. This allowed us to determine

how β-catenin stabilization in these distinct temporal/spatial domains of the pancreatic epithelium affected organogenesis and adult organ function. Interestingly, we observed significantly different pancreatic phenotypes depending on the *Cre* strain employed. Using the *PdxCre* mice generated in the lab of D. Melton which displayed early and robust Cre recombinase activity (*PdxCre^{early}*), we observed a nearly complete loss of pancreatic tissue (Gu et al., 2002). Conversely, slightly delayed and more mosaic Cre recombinase expression in Pdx mice generated in one of our laboratories (*PdxCre^{late}*) drives outgrowth of pancreatic tissue, resulting in a grossly enlarged pancreas (Gannon et al., 2000; Herrera, 2000). Thus, in one instance, β-catenin stabilization drives tissue loss, and in the other culminates in an increase in organ size relative to body mass. Therefore, ectopic stabilization of β-catenin blocks/deregulates the normal mechanisms that control embryonic pancreas formation and postnatal organ growth.

Materials and methods

Mice

Noon of the day when vaginal plugs are detected is treated as e0.5 day post coitum. Mice carrying the floxed exon 3 allele of β-catenin (*β-cat^{active}*)(Harada et al., 1999) were crossed with strains expressing Cre-recombinase under the control of the *Pdx1* promoter (*PdxCre^{early}, PdxCre^{late}, PdxCre^{ER}*)(Gannon et al., 2000; Gu et al., 2002; Herrera, 2000), all of which were maintained in a mixed background. In all experiments presented in this work, the floxed exon 3 allele of β-catenin was maintained as a heterozygote to insure that the level of β-catenin signaling pathway activation was consistent. Thus, the *β-cat^{active}* nomenclature used refers to mice containing one wild type and one floxed exon 3

allele of β-catenin. To verify the expression pattern of Cre-recombinase, a *LacZ* reporter line was used (*R26R*) (Soriano, 1999).

Tamoxifen preparation and injection

10 mg/ml of tamoxifen (Sigma, T5648) was dissolved in corn oil (Sigma, C8267) following 30 minutes of incubation at 37°C and vigorous vortexing. 100 µl (1mg/mouse) was then injected intraperitonealy into the pregnant female at the indicated developmental timepoint using a 21 gauge needle.

Tissue preparation, immunohistochemistry, and microscopy

Embryonic tissues were fixed and paraffin wax imbedded as previously described (Kawahira et al., 2003). Hematoxylin/eosin staining, immunohistochemical and immunofluorescence analysis were performed as previously described (Kim et al., 1997). The primary antibodies used in this study are listed in Table 1. For immunohistochemistry, a biotinylated anti-goat (Vector; BA-9500) was used at a dilution of 1:200. Staining for diaminobenzidine (DAB) was performed with the ABC Elite immuoperoxidase system (Vector). The Alexa series of secondary antibodies from Molecular Probes was used for the immunofluorescent analysis performed in this study. However, in order to amplify the signal from the β-galactosidase antibody, we found it necessary to use the TSA Plus Fluorescence system (Perkin Elmer, fluorescein NEL741). Slides were mounted with Vectashield mounting media containing the nuclear stain, DAPI (Vector). Bright field images were aquired using a Zeiss Axio Imager D1 scope; fluorescent images were captured using a Leica DMIRE2 SP2 confocal microscope.

Staining for β-galactosidase activity and whole mount in situ hybridization

Fixed *PdxCre^early* or *PdxCre^late R26R* were incubated overnight at room temperature in

phosphate-buffered saline (PBS) supplemented with 5-bromo-4-chloro-3-indolyl-D-

galactopyranoside (Xgal: 1mg/ml), 0.02% TritonX-100, 5mM potassium ferricyanide,

and 5 mM potassium ferrocyanide. For whole-mount in situ hybridization, the

gastrointestinal cavity of intact embryos was opened to allow greater penetration of fix

and probe, and then incubated in 4% paraformaldehyde overnight at 4°C. Whole mount

in-situ hybridization with digoxigenin-labeled *FGF10* riboprobe was performed as

previously described (Chuang et al., 2003). Stained tissues were photographed with a

Leica MZ FL3 dissecting microscope equipped with a Leica IM500 system.

Morphometric quantification of proliferation, cell density, islet area, and Pdx1+ cell

number.

Pancreatic paraffin wax imbedded sections (6μm) were cut from both the dorsal and

ventral pancreas. Following immunofluorescent staining for the proliferation marker

phospho-histone H3, positive cells were then scored from 20 non-overlapping fields at

20x magnification from the dorsal and ventral sections of 4 control and 4 *PdxCre^late β-*

cat^active mice. The average number of cells per field was then normalized against the

control. In order to determine endocrine and exocrine cell density, hematoxylin/eosin

stained tissues were used to count cell nuclei from 20 non-overlapping fields at 40x

magnification isolated from 4 control and 4 *PdxCre^late β-cat^active* mice. The average

number of nuclei present in the field was then normalized against control.

For e12.5 and P0 pancreata, the whole pancreas was sectioned and aliquoted as described

previously (Kawahira et al., 2003), in order to obtain representative results. In order to

quantitate the number of Pdx1+ cells present in 3 control, 5 *PdxCre^early β-cat^active*, and 5

PdxCre^late β-cat^active intact e12.5 embryos were paraffin imbedded, cut into 6µm sagittal sections, and aliquotted onto slides. Following immunofluorescence staining for E-cadherin (to mark the epithelium) and Pdx1, the number of Pdx1+ cells within the pancreatic epithelium was counted on 1 section every 96µm until the entire pancreatic bud was evaluated. Islet area was assayed at P0 as described previously (Hebrok et al., 2000; Perez et al., 2005). Error bars represent standard error of the mean, and confidence intervals were determined using a student's t-test analysis.

Pancreas homogenization and hormone radioimmune assays

Approximately 100 mg portions of the dorsal and ventral pancreas from equivalent regions of 6 control and 6 *PdxCre^late β-cat^active* adult pancreata were homogenized in acidified ethanol (750 ul of 85% EtOH, 1.5% HCl) using a TissueTek homogenizer. The relative insulin and glucagon concentrations present in the samples were assayed using Sensitive Rat Insulin RIA and Glucagon RIA kits (Linco, SRI13K, GL32K, respectively). The pancreas hormone concentration values obtained were then standardized based upon the total protein concentration of the sample, determined using a BCA Protein Assay Kit (Pierce, 23225). This hormone concentration was then multiplied by the pancreas weight to generate the total pancreatic hormone content. The total hormone content was normalized against control. Error bars represent standard error of the mean, and confidence intervals were determined using a student t-test analysis.

Glucose tolerance testing

6 control and 6 *PdxCre^late β-cat^active* mice were fasted for 14 hours before intraperitoneal injection of a 20% glucose (w/v) solution at a dose of 2g per kg body mass. Venous blood glucose readings were then taken at the indicated intervals using a Bayer Ascensia

Elite XL to analyze samples collected from tail nicks. Error bars represent standard error

of the mean.

Results

Temporal and spatial difference in Cre recombinase activity in the PdxCre^{early} and

PdxCre^{late} transgenic lines

The *PdxCre^{late}* transgenic mouse was generated using a 4.5 kb promoter fragment,

while the *PdxCre^{early}* transgenic mouse utilized a 5.5 kb fragment of the promoter.

Because the size of the promoter fragment used, the site of integration, and other factors

that can affect the expression of the transgene, we directly compared the activity of the

Cre-recombinase by crossing both *PdxCre* strains to the reporter line *R26R*, which carries

a β-galactosidase gene whose transcription is activated after Cre-mediated recombination

(Soriano, 1999). In this manner, we were able to map the timing and expression of

pancreatic Cre-recombinase. By e10.5, robust lacZ staining was detected in the

pancreatic epithelium of *PdxCre^{early} R26R* animals at the gross and histological levels

(Fig. 1C,F). Moreover, expression was detectable in the majority of Pdx1+ cells

observed (Fig. 1F). Interestingly, no lacZ staining was observed in the *PdxCre^{late} R26R*

animals at this time point (Fig. 1B,E). By e11.5, a few *lacZ* positive cells were found in

the pancreatic epithelium of *PdxCre^{late} R26R*, a delay of approximately 24 hours (data not

shown) from the onset of expression in the *PdxCre^{early}*. Furthermore, comparison of

lacZ/Pdx1 co-stained pancreatic tissue revealed that even at e12.5, the *Cre* expression in

the *PdxCre^{late}* strain was more mosaic than in the *PdxCre^{early}* (Fig 1 H,I).

Analysis of lacZ stained pancreas sections in adult *PdxCre^{late} R26R* mice suggested

that *Cre* expression within the terminally differentiated exocrine and endocrine cells

remained mosaic in the *PdxCre^late* strain (Fig 1K). Interestingly, β-galactosidase can

rarely be detected within the adult pancreatic ducts in *PdxCre^late R26R* mice (Fig. 1N). In

comparison, the majority of endocrine, exocrine, and ductal cells in *PdxCre^early R26R*

mice exhibit β-galactosidase activity (Fig. 1L, O). The higher number of lacZ+ cells in

the adult *PdxCre^early R26R* mice strongly indicates that the onset of *Cre* expression was

not only earlier in timing, but also targeted a greater portion of the pancreatic epithelium.

Control tissue was stained for each of the time points assayed to demonstrate the

specificity of the lacZ staining reaction/immunofluorescence (Fig. 1 A,D,G,J, M).

Therefore, the *PdxCre^late* and *PdxCre^early* mice were used in this study as tools to probe

the effect of increased β-catenin signaling on distinct temporal/spatial populations of

cells in the early embryonic pancreas.

Stabilization of β-catenin results in disruption of pancreas formation in PdxCre^early β-cat^active

    In order to assess the consequences of increased β-catenin signaling on pancreas

organogenesis, we crossed *β-cat^active* animals with the *PdxCre^late* or *PdxCre^early* mice.

Because previous studies have shown that the loss of the third exon of one allele of β-

catenin is sufficient to drive strong increases in Wnt pathway activity, all experiments

were done using mice that were heterozygous for the floxed β-catenin allele (Harada et

al., 1999; Kemler et al., 2004; Zechner et al., 2003). Analysis of gross morphology and

pancreas architecture at e18.5 in the *PdxCre^late β-cat^active* mice did not reveal any overt

changes compared to control littermates (Fig. 2A,B,D,E). In contrast, the *PdxCre^early β-cat^active* animals displayed near total pancreas agenesis, and the pancreatic remnant

contained multiple large cysts (Fig. 2C,F). Histological examination revealed a

significant reduction in the epithelial derived exocrine and endocrine tissues.

Consequently, *PdxCre^{early} β-cat^{active}* survive on average only 7 days after birth, whereas

PdxCre^{late} β-cat^{active} are viable and reproductively active.

Nuclear β-catenin localization was abundant and easily detected by confocal

microscopy in both *PdxCre^{late} β-cat^{active}* and *PdxCre^{early} β-cat^{active}* pancreata at e18.5 (Fig.

2H, I). In control samples, β-catenin was only detected at the plasma membrane (Fig.

2G). Therefore, as has been shown in other tissues (Jamora et al., 2003; Miller and

Moon, 1997; Tolwinski and Wieschaus, 2004), stabilization of β-catenin leads to

increased nuclear β-catenin signaling, and presumably, hyperactivation of the canonical

Wnt signaling pathway in the pancreas.

In addition to its role in the canonical Wnt signaling pathway, the β-catenin protein

also participates in cell adhesion at adherens junctions. β-catenin links the cytoplasmic

domain of transmembrane cadherins to the actin cytoskeleton via its association with the

adaptor protein, α-catenin (reviewed in (Bienz, 2005)). Therefore, β-catenin stabilization

may also impact cell adhesion. However, despite clear evidence of nuclear localization

of β-catenin in *PdxCre^{late} β-cat^{active}* and *PdxCre^{early} β-cat^{active}* mice, E-cadherin remained

properly localized to the plasma membrane (Fig. 2K,L inset), suggesting that adhesion

has not been disrupted. Similarly, other studies utilizing the *β-cat^{active}* mouse strain have

not found adhesion defects in cells expressing the stabilized form of β-catenin (Gounari

et al., 2002; Harada et al., 1999). Using E-cadherin as a marker of epithelial cells,

immunohistochemical analysis revealed the extensive loss of epithelial tissue mass in the

PdxCre^early β-cat^active organ remnant. As expected, the developing cysts are E-cadherin-positive, indicating that the cysts were epithelial in origin (Fig. 2L).

By e18.5, endocrine islets in mice start to form a stereotypical structure consisting of a core of insulin producing β-cells surrounded by glucagon producing α-cells (Fig 2M). Although the *PdxCre^late β-cat^active* mutants displayed islet architecture (Fig 2N) and islet area (supplemental Fig. 1) equivalent to control, *PdxCre^early β-cat^active* mutants had few insulin$^+$ or glucagon$^+$ cells (Fig. 1O). In addition, these endocrine cells were found scattered throughout the remaining organ, rather than organized into discrete islet structures (Fig.2O).

Thus, early and widespread upregulation of the β-catenin signaling pathway in the *PdxCre^early β-cat^active* mouse strain prevents normal formation of the exocrine and endocrine compartments of the pancreas. However, the delayed and more mosaic upregulation of the β-catenin signaling pathway in the *PdxCre^late β-cat^active* mutants appears to be well tolerated and does not result in any obvious developmental defect.

Stabilization of β-catenin at e11.5, but not e13.5, results in pancreas hypoplasia.

Other differences between the *PdxCre^early* and *PdxCre^late* mouse strains, beyond the delay in onset of Cre expression, might account for the difference in phenotypes observed. For example, differences in the specific subset of cells targeted by each Cre after e12.5 when both lines are active might be responsible for driving the pancreas hypoplasia observed. Therefore, we directly assessed the temporal dependence of the phenotype seen in the *PdxCre^early β-cat^active* mice by crossing the *β-cat^active* mouse to an inducible *PdxCre* strain (*PdxCre^ER*)(Gu et al., 2002) containing the same 5.5 kb promoter

fragment as the *PdxCre^early* mouse. In this system, the *Cre* recombinase is expressed as a fusion protein with the estrogen receptor, and remains inactive in the cytoplasm in the absence of tamoxifen ligand. However, once bound to tamoxifen, the Cre recombinase enters the nucleus where it can catalyze recombination (Gu et al., 2002).

Injection of tamoxifen at e11.5 induced accumulation of β-catenin in the nucleus of a large number of pancreatic epithelial cells in *PdxCre^ER β-cat^active* mice (Fig. 3J), resulting in a severe reduction of pancreas mass in all mutants observed (n=9, Fig. 3B). Nuclear localization of β-catenin was not observed in control pancreata (Fig 3I). Moreover, cystic structures similar to those seen in *PdxCre^early β-cat^active* are apparent in histological sections of the pancreas (Fig 3F, indicated by arrows).

Conversely, injection of tamoxifen at e12.5 induced more variable phenotypes. The majority of *PdxCre^ER β-cat^active* mutants exhibited an intermediate phenotype with some reduction of the ventral and dorsal pancreas obvious in examination of the gross morphology of the organ (Fig. 3C). The pancreas histology of these intermediate *PdxCre^ER β-cat^active* mutants (Fig. 3G) appeared equivalent to control (Fig 3E). However, a smaller number of *PdxCre^ER β-cat^active* mutants from litters injected with tamoxifen at e12.5 displayed either pancreas hypoplasia similar to those in the e11.5 injection group (Fig 3B) or appeared unaffected (exact proportion of mutants in each category summarized in Fig 3M). Despite the variability in phenotype, significant numbers of cells with nuclear β-catenin localization were present in the pancreatic epithelium in all mutants analyzed (Fig 3K).

Injection of tamoxifen at e13.5 did not disrupt pancreas formation in any of the 11 *PdxCre^{ER} β-cat^{active}* mutants observed (Fig. 3D, H), despite clear nuclear localization of β-catenin in a large number of pancreatic cells (Fig 3L).

Taken together, these results indicate that β-catenin stabilization can adversely affect pancreas development only during the earlier stages of organ formation. After e12.5, the increased levels of canonical Wnt signaling that the stabilized β-catenin presumably induces are well tolerated. Therefore, it appears likely that the pancreas phenotype seen in the *PdxCre^{early} β-cat^{active}* is dependent on the earlier onset of *Cre* recombinase expression seen when compared to the *PdxCre^{late}* mouse strain.

Pancreatic defects in PdxCre^{early} β-cat^{active} correlate with changes in FGF and Hedgehog signaling, and loss of Pdx1+ progenitor cells.

In order to analyze the defects in *PdxCre^{early} β-cat^{active}* mice in more detail, we performed a series of histological and molecular assays aimed at characterizing the early progression of the phenotype and identifying the underlying molecular mechanisms involved. By e12.5, stabilization of β-catenin within the pancreas of *PdxCre^{early} β-cat^{active}* mice caused the pancreatic epithelium in some mutants to exhibit abnormal dilation not seen in control tissues, representing the earliest histological change that we could detect (Sup. Fig.1A,B). By e15.5, the rudimentary clusters of exocrine cells seen in control embryos (Sup. Fig. 1C) are almost completely absent in the *PdxCre^{early} β-cat^{active}* (Sup. Fig. 1D). In addition, abnormally enlarged pancreatic ducts are frequently observed at this time point in *PdxCre^{early} β-cat^{active}* pancreatic tissues (Sup. Fig. 1D, yellow arrows) and it is likely that these dilated ducts later form the cystic structures seen at e18.5 (Fig 2F 'c').

Numerous studies have shown the importance of mesenchymal-epithelial interactions for proper pancreas formation. One of the mesenchymal molecules known to regulate expansion of pancreatic epithelial cells is fibroblast growth factor 10 (FGF10) (Bhushan et al., 2001). *FGF10* expression is normally detectable within the mesenchyme surrounding the pancreatic bud beginning at e9.5 and peaking at e10.5. By e12.5, *FGF10* expression can no longer be detected. Loss of FGF10 in mice has been shown to disrupt pancreas formation (Bhushan et al., 2001), a phenotype similar to the one we observed in *PdxCre^{early} β-cat^{active}* mice. Therefore, we asked whether stabilization of β-catenin resulted in changes in mesenchymal *FGF10* expression. Whole mount in situ hybridization at e10.5 revealed that *FGF10* expression is decreased in the pancreatic mesenchyme of *PdxCre^{early} β-cat^{active}* animals (Fig. 4C) when compared to control (Fig. 4A). *FGF10* expression appeared normal in the *PdxCre^{late} β-cat^{active}* mutants (Fig. 4B). This observation supports our *R26R* expression analysis, which indicated that *Cre* recombinase is not active in *PdxCre^{late} β-cat^{active}* mice at this time point. Thus, β-catenin stabilization in pancreas epithelium before e11.5 disrupts an important component of the signaling exchange that occurs between the mesenchyme and epithelium, which at least partially explains the dramatic defects in organogenesis observed.

Wnt signaling has also been implicated in maintaining the expression of *Hedgehog* (Hh) ligands in both *Drosophila* wing discs and mouse limb buds (Parr and McMahon, 1995; Pinson et al., 2000; Tabata and Kornberg, 1994). In addition, ectopic Wnt signaling in the epidermis has been shown to upregulate the expression of Hh signaling pathway components (Silva-Vargas et al., 2005). Hedgehog signaling, in turn, stabilizes Wnt expression in *Drosophila* wing (Tabata and Kornberg, 1994), indicating that both

pathways can cross-regulate each other's activity. A previous study has shown that overexpression of the *Hh* ligand, Shh, under the *Pdx1* promotor results in pancreas agenesis (Apelqvist et al., 1997), a phenotype similar to that observed in the *PdxCre^early β-cat^active mice*. To determine whether stabilization of β-catenin activates Hh signaling in pancreatic tissue, we analyzed e12.5 pancreas tissue from WT, *PdxCre^late β-cat^active*, and *PdxCre^early β-cat^active* mice. By immunohistochemistry, protein levels of the Hh receptor, Ptc, a direct transcriptional target of Hh signaling (Goodrich et al., 1996), are significantly upregulated within the pancreatic epithelium of the *PdxCre^early β-cat^active* mice (Fig. 4F) when compared to control or *PdxCre^late β-cat^active* (Fig. 4D,E). Protein levels of Hh ligand, are also increased in the *PdxCre^early β-cat^active* (Fig. 4I) when compared to control or *PdxCre^late β-cat^active* mice (Fig. 4G,H). Therefore, stabilization of β-catenin in the *PdxCre^early β-cat^active* mice results in upregulation of the Hh signaling pathway within the early pancreatic epithelium which may also partially account for the dramatic changes observed during organ formation/morphogenesis.

A previous study indicated that FGF10-/- mice exhibit a marked loss of the Pdx1+ progenitor cells by e12.5-e13.5 (Bhushan et al., 2001). Additionally, loss of Pdx1 in mice has been shown to cause pancreas agenesis (Offield et al., 1996)(Jonsson et al., 1994). Therefore, we examined Pdx1 expression within the e12.5 pancreatic epithelium. Interestingly, *PdxCre^early β-cat^active* mice exhibited a 76% reduction in Pdx1+ progenitor cells (Fig. 4L, quantitated in Sup. Fig. 2A). In contrast, *PdxCre^late β-cat^active* mice had numbers of Pdx1+ progenitor cells (Fig. 4K) that were equivalent to control (Fig. 4J). Moreover, only cells that did not display elevated levels of β-catenin retained Pdx1 expression (Sup. Fig. 2D). Presumably, these cells escaped recombination. Cells with a

29

clear increase in cytoplasmic/nuclear β-catenin were rarely detected in the *PdxCre^late^ β-cat^active^* mutant pancreatic epithelium at e12.5 (Sup. Fig 2C).

Thus, the pancreatic hypoplasia and cyst formation in the *PdxCre^early^ β-cat^active^* appears to be mediated by loss of FGF10 signaling concomitant with an increase in Hh signaling. Together these perturbations in early pancreas specification may contribute to the loss of Pdx1$^+$ pancreatic progenitors.

Stabilization of β-catenin causes increased pancreas organ size in PdxCre^late^ β-cat^active^ mice

While the morphology and histological architecture of pancreata dissected from *PdxCre^late^ β-cat^active^* appeared normal at the end of development (Fig. 2B,E), pancreas mass was not. Despite the fact that mutant pups were equivalent in body mass to control littermates, pancreas mass at day 0 was increased by 53% (Fig. 5B). Pancreas mass continued to increase independent of animal mass after birth, resulting in a grossly enlarged organ (Fig. 5A) that was 2.7 fold greater than control pancreata at 98 days post natal (Fig. 5B). In transgenic mice older than one year, the pancreas had grown 4.6 fold larger than those found in control littermates (Fig. 5B). Strong nuclear β-catenin staining could be detected within the adult exocrine pancreas, suggesting that increased Wnt activity in the *PdxCre^late^ β-cat^active^* mice was responsible for the increase in organ size after birth. In support of this hypothesis, we found a 2.5 fold increase in the number of proliferating adult exocrine cells in the *PdxCre^late^ β-cat^active^* (Fig. 5I), as revealed by staining for the mitotic marker phosphohistone H3 (Figure 5E,F).

Interestingly, *PdxCre^ER^ β-cat^active^* mice injected with tamoxifen 4 weeks after birth, also showed a 2 fold increase in pancreas mass by one year of age (n=8, data not shown).

Injection of *PdxCre^ER R26R* mice with tamoxifen results in clear Cre recombinase activity (as indicated by lacZ staining) in a significant portion of the exocrine pancreas at this stage (data not shown). Thus, as has been shown for other tissues (Bierie et al., 2003; Huelsken and Birchmeier, 2001), β-catenin signaling, as a part of the canonical Wnt signaling pathway, can act as a proliferative signal in mature exocrine pancreas. In addition, the density of cells within the exocrine pancreas, as determined by counting the number of nuclei present in a defined histological field, is also increased 1.8 fold in *PdxCre^late β-cat^active* when compared to controls (Fig. 5G,H,J). In contrast, the density of endocrine cells within the mutant is normal. While these data suggest that exocrine cell size is reduced in *PdxCre^late β-cat^active* mutants, the mechanism driving this phenomenon is unclear. Stabilization of β-catenin within the adult exocrine tissue may directly deregulate cell size. However, it is also possible that the rapidly proliferating exocrine cells do not need to reach their normal size before dividing again. Electron microscopy will be used in future studies to further characterize how this mutation affects pancreatic cellular ultrastructure.

Despite the dramatic increase in exocrine cell proliferation and the resultant increase in organ mass, pancreatic tumors have not been observed in any of the *PdxCre^late β-cat^active* mutants, up to one year of age. The mice are viable, fertile, and appear healthy.

β-cell differentiation and islet function appear normal in the PdxCre^late β-cat^active mouse at 3 months

As shown in figure 1K, islets within the *PdxCre^late* strain were mosaic for Cre activity. Therefore, only a subset of β-cells were targeted for stabilization of β-catenin in

the *PdxCre^late β-cat^active* mouse. Immunofluorescence staining indicated that *PdxCre^late β-cat^active* adult mutants exhibit stereotypical murine islet architecture, consisting of a central core of insulin producing β-cells and a periphery of glucagon producing α-cells (Fig. 6 A,B). Despite the increase in overall organ size at birth, the total cross sectional area of endocrine islets remained equivalent to control (Sup. Fig. 3A), suggesting that the ratio of endocrine content to animal mass was not perturbed. In addition, analysis of relative hormone content in pancreas homogenates at three months of age indicated that the total amount of insulin and glucagon present in the *PdxCre^late β-cat^active* is equivalent to control (Sup. Fig. 3B). Thus, in contrast to the vast expansion of the exocrine compartment of the pancreas, the size of the endocrine compartment remains largely unaffected (shown in schematic, Sup. Fig 3C).

As expected from the *R26R* expression data, the majority of β-cells in adult *PdxCre^late β-cat^active* mutants exhibited plasma membrane localization of β-catenin that appeared equivalent to control (Fig. 6C,D, higher magnification F,G) and only a subset of β-cells was marked by upregulated ß-catenin levels. However, unlike the exocrine compartment (Fig. 5D), confocal analysis revealed that Cre-mediated excision in β-cells did not result in a significant increase in nuclear β-catenin, but instead in an increase in cytoplasmic β-catenin levels (Fig 6E, higher magnification, 6H).

Within the β-cells marked by high levels of cytoplasmic β-catenin protein, expression of insulin (Fig. 6H), adult β-cell transcription factors Pdx1 (Fig. 6J) and Nkx6.1 (data not shown), and the glucose transporter, Glut 2 (data not shown) appear equivalent to control (Fig. 6 F,I). These results demonstrate that the β-cells are fully differentiated despite the dramatic increase in cytoplasmic β-catenin. Additionally, fasting glucose tolerance is

normal in *PdxCre^{late} β-cat^{active}* animals (Fig. 6J), suggesting that either β-cell function is normal in these mutants or that the number of β-cells expressing the stabilized form of β-catenin is insufficient to affect this physiological assay. Future experiments utilizing cultured islets are necessary to determine what biochemical mechanisms might protect pancreatic endocrine cells from accumulating nuclear β-catenin.

Abnormal cells with nuclear localization of β-catenin are present in a subset of islets in 1 year old PdxCre^{late} β-cat^{active} mice.

Surprisingly, analysis of β-catenin expression patterns in 1 year old mice revealed the presence of cells within a small subset of islets that exhibited nuclear localization of β-catenin (Fig. 7B, higher magnification 7D), a phenomenon not seen in younger mice. Despite their location in the center of islets where β-cells typically are found, these cells do not express insulin (Fig. 7B, higher magnification 7D). These cells also lack expression of β-cell markers including, Pdx1 (Fig. 7 F, higher magnification 7H), Nkx6.1, and glut2 or markers of other endocrine cell populations (glucagon, somatostatin, PP; data not shown). Moreover, these cells do not express the pancreatic duct marker Mucin-1 or the exocrine marker, amylase (data not shown). Fasting glucose tolerance is also normal in *PdxCre^{late} β-cat^{active}* mutants at 1 year of age (data not shown) indicating that the presence of these abnormal cells in a subset of islets has not impacted this physiological assay. Given the lack of expression of pancreatic endocrine, exocrine, or ductal markers, these cells potentially represent a subpopulation of cells that have dedifferentiated as a result of the accumulation of nuclear β-catenin. Further genetic experimentation is necessary to identify the lineage of this cell population.

Discussion

Our studies underscore the fact that important differences in Cre-activity can be found in mouse Cre-lines that utilize similar promoter elements of the same gene. Differences in the site of integration, the length of the promoter fragment used, and gene silencing can all exert significant influence over the transgenic expression of Cre recombinase. Here, we show how differences in the temporal/spatial stabilization of the β-catenin protein within the developing pancreas result in dramatically different phenotypes: organ ablation versus organ enlargement. The $PdxCre^{early}$ mouse strain efficiently targets all three pancreatic lineages: endocrine, exocrine, and duct, and is expressed early in pancreatic development. In contrast, the $PdxCre^{late}$ strain targets a subset of the endocrine and exocrine cell lineages, but does not appear to be expressed in a significant number of duct cells.

Wnt, Hh, and FGF interaction during pancreas development

Our observation that stabilization of β-catenin in $PdxCre^{early}$ $βcat^{active}$ mice results in upregulation of Hh signaling components concomitant with a loss of FGF10 suggests that the activities of these three major embryonic signaling pathways are intimately linked during this stage of pancreas development. While we cannot exclude that Wnt signaling in the epithelium directly affects the expression of mensenchymal FGF10, it is interesting to note that upregulation of Hh signaling resulting from loss of the Hh inhibitor, *Hhip*, is known to cause a delay in *FGF10* expression in the pancreatic mesenchyme (Kawahira et al., 2003). Therefore, our results are consistent with the idea that at least some of the defects observed in epithelium and mesenchyme are mediated via increased Hh activity. A reduction of pancreas size has also been observed in transgenic mice expressing Wnt-1

under the control of the Pdx1 promoter (Heller et al., 2003). The phenotype observed in the *PdxCre^{early} βcat^{active}* mice results from upregulation of β-catenin signaling in a cell autonomous fashion within the epithelium. However, transgenic expression of the soluble Wnt-1 ligand presumably exerts a direct effect on both the pancreatic mesenchyme and epithelium. Therefore, it would be interesting to compare whether Hh and FGF signaling are also affected in the Pdx-Wnt1 mice. Moreover, future studies are necessary to determine the precise signaling hierarchy between the Wnt, Hh, and FGF signaling pathways during normal pancreas specification and organogenesis.

β-catenin activation influences pancreas morphogenesis and growth

Despite the 4.6 fold increase in mass, the pancreas of *PdxCre^{late} β-cat^{active}* mutant remains functional. *PdxCre^{late} β-cat^{active}* animals have a body mass equivalent to control littermates, suggesting that the duodenum still receives the pancreatic enzymes necessary for digestion, and their glucose tolerance profile is normal, indicating that the endocrine function of the pancreas is intact. Moreover, the shape of the organ is also conserved; it is simply bigger. Despite the increased proliferation, the *PdxCre^{late} β-cat^{active}* mice do not appear to develop tumors.

Interestingly, while the pancreas becomes grossly enlarged, the exocrine cells that comprise it appear smaller. Modulation of Wnt signaling has been implicated in increasing the size of skeletal muscle cells after mechanical overload (Armstrong and Esser, 2005). In addition, Wnt activation via overexpression of a canonical Wnt ligand has been shown to result in chondrocyte hypertrophy (Day et al., 2005). While the opposite was observed in the *PdxCre^{late} β-cat^{active}* mice, it is possible that deregulation of

Wnt signaling in pancreatic exocrine cells may directly impact cell size. However, exocrine cells contain a large number of granules whose digestive enzyme content is emptied into the gut in response to feeding. Because the *PdxCre^late β-cat^active* mutant pancreas contains significantly more exocrine cells than are present in the wild type, a feedback mechanism might exist that causes a reduction in the number of granules in each cell, thereby reducing cell size. Ultrastructural analysis is required to precisely determine how β-catenin stabilization affects pancreatic exocrine cell morphology.

β-catenin activation and adult β-cell function

The absence of a proliferative response or enlargement of the β-cell compartment, within *PdxCre^late β-cat^active* mutants may reflect differences in the way in which exocrine and endocrine cells respond to activation of β-catenin. Alternatively, β-cells may have a mechanism that allows for the active exclusion of stabilized β-catenin from the nucleus, which then prevents downstream activation of the canonical Wnt signaling pathway. A recent study involving β-catenin stabilization in preimplantation embryos also observed similar cytoplasmic localization of β-catenin (Kemler et al., 2004). The authors propose several mechanisms that might prevent localization of the stabilized form of β-catenin in the blastomere nuclei. Among these are the presence of an alternative ubiquitylation pathway which can degrade even the stabilized form of β-catenin or the activity of endogenous inhibitors that might prevent β-catenin from exerting its nuclear activity. Endocrine cells may lack, or have low levels of nuclear transport proteins required for normal translocation and retention of β-catenin in the nucleus. Experiments utilizing cultured islets and known inhibitors of nuclear transport might prove instructive in

uncovering the mechanism underlying the pancreatic endocrine cell's resistance to nuclear accumulation of β-catenin.

One of the truly puzzling findings of our study is that a low number of cells with clear nuclear localization of β-catenin can be found only in the islets of one year old *PdxCre^late β-cat^active* animals. Thus, it is possible that pancreatic endocrine cells possess some kind of innate mechanism to prevent nuclear localization of β-catenin that was gradually circumvented over time. Alternatively, it might be a matter of the cellular dosage of the stabilized β-catenin; it might take time for enough of the protein to accumulate to affect cell function.

Moreover, the location of these cells within the center of the islet raises the intriguing possibility that these are β-cells that have undergone de-differentiation, after accumulating sufficient levels of nuclear β-catenin. Genetic cell lineage tracing experiments would need to be performed to confirm this hypothesis. The absence of Pdx1 expression in these cells is consistent with the fact that the pancreatic epithelial cells with nuclear β-catenin accumulation in the *PdxCre^early β-cat^active* also display a loss of Pdx1 expression at e12.5. However, the absence of normal pancreatic cell lineage markers makes it impossible to conclude what these cells were/are without further experimentation.

Given the fact that less than 30% of β-cells are marked by cytoplasmic β-catenin staining, it is also possible that potential β-cell defects in β-catenin activated cells are masked by the remaining wild type cells. Therefore, while the results presented here are intriguing, future studies using a transgenic strain that expresses Cre in a higher

percentage of β-cells are necessary to clarify these findings regarding the effect of β-catenin stabilization on β-cell differentiation, expansion, and function.

Conclusion

Our findings further illustrate the dual nature of β-catenin signaling. In one context, β-catenin activation prevents proper differentiation and expansion of early pancreatic progenitor cells, while in another context β-catenin activation acts as a proliferative cue that induces gross enlargement of the exocrine pancreas. Conversely, deletion of β-catenin has been shown to cause loss of exocrine cell mass (Murtaugh et al., 2005) and in a different context, reduction of endocrine islet mass (Dessimoz et al., 2005). Taken together, these results highlight the complex roles β-catenin signaling plays in pancreas organ growth and the determination of the exocrine:endocrine cell ratio.

References

Apelqvist, A., Ahlgren, U. and Edlund, H. (1997). Sonic hedgehog directs specialised mesoderm differentiation in the intestine and pancreas [published erratum appears in Curr Biol 1997 Dec 1;7(12):R809]. *Curr Biol* **7**, 801-4.

Armstrong, D. D. and Esser, K. A. (2005). Wnt/{beta}-catenin signaling activates growth-control genes during overload induced skeletal muscle hypertrophy. *Am J Physiol Cell Physiol*.

Bhushan, A., Itoh, N., Kato, S., Thiery, J. P., Czernichow, P., Bellusci, S. and Scharfmann, R. (2001). Fgf10 is essential for maintaining the proliferative capacity of epithelial progenitor cells during early pancreatic organogenesis. *Development* **128**, 5109-17.

Bienz, M. (2005). beta-Catenin: a pivot between cell adhesion and Wnt signalling. *Curr Biol* **15**, R64-7.

Bierie, B., Nozawa, M., Renou, J. P., Shillingford, J. M., Morgan, F., Oka, T., Taketo, M. M., Cardiff, R. D., Miyoshi, K., Wagner, K. U. et al. (2003). Activation of beta-catenin in prostate epithelium induces hyperplasias and squamous transdifferentiation. *Oncogene* **22**, 3875-87.

Chuang, P. T., Kawcak, T. and McMahon, A. P. (2003). Feedback control of mammalian Hedgehog signaling by the Hedgehog-binding protein, Hip1, modulates Fgf signaling during branching morphogenesis of the lung. *Genes Dev* **17**, 342-7.

Day, T. F., Guo, X., Garrett-Beal, L. and Yang, Y. (2005). Wnt/beta-catenin signaling in mesenchymal progenitors controls osteoblast and chondrocyte differentiation during vertebrate skeletogenesis. *Dev Cell* **8**, 739-50.

Dessimoz, J., Bonnard, C., Huelsken, J. and Grapin-Botton, A. (2005). Pancreas-specific deletion of beta-catenin reveals Wnt-dependent and Wnt-independent functions during development. *Curr Biol* **15**, 1677-83.

Gannon, M., Herrera, P. L. and Wright, C. V. (2000). Mosaic Cre-mediated recombination in pancreas using the pdx-1 enhancer/promoter. *Genesis* **26**, 143-4.

Goodrich, L. V., Johnson, R. L., Milenkovic, L., McMahon, J. A. and Scott, M. P. (1996). Conservation of the hedgehog/patched signaling pathway from flies to mice: induction of a mouse patched gene by Hedgehog. *Genes Dev* **10**, 301-12.

Gounari, F., Signoretti, S., Bronson, R., Klein, L., Sellers, W. R., Kum, J., Siermann, A., Taketo, M. M., von Boehmer, H. and Khazaie, K. (2002). Stabilization of beta-catenin induces lesions reminiscent of prostatic intraepithelial neoplasia, but terminal squamous transdifferentiation of other secretory epithelia. *Oncogene* **21**, 4099-107.

Gu, G., Dubauskaite, J. and Melton, D. A. (2002). Direct evidence for the pancreatic lineage: NGN3+ cells are islet progenitors and are distinct from duct progenitors. *Development* **129**, 2447-57.

Harada, N., Tamai, Y., Ishikawa, T., Sauer, B., Takaku, K., Oshima, M. and Taketo, M. M. (1999). Intestinal polyposis in mice with a dominant stable mutation of the beta-catenin gene. *Embo J* **18**, 5931-42.

Hebrok, M., Kim, S. K., St.Jacques, B., McMahon, A. P. and Melton, D. A. (2000). Regulation of pancreas development by Hedgehog signaling. *Development* **127**, 4905-4913.

Heller, R. S., Klein, T., Ling, Z., Heimberg, H., Katoh, M., Madsen, O. D. and Serup, P. (2003). Expression of Wnt, Frizzled, sFRP, and DKK genes in adult human pancreas. *Gene Expr* **11**, 141-7.

Herrera, P. L. (2000). Adult insulin- and glucagon-producing cells differentiate from two independent cell lineages. *Development* **127**, 2317-22.

Huelsken, J. and Birchmeier, W. (2001). New aspects of Wnt signaling pathways in higher vertebrates. *Curr Opin Genet Dev* **11**, 547-53.

Jamora, C., DasGupta, R., Kocieniewski, P. and Fuchs, E. (2003). Links between signal transduction, transcription and adhesion in epithelial bud development. *Nature* **422**, 317-22.

Jonsson, J., Carlsson, L., Edlund, T. and Edlund, H. (1994). Insulin-promoter-factor 1 is required for pancreas development in mice. *Nature* **371**, 606-9.

Kawahira, H., Ma, N. H., Tzanakakis, E. S., McMahon, A. P., Chuang, P. T. and Hebrok, M. (2003). Combined activities of hedgehog signaling inhibitors regulate pancreas development. *Development* **130**, 4871-9.

Kemler, R., Hierholzer, A., Kanzler, B., Kuppig, S., Hansen, K., Taketo, M. M., de Vries, W. N., Knowles, B. B. and Solter, D. (2004). Stabilization of beta-catenin in the mouse zygote leads to premature epithelial-mesenchymal transition in the epiblast. *Development* **131**, 5817-24.

Kielman, M. F., Rindapaa, M., Gaspar, C., van Poppel, N., Breukel, C., van Leeuwen, S., Taketo, M. M., Roberts, S., Smits, R. and Fodde, R. (2002). Apc modulates embryonic stem-cell differentiation by controlling the dosage of beta-catenin signaling. *Nat Genet* **32**, 594-605.

Kim, S. K. and Hebrok, M. (2001). Intercellular signals regulating pancreas development and function. *Genes Dev* **15**, 111-27.

Kim, S. K., Hebrok, M. and Melton, D. A. (1997). Pancreas development in the chick embryo. *Cold Spring Harb Symp Quant Biol* **62**, 377-83.

Miller, J. R. and Moon, R. T. (1997). Analysis of the signaling activities of localization mutants of beta-catenin during axis specification in Xenopus. *J Cell Biol* **139**, 229-43.

Murtaugh, L. C., Law, A. C., Dor, Y. and Melton, D. A. (2005). Beta-catenin is essential for pancreatic acinar but not islet development. *Development* **132**, 4663-74.
Nelson, W. J. and Nusse, R. (2004). Convergence of Wnt, beta-catenin, and cadherin pathways. *Science* **303**, 1483-7.

Offield, M. F., Jetton, T. L., Labosky, P. A., Ray, M., Stein, R. W., Magnuson, M. A., Hogan, B. L. and Wright, C. V. (1996). PDX-1 is required for pancreatic outgrowth and differentiation of the rostral duodenum. *Development* **122**, 983-95.

Papadopoulou, S. and Edlund, H. (2005). Attenuated Wnt signaling perturbs pancreatic growth but not pancreatic function. *Diabetes* **54**, 2844-51.

Parr, B. A. and McMahon, A. P. (1995). Dorsalizing signal Wnt-7a required for normal polarity of D-V and A-P axes of mouse limb. *Nature* **374**, 350-3.

Perez, S. E., Cano, D. A., Dao-Pick, T., Rougier, J. P., Werb, Z. and Hebrok, M. (2005). Matrix metalloproteinases 2 and 9 are dispensable for pancreatic islet formation and function in vivo. *Diabetes* **54**, 694-701.

Pinson, K. I., Brennan, J., Monkley, S., Avery, B. J. and Skarnes, W. C. (2000). An LDL-receptor-related protein mediates Wnt signalling in mice. *Nature* **407**, 535-8.

Silva-Vargas, V., Lo Celso, C., Giangreco, A., Ofstad, T., Prowse, D. M., Braun, K. M. and Watt, F. M. (2005). Beta-catenin and Hedgehog signal strength can specify number and location of hair follicles in adult epidermis without recruitment of bulge stem cells. *Dev Cell* **9**, 121-31.

Soriano, P. (1999). Generalized lacZ expression with the ROSA26 Cre reporter strain. *Nat Genet* **21**, 70-1.

Tabata, T. and Kornberg, T. B. (1994). Hedgehog is a signaling protein with a key role in patterning Drosophila imaginal discs. *Cell* **76**, 89-102.

Tolwinski, N. S. and Wieschaus, E. (2004). A nuclear function for armadillo/beta-catenin. *PLoS Biol* **2**, E95.

Willert, K. and Nusse, R. (1998). Beta-catenin: a key mediator of Wnt signaling. *Curr Opin Genet Dev* **8**, 95-102.

Zechner, D., Fujita, Y., Hulsken, J., Muller, T., Walther, I., Taketo, M. M., Crenshaw, E. B., 3rd, Birchmeier, W. and Birchmeier, C. (2003). beta-Catenin signals

regulate cell growth and the balance between progenitor cell expansion and differentiation in the nervous system. *Dev Biol* **258**, 406-18.

FIGURE LEGENDS

Figure 1. Temporal and spatial differences in Cre recombinase activity in the *PdxCre^early^*

and *PdxCre^late^* transgenic lines.   LacZ staining marks cells that have undergone Cre-

mediated recombination in *PdxCre^late^* and *PdxCre^early^ R26R* mice. Gross and histological

examination of the *PdxCre^early^ R26R* e10.5 embryo reveals strong β-galacotosidase

staining at e10.5 within the pancreas (C, pancreas indicated by black arrow, F). No

staining is detectable within the *PdxCre^late^ R26R* embryo at e10.5 (B, E). Histological

examination of pancreas sections from the *PdxCre^early^ R26R* animal immunostained for

Pdx1 (brown) and enzymatically stained for β-galactosidase activity (blue) (F) indicates

that the majority of Pdx1$^+$ cells, are also positive for lacZ at e10.5. At e12.5, β-

galactosidase staining (blue) is detectable within a subset of the Pdx1$^+$ (brown) cells in

the *PdxCre^late^ R26R* animals (H). Equivalent pancreas sections of a *PdxCre^early^ R26R*

animal (I) at e12.5 show robust β-galactosidase staining (blue) in the majority of Pdx1$^+$

cells (brown). In the adult *PdxCre^late^ R26R* animal, only a subset of islet cells exhibit β-

galactosidase staining (blue, islets are marked by black circles). Cre expression within

the exocrine tissue is also mosaic in these animals. A greater percentage of islet cells

(circled in black) and exocrine cells exhibit strong β-galactosidase staining (blue) in the

adult *PdxCre^early^ R26R* pancreas (L). The majority of pancreatic ducts (stained with an

antibody against mucin-1, red) are also β-galactosidase $^+$ (green) in the *PdxCre^early^ R26R*

pancreas (O, non-specific staining sometimes encountered within the center of ducts

indicated with an asterisk). β-galactosidase$^+$ cells are seldom encountered within the

PdxCre^late^ R26R pancreas (N).   No β-galactosidase staining is observed in control animals at any of the time points characterized (A,D,G,J, islet circled in black, and M). A magnification of 40x was used for all histological images shown (D-L); a magnification of 63x was used for confocal images shown (M-O). Scale bars represent 25 μm.

Figure 2. Stabilization of β-catenin results in disruption of pancreas formation in *PdxCre^early^ β-cat^active^* mice. Examination of pancreas gross morphology reveals that the majority of the dorsal pancreas (dp) and ventral pancreas (vp) has been lost in *PdxCre^early^ β-cat^active^* mice (C) at e18.5. In contrast, *PdxCre^late^ β-cat^active^* pancreas morphology (B) appears equivalent to control (A) at e18.5. The stomach (s), spleen (sp) and duodenum (d) are labeled accordingly. Hematoxylin and eosin staining was performed on paraffin sections at 20x magnification from e18.5 tissue from either control (D), *PdxCre^late^ β-cat^active^* (E), or *PdxCre^early^ β-cat^active^* (F) animals. While *PdxCre^late^ β-cat^active^* pancreas structure (E) is normal, the *PdxCre^early^ β-cat^active^* pancreatic remnant (F) contains very little exocrine tissue and exhibits multiple pronounced cyst structures (c). The majority of the remaining tissue appears mesenchymal in *PdxCre^early^ β-cat^active^* mutants. Staining of pancreas sections for β-catenin (green) and the nuclear co-stain DAPI (blue) reveals that β-catenin is localized exclusively to the membrane in control animals (G). Significant levels of nuclear β-catenin can be detected in both the *PdxCre^late^ β-cat^active^* and *PdxCre^early^ β-cat^active^* mutants (H,I). Insets show increased magnification of equivalent fields in each image; scale bars represent 50 μm. Cysts are labeled (c) in the *PdxCre^early^ β-cat^active^* mutant. Staining for the epithelial marker E-cadherin (green)

indicates the dramatic loss of epithelial tissue in the *PdxCre^early β-cat^active* mutant (L) when compared to both the *PdxCre^late β-cat^active* (K) and control (J). The *PdxCre^early β-cat^active* cysts (c) are lined by E-cadherin positive cells. Insets show increased magnification of equivalent fields in each image to show proper plasma membrane localization of E-cadherin in both *PdxCre^late β-cat^active* and *PdxCre^early β-cat^active* mutants; scale bars represent 100μm. Staining for glucagon (green) and insulin (red), along with the nuclear marker DAPI (blue), reveal islet structure in the *PdxCre^late β-cat^active* mutant (N) that is equivalent to control (M). In contrast, insulin$^+$ and glucagon $^+$ cells are scattered within the walls of the cysts (c) and surrounding mesenchyme in the *PdxCre^early β-cat^active* mutant tissue (O). Scale bars represent 100 μm.

Figure 3. Stabilization of β-catenin at e11.5, but not e13.5, results in pancreas hypoplasia. Tamoxifen injection at e11.5 effectively targets a large number of cells within the *PdxCre^ER β-cat^active* pancreatic epithelium, indicated by the accumulation of nuclear β-catenin (J) that is not seen in control tissue (I). Consequently, these mutants display a dramatic loss of pancreas mass in (B), and gross histological abnormalities, including the formation of large cysts (F, cysts indicated with black arrows). Tamoxifen injection at e12.5 also results in detectable β-catenin within the nuclei of a significant number of cells within the *PdxCre^ER β-cat^active* pancreatic epithelium (K). In the majority of cases, the dorsal and ventral pancreas appear moderately reduced (C), while pancreas histology (G) appears similar to control. Despite the presence of a large number of cells that exhibit nuclear β-catenin within the pancreatic epithelium of *PdxCre^ER β-cat^active* animals exposed to tamoxifen at e13.5 (L), pancreas gross morphology (D) and histology

(H) appear normal. The table provided (M) summarizes the number of mutants seen at each tamoxifen injection time point, and the severity of the pancreas phenotype observed. All images were from embryos at e18.5; images E-H were aquired at 20x magnification; scale bars represent 50μm. The stomach (s), spleen (sp), duodenum (d), dorsal pancreas (dp), and ventral pancreas (vp) are labeled accordingly.

Figure 4. Pancreatic defects in $PdxCre^{early}$ β-cat^{active} correlate with changes in FGF and Hedgehog signaling, and loss of Pdx1^{+} progenitor cells. Whole mount in situ hybridization reveals that *FGF10* expression is down regulated in the dorsal pancreatic (dp) and ventral pancreatic (vp) mesenchyme of the $PdxCre^{early}$ β-cat^{active} mutants (C) at e10.5. *FGF10* expression within the pancreatic mesenchyme of $PdxCre^{late}$ β-cat^{active} mutants (B) is equivalent to control (A). Stomach, s. Immunohistochemical staining of pancreatic sections at e12.5 for the Hedgehog (Hh) receptor, Ptc, reveals increased levels of Ptc within the pancreatic epithelium (circled in blue) of the $PdxCre^{early}$ β-cat^{active} mutants (F) when compared with control pancreas (D). Ptc staining in $PdxCre^{late}$ β-cat^{active} (E) pancreatic sections is equivalent to control (D). Similarly, the $PdxCre^{early}$ β-cat^{active} pancreatic epithelium (circled in blue, I) also exhibits increased levels of Hh ligand when compared to control (G) and $PdxCre^{late}$ β-cat^{active} pancreas tissue (H). Images H-M were acquired at a magnification of 40x. Staining of e12.5 pancreata with E-cadherin (green) to mark the pancreatic epithelium and Pdx1 (red) reveals a dramatic loss of Pdx1+ progenitor cells in the $PdxCre^{early}$ β-cat^{active} mutants (L). In contrast, the $PdxCre^{late}$ β-cat^{active} (K) display Pdx1^{+} cell numbers that are equivalent to control (J). Scale bars represent 50 μm (J-L).

Figure 5. Stabilization of β-catenin causes increased pancreas organ size in *PdxCre*^{late} *β-cat*^{active} mice. Gross morphology of pancreata from a control and *PdxCre*^{late} *β-cat*^{active} mutant (A). Quantitative measurements revealed a 4.6 fold increase in pancreas mass in *PdxCre*^{late} *β-cat*^{active} mutants between birth and 1 year (Fig 4B, n≥7 for each time point analyzed, control:blue, *PdxCre*^{late} *β-cat*^{active}: orange). High levels of β-catenin (green) can be detected in the DAPI stained (blue) nuclei of adult *PdxCre*^{late} *β-cat*^{active} exocrine cells (D), identified by amylase staining (red). In contrast, β-catenin is localized exclusively to the plasma membrane of control cells (C). Scale bars represent 10 μm. Staining of pancreatic sections for the proliferation marker, phospho-histone H3 (PH3, red) and costained for DAPI (blue) reveals an increase in the number of proliferating cells in the *PdxCre*^{late} *β-cat*^{active} mutant (F) when compared to control (E). Scale bars represent 100 μm. Quantification of PH3 positive cells (n=4 per genotype analyzed) indicates that the relative number of proliferating cells in the *PdxCre*^{late} *β-cat*^{active} mutant (orange) is increased 2.5 fold over control (blue) at 21 days post natal (I). Hematoxylin and eosin staining of adult pancreas sections from *PdxCre*^{late} *β-cat*^{active} mice (H) reveals an increase in cell density within the exocrine pancreas, but not the endocrine islet (at center) when compared to control (G). Quantification of the relative number of nuclei per field confirms that the density of cells within the exocrine pancreas of *PdxCre*^{late} *β-cat*^{active} mice (orange) is increased 1.8 fold over control (blue), while the endocrine cell density is normal (J, n=4, magnification=40x). Confidence intervals calculated using student's t-test. P values: #, not significant; *, $p < 0.05$; **, $p < 0.01$. Error bars represent standard error of the mean.

Figure 6. Pancreas insulin content and islet function appear normal in the *PdxCre^late β-cat^active* mouse. The islet architecture of adult *PdxCre^late β-cat^active* mutant mice (B) is comparable to control (A) as revealed by glucagon (green) and insulin (red) staining of pancreas sections. DAPI stained nuclei are indicated in blue. Scale bars represent 50 μm (A-B). The majority of β-cells, identified by insulin staining (red), in the adult *PdxCre^late β-cat^active* mutant (D, higher magnification, G) display localization of β-catenin (green) to the plasma membrane that is equivalent to control (C, higher magnification, F). However, a subset of β-cells in the *PdxCre^late β-cat^active* mutants (E, higher magnification, H) exhibit high levels of cytoplasmic β-catenin staining. Scale bars indicate 100 μm (C-E) and 15 μm (F-H). The β-cells that exhibit strong cytoplasmic β-catenin localization (green) in the *PdxCre^late β-cat^active* mutant (J) still stain positive for the adult β-cell transcription factor Pdx1 (red), a characteristic of properly differentiated β-cells. β-cells present in equivalent adult pancreas sections from control animals are shown stained for Pdx1 (I). Resolution of a fasting glucose challenge is equivalent in control (blue) and *PdxCre^late β-cat^active* (orange) animals (K, n=6 for each genotype, error bars represent standard error of the mean).

Figure 7. Abnormal cells with nuclear localization of β-catenin are present in a subset of islets in 1 year old PdxCre^late β-cat^active mice. Cells within a small subset of islets in one year old *PdxCre^late β-cat^active* mutant pancreata exhibit nuclear localization of β-catenin (Fig. 5 B,D,F,H). These cells do not express insulin or Pdx1 (B, higher magnficiation D, F, higher magnification H) seen in control islets (A, higher magnification C, E, higher magnificiation G.) Scale bars represent 50 um (A,B, E,F) and 25 um (C, D,G, H).

Supplemental Figure 1. Pancreatic defects in *PdxCre^{early} β-cat^{active}* are detectable early in organogenesis. Analysis of hematoxylin and eosin stained 12.5 pancreatic buds at 20x magnification reveals abnormal dilation of the early pancreatic epithelium in some *PdxCre^{early} β-cat^{active}* mutants (B) when compared to equivalent sections in control animals (A). By e15.5, the clearly defined exocrine cell clusters that are seen in the control (C) can not be detected in the equivalent sections from the *PdxCre^{early} β-cat^{active}* mutant (D). In addition, numerous abnormally enlarged ductal structures (yellow arrows) are present in the *PdxCre^{early} β-cat^{active}* mutant (D). Magnification in A-D is 20x.

Supplemental Figure 2. The number of Pdx1$^+$ progenitor cells within the pancreatic epithelium at e12.5 is significantly reduced in the *PdxCre^{early} β-cat^{active}* mutants (red, n=5) when compared to control (blue, n= 3) and *PdxCre^{late} β-cat^{active}*(orange, n=5) mutants (A). Error bars indicate standard deviation. Confidence intervals were determined using the student's t-test; # = not significant, ** = p<0.01. Pdx1 protein can no longer be detected within cells that exhibit increased levels of β-catenin staining in the *PdxCre^{early} β-cat^{active}* e12.5 pancreatic epithelium (D). In contrast, the level of β-catenin staining in the *PdxCre^{late} β-cat^{active}* (C) appears equivalent to control (B). Scale bars indicate 25 μm (A-D).

Supplemental Figure 3. Islet area in the *PdxCre^{late} β-cat^{active}* (orange) at P0 is equivalent to control (blue), n= 4 for each genotype (A). Relative pancreas insulin and

glucagon content in the *PdxCre^late β-cat^active* (orange) is equivalent to control (blue), n=6

for each genotype (B). P values: # not significant (determined using student's t-test),

error bars represent standard error of the mean. Schematic showing selective expansion

of the pancreatic exocrine compartment in the *PdxCre^late β-cat^active* mutants, while the

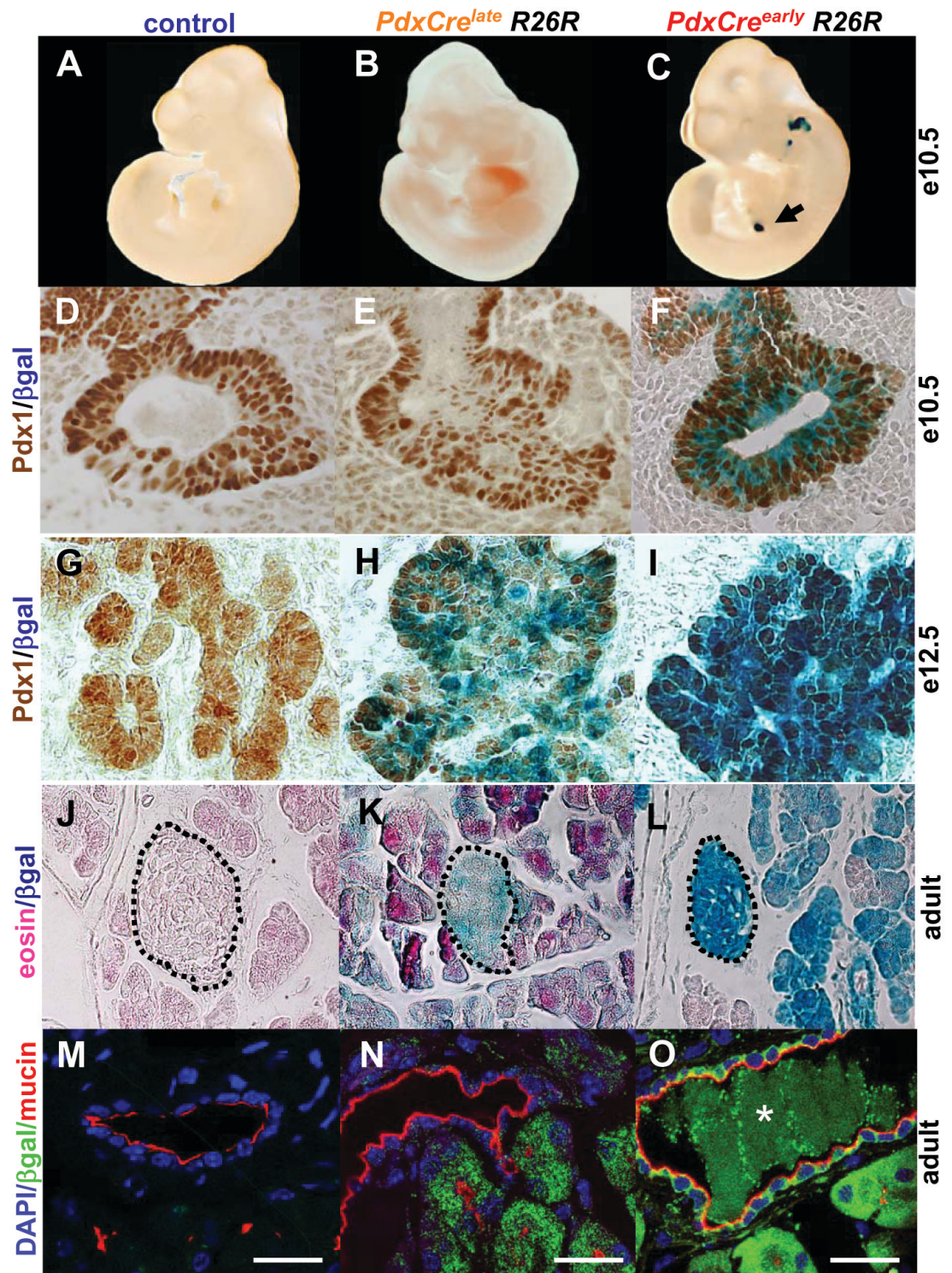size of the pancreatic endocrine compartment remains unchanged (C).

Table 1: Antibodies used in this study

Antigen	Species	Source	Dilution
amylase	rabbit	Sigma, A8273	1:800
β-catenin	mouse	BD, 610154	1:200
β-galactosidase	rabbit	ICN, 55976, lot 03660	1:200
E-cadherin	mouse	BD, 610181	1:200
glucagon	rabbit	Linco, 4030-01f	1:400
Glut2	rabbit	Chemicon, AB1342	1:100
insulin	guinea pig	Linco, 4011-01	1:400
Mucin-1	hamster	NeoMarkers, HM-1630	1:500
Nkx6.1	rabbit	Gift of Michael German, UCSF	1:1,000
pancreatic polypeptide	guinea pig	Linco, 4041-01	1:400
Pdx-1	rabbit	Gift of Michael German, UCSF	1:1,000
phospho-histone H3	rabbit	Upstate Laboratories 65-570	1:200
Ptc	goat	Santa Cruz, SC6149, lot E142	1:100
somatostatin	rabbit	DAKO, A0566	1:200
Sonic hedgehog**	goat	Santa Cruz, SC1194, lot F262	1:100

Antibodies were used at the stated dilution on paraffin imbedded tissues.

**Please note that we have found that this particular antibody recognizes multiple Hedgehog ligands. Therefore, in the figure legend we have denoted the staining as Hedgehog ligand, rather than claiming specificity for Sonic
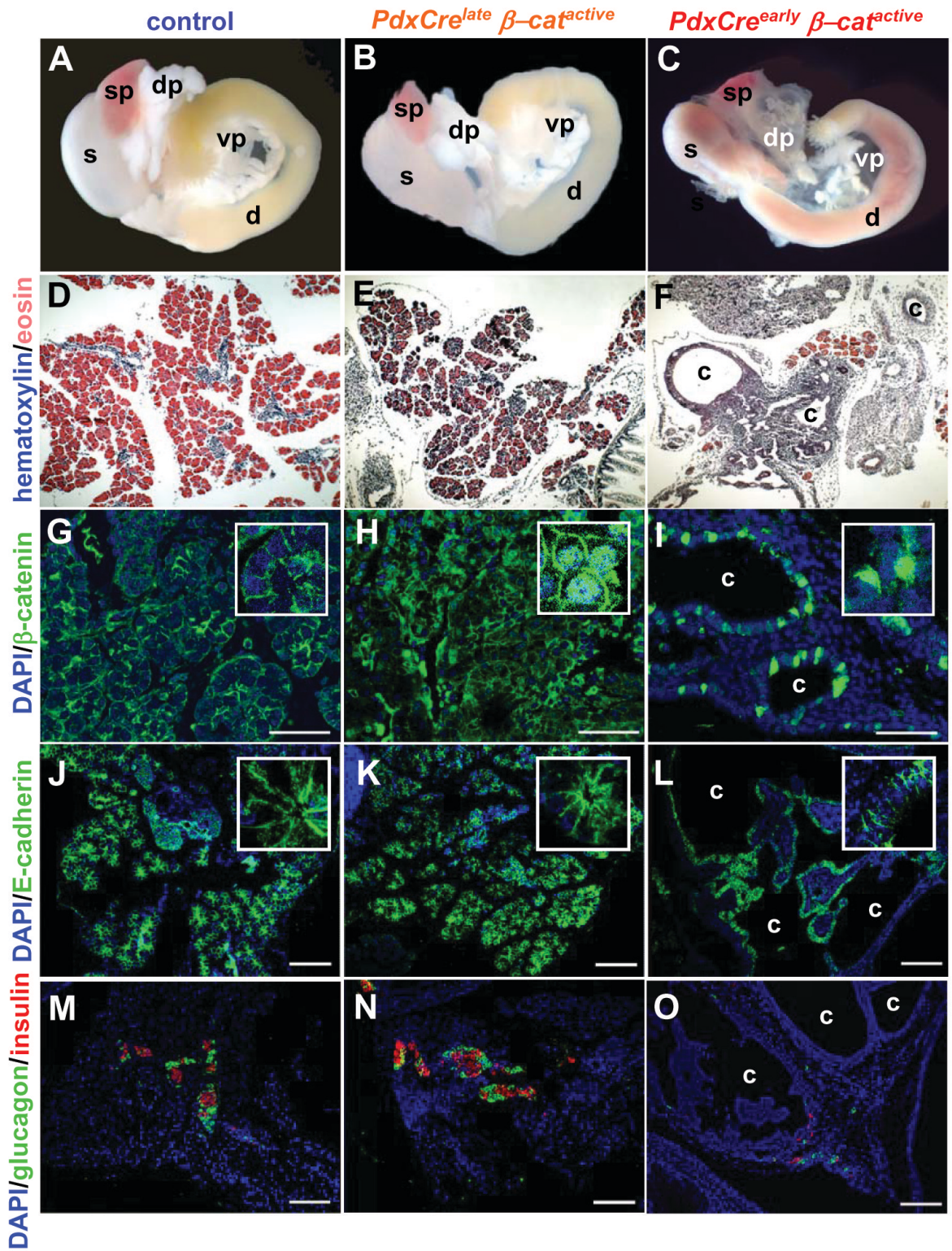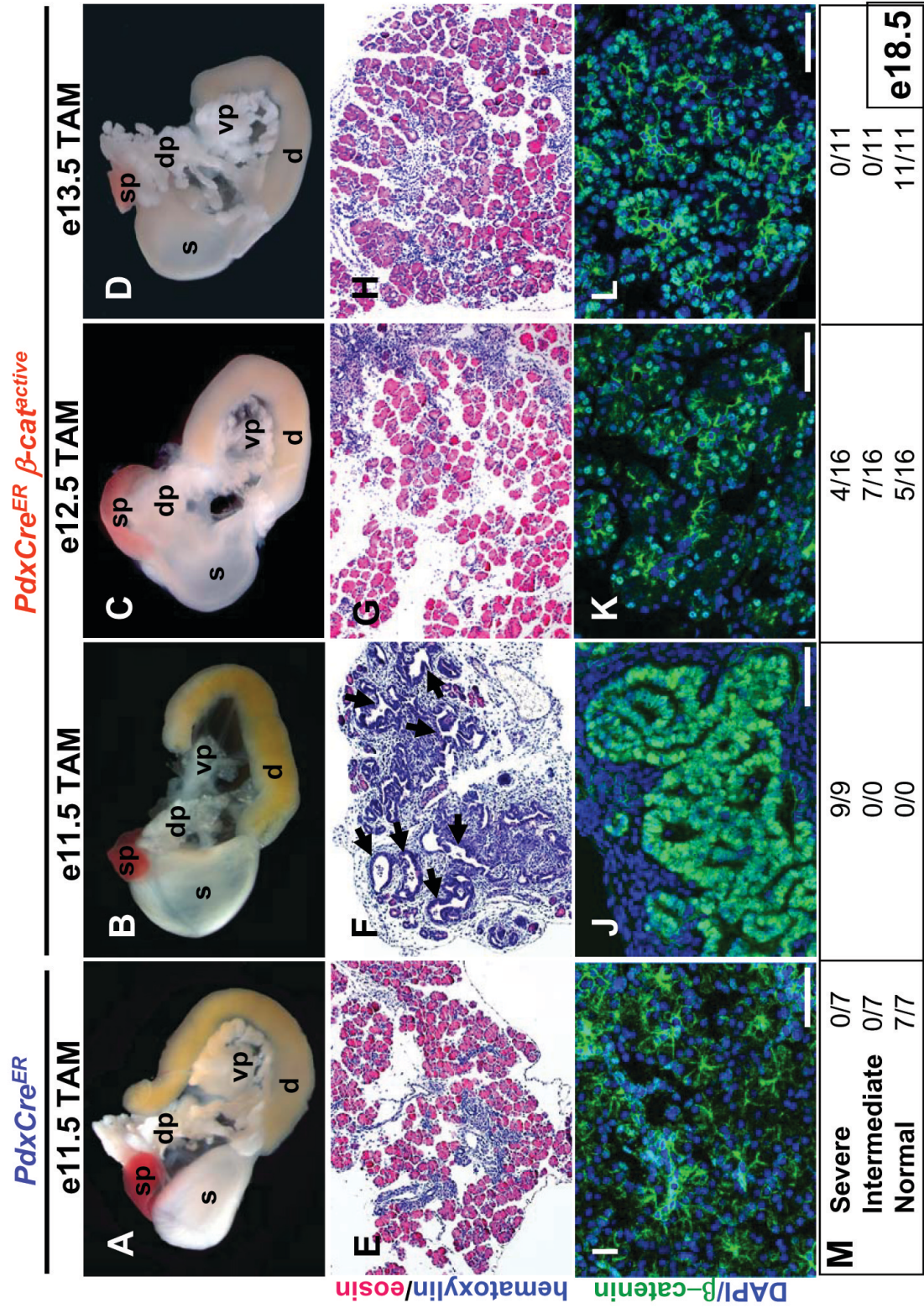
Figure 1

Figure 2

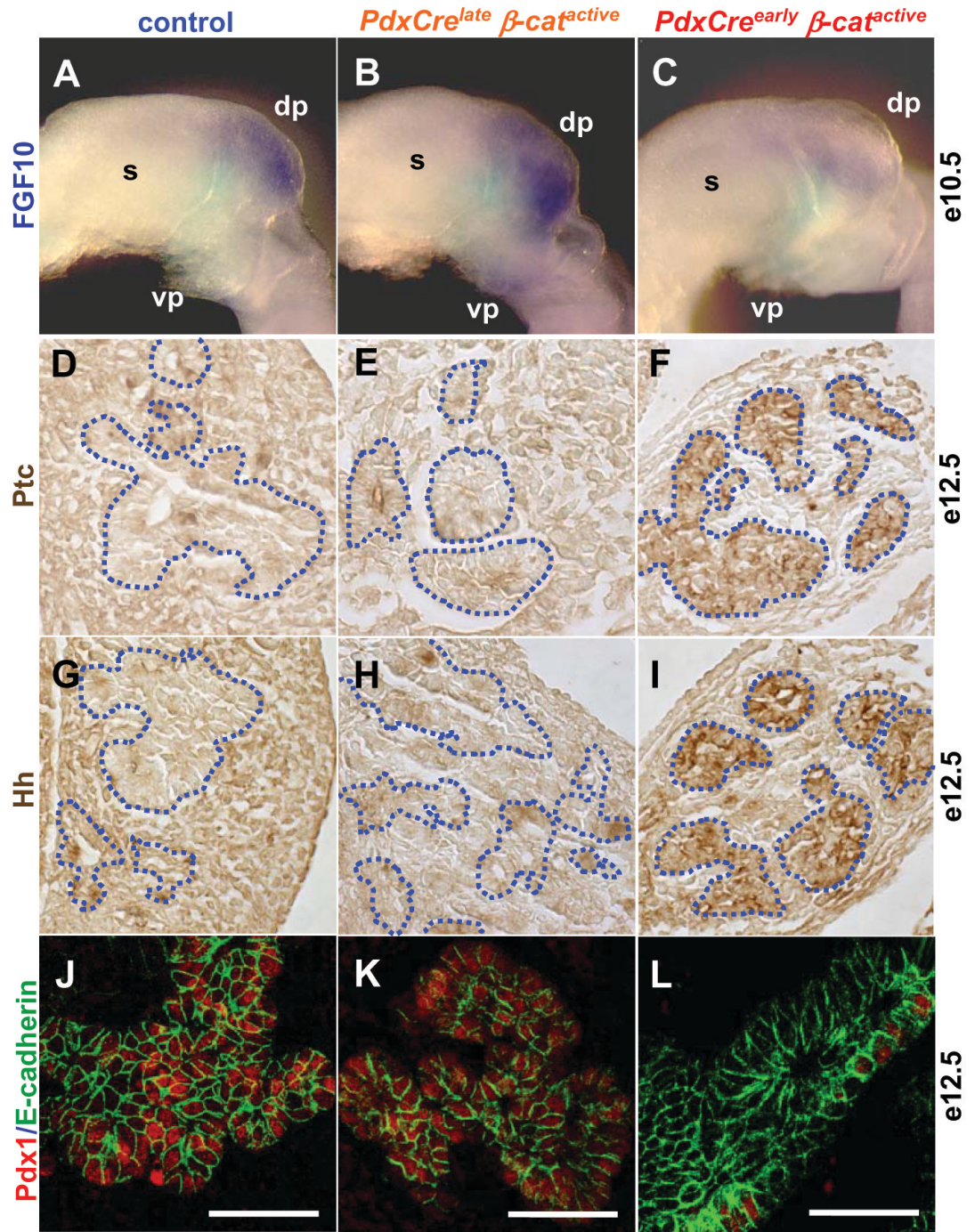**control**   *PdxCre^late^ β–cat^active^*   *PdxCre^early^ β–cat^active^*
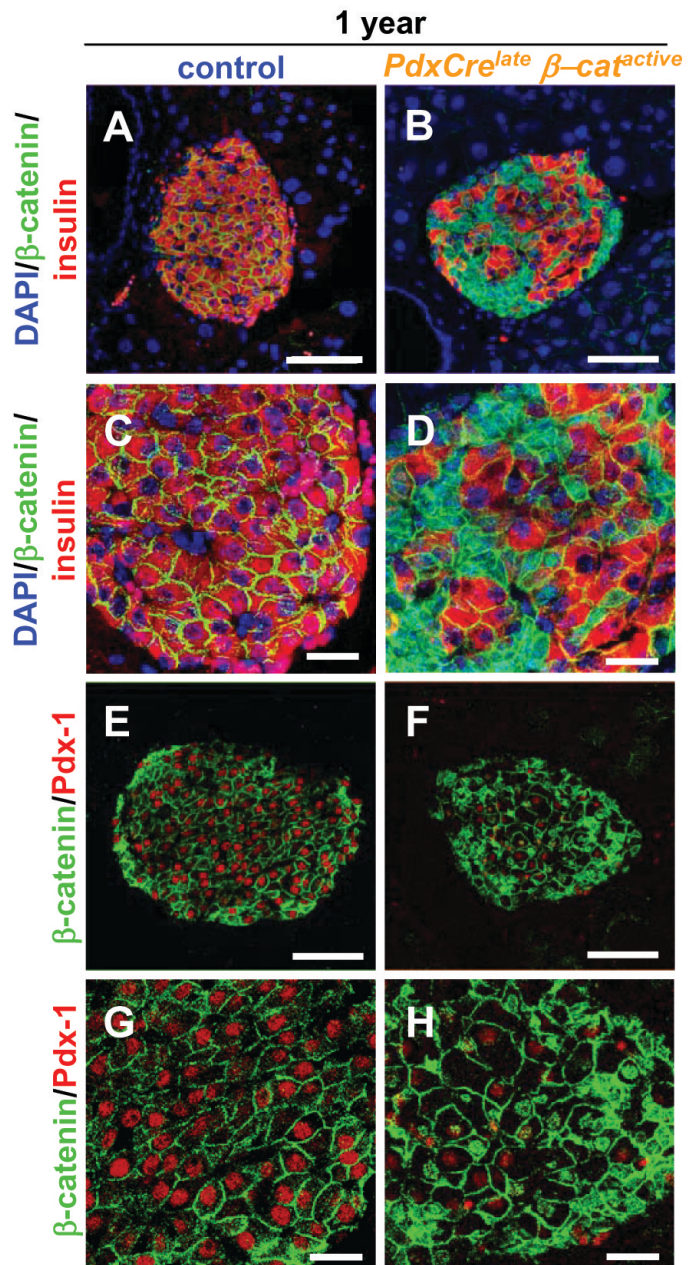
Figure 3
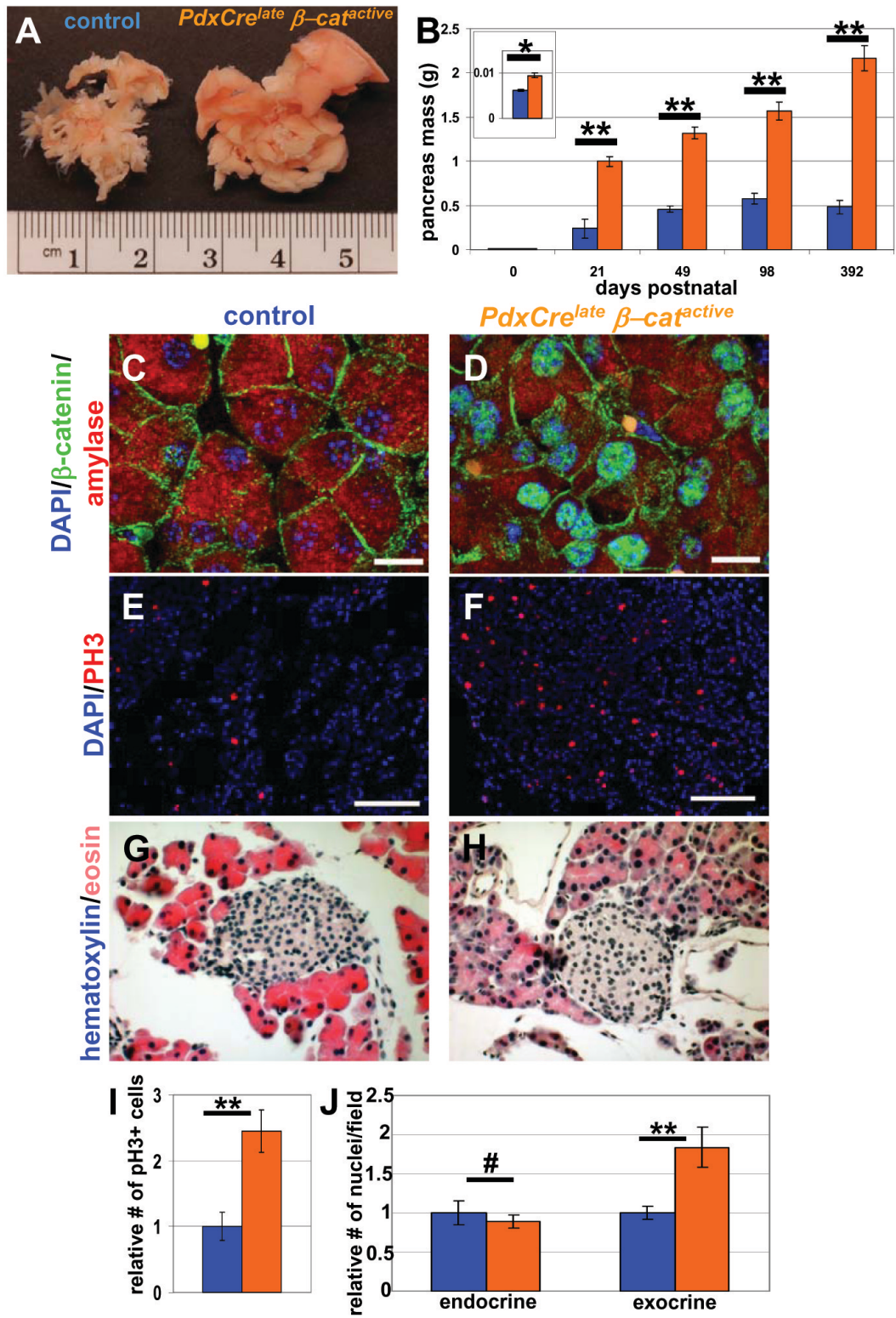
Figure 4

Figure 5

Figure 6
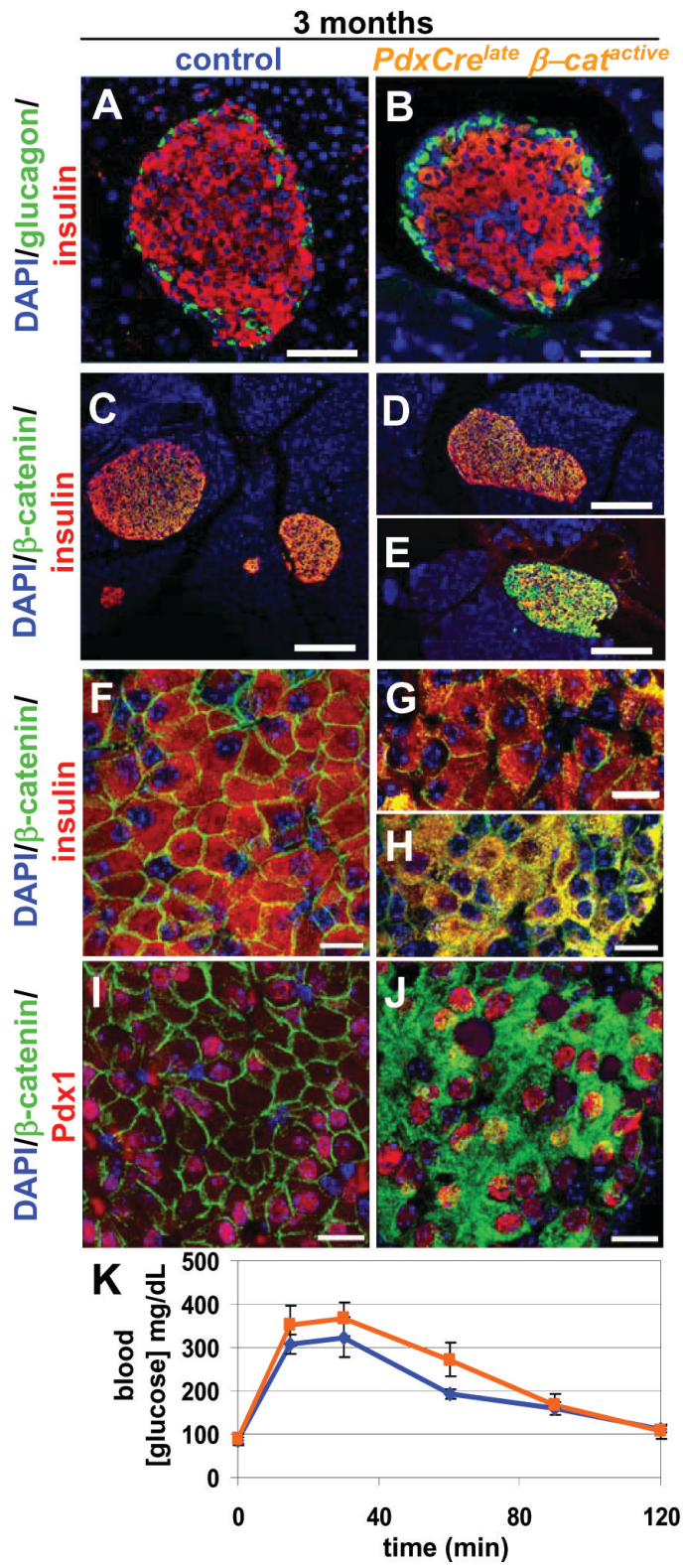
Figure 7

Supplemental Figure 1

Supplemental Figure 2

A

e12.5

Relative # of Pdx1+ cells

control

*PdxCre^late^ β-cat^active^*

*PdxCre^early^ β-cat^active^*

control

*PdxCre^late^ β-cat^active^*

*PdxCre^early^ β-cat^active^*

Pdx1/β-catenin

e12.5

Supplemental Figure 3

A

B

C
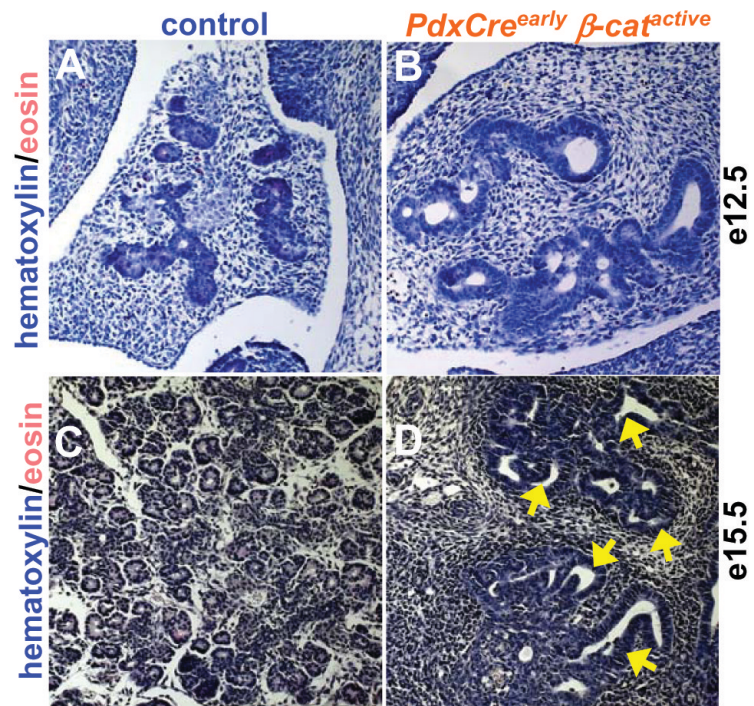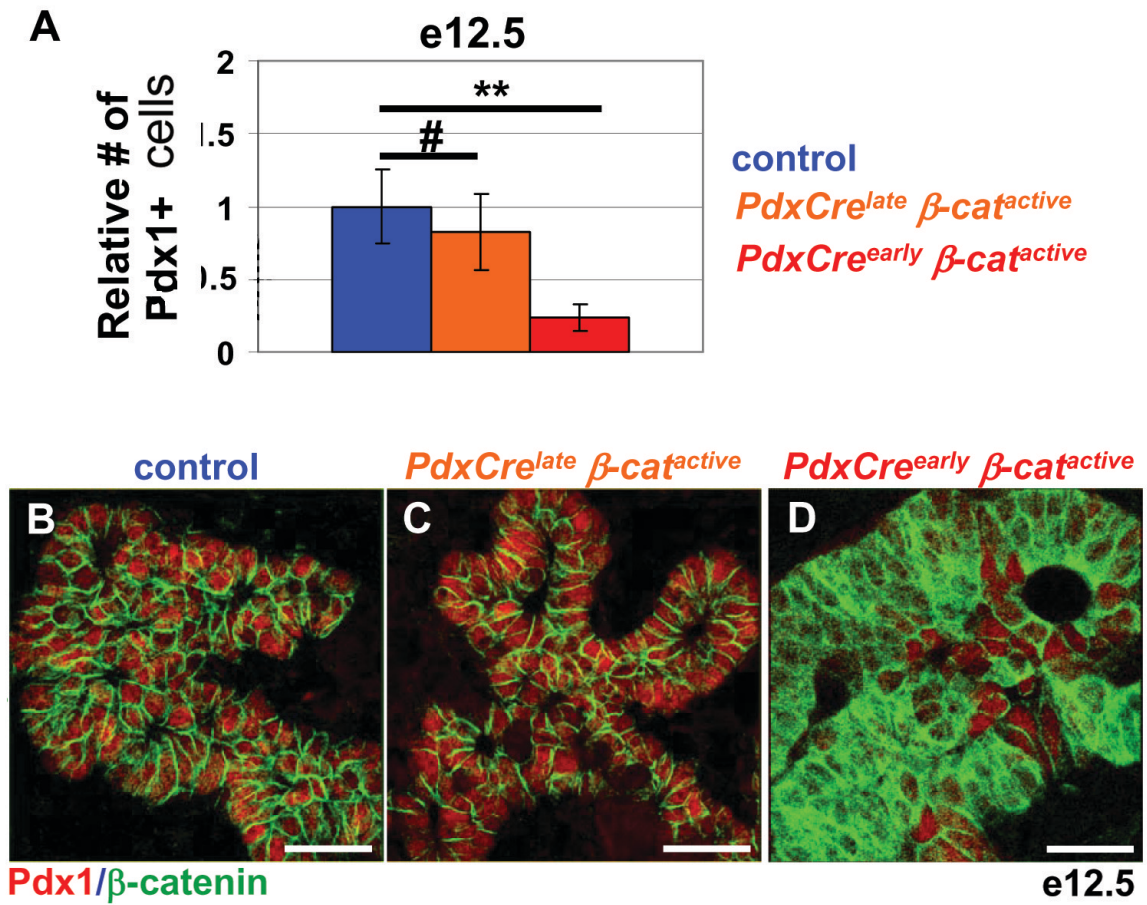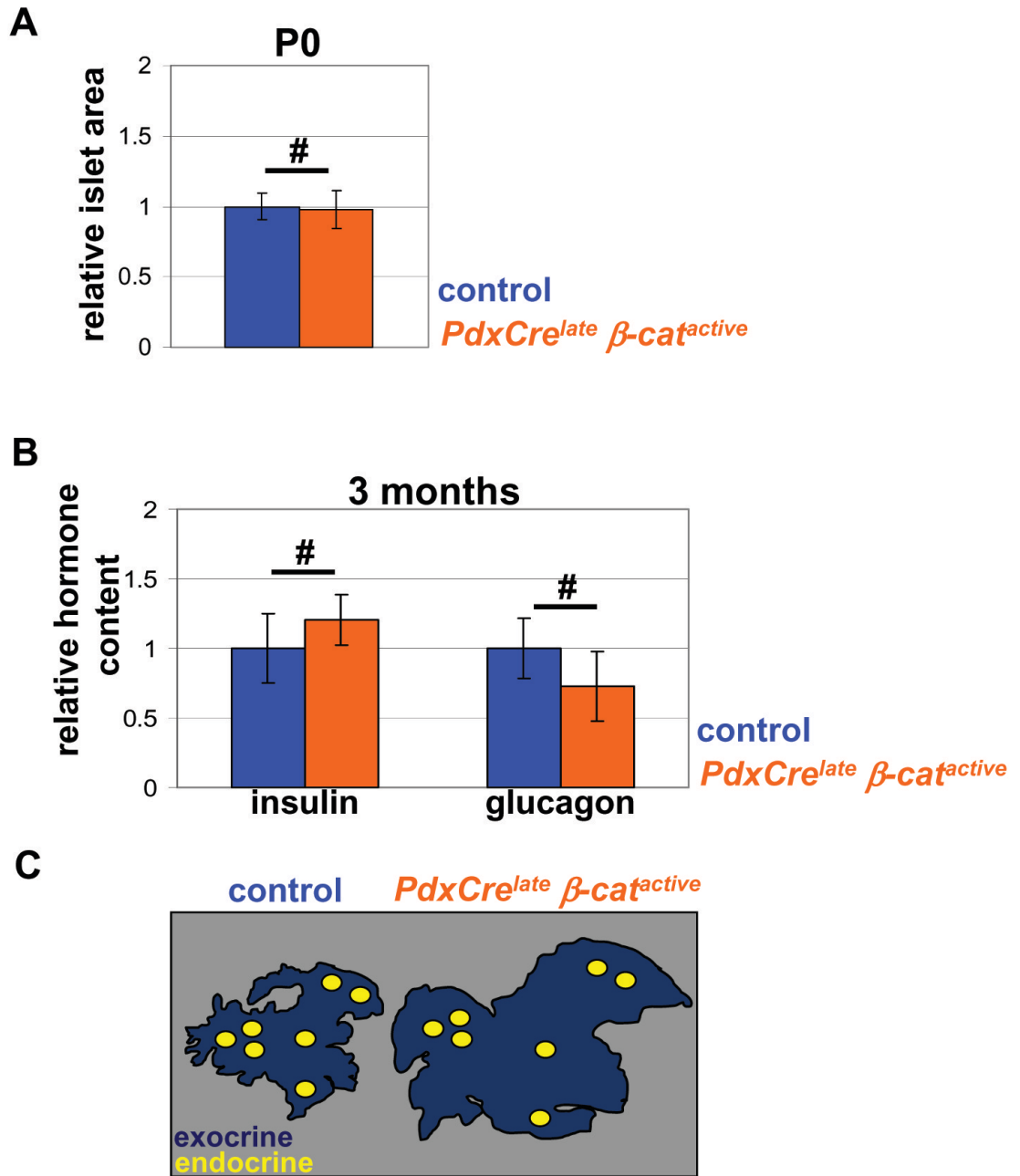
Chapter 3

Wnt signaling regulates pancreatic β-cell proliferation

Abstract

There is widespread interest in defining factors and mechanisms that stimulate proliferation of pancreatic islet cells. Wnt signaling is an important regulator of organ growth and cell fates, and genes encoding Wnt signaling factors are expressed in the pancreas. However, it is unclear if Wnt signaling regulates pancreatic islet proliferation and differentiation. Here we provide evidence that Wnt signaling stimulates islet b-cell proliferation. Addition of purified Wnt 3a protein to cultured β-cells or islets promoted expression of Pitx2, a direct target of Wnt signaling, and Cyclin D2, an essential regulator of ß-cell cycle progression, and led to increased b-cell proliferation in vitro. Conditional pancreatic ß-cell expression of activated ß–catenin, a crucial Wnt signal transduction protein, produced similar phenotypes in vivo, leading to ß-cell expansion, increased insulin production and serum levels, and enhanced glucose handling. Conditional ß-cell expression of Axin, a potent negative regulator of Wnt signaling, led to reduced Pitx2 and Cyclin D2 expression by ß-cells, resulting in reduced neonatal ß-cell expansion and mass, and impaired glucose tolerance. Thus, Wnt signaling is both necessary and sufficient for islet ß-cell proliferation, and our study provides unique evidence for a mechanism governing endocrine pancreas growth and function.

Introduction

Relative or absolute deficiency of pancreatic ß-cell mass underlies the pathogenesis of type 1 and type 2 diabetes (1, 2). Thus, there is considerable interest in understanding the mechanisms that stimulate pancreatic islet cell growth and differentiation. Recent studies identified several cellautonomous factors, including Cyclin D2, c-Myc, cyclin dependent kinase 4 (CDK4), menin, and other nuclear proteins that are essential for regulating growth of pancreatic islet ß-cells, the sole source of insulin in post-natal animals (3, 4). However, little is known about the signaling factors that control expression or activity of these ß-cell autonomous growth regulators.

Wnt proteins are a family of highly conserved secreted proteins that regulate multiple developmental processes including proliferation of organ-specific stem/progenitor cell populations, growth control and cell fate determination in diverse organs, and tissue patterning (5). In the canonical Wnt signaling pathway, binding of Wnt ligand to cognate membrane-spanning receptor proteins called Frizzleds (Fz), triggers a signaling cascade that results in the stabilization and nuclear localization of ß-catenin, whose interactions with TCF/LEF transcription factors control transcription of target genes like Pitx2 (6, 7). In the absence of Wnt signaling, cytoplasmic ß-catenin in Wnt-responsive cells is targeted for proteosome-mediated degradation by a heteromeric protein complex that includes Axin, glycogen synthase kinase 3ß (GSK-3ß), and other proteins (8-10).

Recent studies document expression of several Wnt ligands and Fz receptors in the embryonic and post-natal pancreas. In one study, conditional disruption of pancreatic ß-catenin expression produced pancreatitis, and reduced islet mass, but the mechanism for impaired islet cell proliferation was not identified (11). In other studies, Wnt signaling

64

disruption led to clear changes in exocrine pancreas growth without detectable changes in

endocrine cell proliferation (12-14). Thus, it remains unclear if Wnt signaling controls

islet cell growth. Here we use gain- and loss-of function approaches to show that Wnt

signaling controls islet ß-cell proliferation, and to unveil a mechanism underlying this

regulation.

MATERIALS & METHODS

Animal Breeding RIP-Cre (24), ß-cat$_{active}$ (26), *Pdx1*-tTA (27, 28) and TRE-*Axin* mice

(27) have been previously described. Dox (2mg/ml; Sigma) was administered via

drinking water as described previously (29)

Immunohistochemistry Tissue was fixed in 4% paraformaldehyde (Electron

Microscopy

Sciences) or in Z-fix (Anatech Ltd.). Immuno-histochemistry was performed paraffin-

embedded tissue and immunofluorescence studies were performed on either paraffin- or

cryo-preserved tissue, depending on antibody requirements. Antigen retrieval, antisera

and detection methods used here are described in *Supporting Materials and Methods*,

which is included below. Images were captured using a Leica SP2 AOBS confocal

microscope (Cell Sciences Imaging Facility, Stanford Medical Center). Light images

were captured using a Zeiss Axioplan 2 microscope and software. Cell counting, point-

counting morphometry, and β-cell quantification were performed using standard

morphometric techniques (14, 44, 45) or as described in *Supporting Materials and*

Methods. For quantification of immunostained cells, pancreas tissue was obtained from at

least 4 mice per genotype. All data are presented as the average ± s.e.m.. Two-tailed T

tests were conducted to determine statistical significance.

Physiologic studies and islet isolation Glucose challenge studies were performed as

described (45). Pancreatic insulin content was measured with a Mouse Insulin ELISA kit

(Alpco Diagnostics). Islets were isolated from C57BL/6 mice on postnatal days 4-8.

Pancreata were digested with collagenase (Sigma-Aldrich), and islets were purified using

a multi-layer islet-specific ficoll gradient (Mediatech).

Isolation of RNA, protein, and quantitative PCR analysis

The murine insulinoma cell line MIN6 (18) was used for in vitro studies. MIN6 cells or

postnatal islets were treated with purified Wnt3a (ref. 16; final concentration 100 ng/ml,

equal to 2.4 nM), vehicle only, or Wnt3a plus Fz8-CRD (final concentration 200 ng/ml,

equal to 3.3 nM). Following treatment, RNA was isolated using TriZol (Invitrogen). 1.5

mg of total RNA was then reverse transcribed into cDNA using the RetroScript Kit

(Ambion, Inc.). Quantitative PCR analysis was performed on an Applied Biosystems

7300 Real Time Machine PCR machine with Taqman probe sets for *Pitx2, cyclin D2,*

cyclin D1, CDK4. All transcript levels were normalized against β-*actin*. ChIP assays

were performed on MIN6 cells and islets as described (19). Before ChIP analysis and

proliferation analysis, islets were maintained for 24 hours in RPMI,

Penicillin/Streptomycin, HEPES, fungizone, and L-Glutamine (Invitrogen-GIBCO)

containing 10% fetal bovine serum (Hyclone) at 37ₒC. We used monoclonal antibody

specific for Pitx2 (1:100, Santa Cruz Biotechnology, Inc.). Primers specific for c*yclin D2*

proximal promoter sequences and regions of the *cyclin D1* and *cdk4* promoters are

available in *Supporting Materials and Methods*, which is described below.

Results

Wnt signaling stimulates expression of essential ß-cell cycle regulators

To test if Wnt signaling controls islet ß-cell growth, we exposed isolated pancreatic islets to

purified Wnt3a, a Wnt family member that is expressed in the developing pancreas and in

adult human islets (15). In prior studies we showed that purified Wnt3a led to ß-catenin

stabilization and induction of established Wnt target genes (16). To quantify ß-cell

proliferation, we measured expression of Ki67, a marker of late G1, S, G2 and M phases

previously used to assess ß-cell cycle progression. In islets treated with Wnt3a we found

a 2-fold increase of Ki67+ ß-cells (Fig. 1A), which characteristically co-expressed insulin

and the transcription factor Nkx6.1, markers not expressed by other mature islet cells

[Supporting Information (SI) Fig. 1; ref. 17]. Addition of soluble Frizzled 8-Cysteine

Rich Domain (Fz8-CRD), a potent specific Wnt inhibitor (16, D. ten Berge and R. Nusse,

unpubl. results) eliminated this stimulatory effect of Wnt3a, indicating that active Wnt

signaling was assessed (Fig. 1A). Consistent with these data, we found that growth of

MIN6 cells, a transformed mouse ß-cell line responsive to normal growth cues (18, 19),

was significantly increased by purified Wnt3a, compared to treatment with vehicle alone

(Fig 1B). To test if Wnt3a promoted MIN6 cell proliferation, we measured incorporation

of bromodeoxyuridine

(BrdU), which proved more consistent than Ki67 as a proliferation marker in our MIN6

cultures.

Compared to vehicle-treated controls, Wnt3a-treated cells had a 3-fold increase in BrdU incorporation (Fig. 1C). Collectively, these results show that Wnt3a exposure in vitro was sufficient to increase proliferation by ß-cells. Several cell cycle regulators including Cyclin D1, Cyclin D2, CDK4, and c-myc have been shown to control ß-cell proliferation in vivo (20-23). To identify the mechanism of Wnt-stimulated ß-cell proliferation, we tested if expression of these established ß-cell cycle regulators was controlled by Wnt signaling. Cyclin D2 expression in islet ß-cells peaks between postnatal day 4-6, corresponding with a period of increased ß-cell proliferation and expansion (21), suggesting competence for endogenous signals that regulate proliferation. Thus, we tested if expression of *cyclin D2* and other cell cycle regulators was stimulated by Wnt3a protein in islets from mice at postnatal day 4. Wnt3a-treatement of islets for 24 hours led to significantly increased mRNA levels of *cyclin D1,* c*yclin D2* and *CDK4* compared to controls, a response that was completely abolished by Fz8-CRD (Fig 1D). To test if Wnt3a affected ß-cells, we then exposed MIN6 cells to Wnt3a. Similar to our finding in islets, mRNA levels of *cyclin D1*, c*yclin D2*, and *CDK4* were clearly increased by Wnt3a exposure (Fig. 1E). Addition of soluble Fz8-CRD eliminated the stimulatory effects of Wnt3a on each of these targets (Fig 1D). Thus, Wnt3a was sufficient to stimulate expression of cell cycle regulators in purified islets and cultured ß-cells, matched by increased ß-cell proliferation. To test if Wnt signaling regulation of cell cycle regulators was conserved, we assessed effects of Wnt3a exposure on cultured human islets. Real-time RT-PCR studies revealed that Wnt3a increased mRNA levels of *cyclinD2* and *Pitx2*, a direct transcriptional regulator of *cyclinD2* (see below), an effect

that was blocked by Fz8-CRD (SI Fig 2). Additional studies are needed to assess if Wnt

signaling is sufficient to stimulate expansion of cultured human islet cells.

Wnt3a promotes direct association of Pitx2 with regions of the *cyclin D2* gene in b-

cells

In neuroendocrine cells Wnt signaling stimulates expression of the transcription

factor Pitx2, which in turn can activate transcription of *cyclin D2* and *c-myc* (7). We

found that exposure of MIN6 cells or islets to purified Wnt3a led to a 4-fold increase in

Pitx2 mRNA levels, an effect abolished by Fz8-CRD (Figs 1D-E, SI Fig 2). To determine

if Wnt signaling promotes the direct association of Pitx2 with target genes, we performed

chromatin immunoprecipitation (ChIP) studies in MIN6 cells and postnatal pancreatic

islets. Prior to Wnt3a exposure, Pitx2 was not detectably associated with the region –980

to -525 base pairs (bp) immediately 5' of the *cyclin D2* transcriptional start site (Fig. 2A).

After exposure of islets (Fig. 2B) and MIN6 cells (Fig. 2C) to purified Wnt3a protein,

ChIP analysis revealed Pitx2 association with elements within –980 bp of the

transcription start site of *cyclin D2* (Fig. 2A-B), a region that contains consensus *bicoid*-

like binding sites (red boxes) known to bind Pitx2 (7). By contrast, we did not detect

Pitx2 association with regions in the *cyclinD2* locus distal to -1000bp that lack these

consensus sites (Fig 2B) or in regions proximal to -525. Although Wnt3a stimulation

results in increased transcription of *cyclin D1* and *Cdk4* in MIN6 cells and purified islets

(Figs 1D-E), we did not observe direct association of Pitx2 with these genes by ChIP

analysis (data not shown). Thus, Wnt3a stimulated Pitx2 association with *cyclin D2* in

islets. Collectively, our results provide the first evidence, to our knowledge, that Wnt

signaling is sufficient to induce Pitx2 binding to elements of *cyclin D2* in ß cells, promoting increased Cyclin D2 expression and proliferation.

Expression of activated ß-catenin is sufficient to stimulate islet ß-cell expansion

To test if Wnt signaling activation is sufficient to promote ß-cell proliferation in vivo, we intercrossed mice to create strains expressing Cre-recombinase in ß-cells from the rat insulin promoter (RIP-Cre; 24-25) and harboring the ß-cat$_{active}$ allele, which encodes a loxP-flanked constitutively-active form of ß-catenin (see Methods; 14, 26). Previously, we used mice expressing Cre-recombinase under the control of the *Pdx1* promoter (24) to induce expression of ß-cat$_{active}$ in adult islets, but expression of Cre-recombinase was mosaic in islet ß-cells, and did not result in significant changes in ß-cell mass (14). In 3 month-old bitransgenic RIP-Cre, ß-cat$_{active}$ mice, immunohistology revealed increased ß-catenin levels and nuclear localization in ß–cells when compared to controls (Fig 3A-B, SI Fig 3). Expression of Ki67 by ß-cells in adult RIP-Cre, ß-cat$_{active}$ mice was increased 3 fold, corresponding well with a 2.5 fold increase in ß-cell mass (Fig 3C-F). Consistent with our in vitro islet studies, the in vivo expression of Cyclin D2 was increased in ß-cells of RIP-Cre, ß-cat$_{active}$ mice (Fig 3G-H). Real-time RT-PCR measures revealed a 2-fold increase of *cyclinD2* and *Pitx2* mRNA levels in RIP-Cre, ß-cat$_{active}$ islets compared to controls (Fig

3I). In 3 month old RIP-Cre, ß-cat$_{active}$ mice, cyclinD2$_+$ ß-cells maintained expression of insulin (Fig 3G-H). Moreover, expression of adult b-cell markers including, Pdx1, Glut2, and Nkx6.1 were also maintained in the islet cells of 3 month old RIP-Cre, B-cat$_{active}$ mice (data not shown). Together, this suggests that activation of ß-catenin was sufficient to stimulate expansion of ß-cells that maintained their differentiated fate. In support of

70

this conclusion, physiologic studies revealed evidence of increased ß-cell mass in RIP-Cre, ß-cat$_{active}$ mice. Serum insulin levels in RIP-Cre, ßcat$_{active}$ mice were increased approximately 3-fold (Fig 3J). However, insulin content per islet cell was not detectably changed in RIP-Cre, ß-cat$_{active}$ mice (SI Fig 3). Moreover, compared to islets from control mice, insulin secretion by islets from RIP-Cre, ß-cat$_{active}$ mice following stimulation with glucose (Fig 3K) or other secretogogues like arginine (SI Fig 3) was indistinguishable. Consistent with these findings, blood glucose concentration in fasted RIP-Cre, ß-cat$_{active}$ mice was significantly reduced and intraperitoneal glucose challenge revealed that glucose disposal was improved in RIP-Cre, ß-cat$_{active}$ mice compared to controls (Fig 3L). Collectively, these results support the conclusion that hyperinsulinemia in RIP-Cre, ß-cat$_{active}$ mice principally reflects increased ß-cell mass. Thus, induction of ß-catenin *in vivo* was sufficient to promote expansion of functional pancreatic ß-cells.

Conditional Axin expression impairs Pitx2 expression and ß-cell expansion

To address if Wnt signaling was required for normal ß-cell expansion in vivo, we generated

transgenic mice that permitted conditional pancreatic expression of Axin, a potent inhibitor of Wnt signaling. Intercrosses produced mice that harbor a transgene encoding Axin adjacent to a tetracycline response element (TRE) promoter (TRE-Axin; 27) and the *Pdx1*-tTA transgene (28, 29) in which the tetracycline-regulated transactivator (tTA) replaces the coding region of *Pdx1*, a gene expressed in pancreatic progenitor cells and mature b-cells (30-32). Bi-transgenic *Pdx1*-tTA/TREAxin progeny and mice of other genotypes from this intercross were obtained at mendelian frequency from over 20 litters. Transgenic Axin expression in *Pdx1*-tTA/TRE-Axin islets was clearly detectable by

immunohistochemistry (Fig 4) and by western blotting (SI Fig 4). Axin was detected in the islet core, where Pdx1-expressing ß-cells reside, in pancreatic islets of bi-transgenic mice, but not littermate controls on post-natal day (P) 4 (Fig. 4A, B), a neonatal stage when ß-cells are actively proliferating (21). As expected, continuous exposure of *Pdx1-tTA/TRE-Axin* mice to doxycycline (Dox), a tetracycline analogue, from the time of conception prevented expression of TRE-Axin in Pdx1+ cells (Fig. 4C; see Methods). Thus, in *Pdx1*-tTA/TRE-Axin mice, TRE-Axin was expressed in Pdx1+ cells, and conditionally repressed by Dox exposure. To assess Axin effects on Wnt signaling in *Pdx1*-tTA/TRE-Axin mice at P4, we analyzed expression of *Pitx2*, a direct Wnt signaling target (7). Immunohistology showed that Pitx2 was localized to ß-cell nuclei (Fig 4D-I). Compared to wildtype controls or to *Pdx1*-tTA/TRE-Axin mice administered Dox, the percentage of Pitx2+ ß-cells per pancreas was reduced by 75% in *Pdx1*-tTA/TRE-Axin mice (Fig 4D-J). Thus, conditional Axin induction reduced *Pitx2* expression, providing evidence of Wnt-signaling disruption in the endocrine pancreas of *Pdx1*-tTA/TRE-Axin mice.

Prior studies showed that Cyclin D2-deficient mice have a 70% reduction in ß-cell mass and glucose intolerance without changes in total pancreatic mass (21), phenotypes that are reminiscent of the changes we noted in *Pdx1*-tTA/TRE-Axin mice. Based on these findings and our in vitro studies, we postulated that *cyclin D2* expression by nascent ß-cells in *Pdx1*-tTA/TRE-Axin mice might be impaired. Immunohistology showed that Cyclin D2 protein co-localized with Nkx6.1+ cells in wild type and *Pdx1*-tTA/TRE-Axin mice, consistent with our in studies of MIN6 cells and cultured islets (Fig. 4K-S). However, analysis of *Pdx1*-tTA/TRE-Axin mice revealed a 60% reduction of Cyclin D2

expression in Nkx6.1+ cells, an effect reversed by Dox (Fig 4K-T). These changes correlated with a significant reduction of BrdU incorporation by Nkx6.1+ cells (SI Fig. 4). In contrast to these proliferation phenotypes, we did not detect changes in pancreatic apoptosis using TdT-mediated dUTP nick-end labeling (data not shown). Collectively, these studies suggest that Wnt signaling regulates in vivo expression of Cyclin D2, an essential regulator of ß-cell proliferation.

To identify effects of Axin expression on pancreas islets, we analyzed pancreata from *Pdx1*-tTA/TRE-Axin and control mice. The morphology of the pancreas from *Pdx1*-tTA/TRE-Axin mice appeared grossly normal and changes in acinar or ductal cell morphology and number were not detected (data not shown). However, immunohistology and morphometry revealed several defects in postnatal pancreatic islet composition and morphology in *Pdx1*-tTA/TRE-Axin pancreata (Fig.5). Compared to islets from wildtype mice or bi-transgenic mice exposed to Dox, islets from bitransgenic *Pdx1*-tTA/TRE-Axin mice had a significant reduction of b-cells (Fig. 5B-E), and lacked the characteristic architecture of insulin+ cells surrounded by glucagon+ cells. The number of non-bislet cells, including glucagon+ cells, somatostatin+ cells and PP+ cells and the total number of islets, was not significantly altered in bi-transgenic mice (Fig. 5B, E-F and data not shown). At weaning, *Pdx1*-tTA/TRE-Axin mice had persistent ß-cell hypoplasia, with a 50-60% reduction of b-cells compared to littermate controls (Fig. 5G). Compared to controls, including *Pdx1-tTA* mice, total pancreatic insulin content in *Pdx1*-tTA/TRE-Axin mice was reduced (Fig. 5H). While weight gain, blood glucose, and serum insulin levels during random feeding appeared normal in *Pdx1*-tTA/TREAxin mice (data not shown), intraperitoneal glucose challenge revealed impaired glucose tolerance that was

more severe than in *Pdx1*-tTA mice, which have mild glucose intolerance (28; SI Fig. 5) or in other littermate controls. Thus, glucose tolerance was significantly worsened by Axin expression in *Pdx1*-tTA/TRE-Axin mice.

Discussion

These studies reveal that pancreatic Wnt signaling controls islet ß-cell proliferation. Prior studies provided evidence that pancreatic growth and differentiation is regulated by Wnt signaling (11-15, 33, 34). However, these reports did not present a mechanism for the Wnt-mediated action, nor test if Wnt signaling was sufficient to stimulate ß-cell proliferation in pancreatic islets. Here, treatment of ß-cells with purified Wnt protein, or stimulation with activated ß-catenin, permitted us to test if Wnt pathway activation might promote islet ß-cell proliferation, and allowed elucidation of mechanisms underlying Wnt-mediated ß -cell growth. Here we show that Wnt signaling stimulated expression of multiple ß-cell cycle regulators, including Cyclins D1 and D2, resulting in enhanced islet proliferation. Previous studies showed that these D-type cyclins, c-myc and other cell autonomous factors control ß-cell proliferation in pancreas development (21-23, 35), but did not reveal how expression of these factors was controlled. Our studies reveal that Wnt signals promote expression of Pitx2, a transcriptional activator that directly associates with *cis*-regulatory elements in the *cyclin D2* gene. Based on these results, we hypothesize that Wnt signaling induction of Pitx2 promotes *cyclin D2* expression to drive proliferation of nascent ß-cells. Pitx2 has also been shown to regulate expression of *c-Myc* and *cyclin D1* (6, 36), but we did not detect direct association of Pitx2 with promoter-proximal sequences in these genes. Thus, the basis of enhanced expression of *c-*

74

Myc, *cyclin D1* and CDK4 in Wnt-treated ß-cells, and the contribution of these factors to

Wnt-stimulated ß-cell proliferation requires further investigation. Following Wnt

stimulation, ß-cell proliferation was not accompanied by loss of characteristic ß-cell

markers, like insulin or Nkx6.1 (37). On the contrary, our studies of RIP-Cre, ß-cat*active*

mice show that Wnt signaling had a clear physiologic impact by enhancing serum insulin

levels and glucose disposal. Thus, exposure to Wnt signals in some contexts can promote

islet growth and hallmark ß-cell features, although prolonged activation of Wnt signaling

may affect the differentiation state of islet ß-cells (14). Exposure to purified mouse

Wnt3a protein can stimulate expression of *Pitx2* and *cyclinD2* in cultured human

cadaveric islets, but we have not yet found that Wnt signaling is sufficient to induce ß-

cell expansion in human islets. Thus, further studies are needed to test the possibility that

Wnt signaling may be useful for expanding functional islets for therapeutic goals. We

also showed that conditional Axin expression impaired proliferation of neonatal ß-cells,

demonstrating a requirement for Wnt signaling during ß-cell expansion in vivo.

Consistent with our findings, a prior study (11) reported comparable ß–cell hypoplasia

following conditional inactivation of ß-catenin, but no mechanism for reduced islet cell

proliferation was described, nor was impaired glucose control detected in that study.

Here, we showed that Axin expression impaired normal expression of islet Pitx2 and

cyclinD2. Together with in vitro studies of Wnt-stimulated islets, our results collectively

suggest that Wnt signaling is required for ß-cell Pitx2 and Cyclin D2 expression to

promote *in vivo* ß–cell growth. Mutations in *Pitx2* are associated with Rieger syndrome in

humans, an autosomal dominant condition that includes impaired glucose tolerance,

reduced circulating insulin levels, and overt diabetes mellitus (38). The basis for these

metabolic anomalies is not known. Mice with targeted mutations in *Pitx2* have been previously described, and manifest exhibit numerous developmental malformations (7, 39-42), but pancreatic islet defects have not yet been described, to our knowledge. Thus, further studies are needed to show if Pitx2 is sufficient or required for pancreatic ß-cell proliferation. Another study (14) provided evidence that the timing or extent of Wnt pathway modulation can significantly alter the outcome of mouse embryonic and peri-natal pancreas development. Thus, the range of non-endocrine and endocrine pancreatic phenotypes reported by us and others (11-14) likely reflects the distinct experimental strategies and transgenic strains used to disrupt in vivo pancreatic Wnt signaling in these studies.

Proliferation of post-natal islet cells is relatively low compared to tissues like intestines or bone marrow, except in states favoring robust ß-cell growth such as pregnancy, insulin resistance, and obesity (3). Could Wnt signaling regulate adult ß-cell growth? Fujino et al. (43) reported that older mice lacking LRP5, a Wnt co-receptor, had impaired ß-cell function and impaired glucose tolerance when challenged with a high-fat diet (43). This finding suggests that Wnt signaling may be required to maintain islet functions in physiologic conditions demanding adaptive ß-cell responses. Multiple Wnt ligands, receptors, and signal transduction factors are expressed in the embryonic and adult pancreas (12, 13, 33) and it is unclear which endogenous factors might mediate Wnt signaling in ß-cell proliferation. Further studies to clarify these issues may prove useful for generating methods to control pancreatic islet cell proliferation, and to test if Wnt signaling dysregulation might underlie some forms of neuroendocrine tumor pathogenesis.

ACKNOWLEDGEMENTS

REFERENCES

1. Butler AE, Janson J, Bonner-Weir S, Ritzel R, Rizza RA, Butler PC (2003) *Diabetes* 52:102-110.

2. Ryan EA, Paty BW, Senior PA, Bigam D, Alfadhli E, Kneteman NM, Lakey JR, Shapiro AM (2005) *Diabetes* 54:2060-2069.

3. Heit JJ, Karnik SK, Kim SK (2006) *Annu Rev Cell Dev Biol* 22:311-338.

4. Cozar-Castellano I, Fiaschi-Taesch N, Bigatel TA, Takane KK, Garcia-Ocana A, Vasavada R, Stewart AF (2006) *Endocr Rev* 27:356-370.

5. Logan CY, Nusse R (2004) *Annu Rev Cell Dev Biol* 20:781-810.

6. Baek SH, Kioussi C, Briata P, Wang D, Nguyen HD, Ohgi KA, Glass CK, Wynshaw-Boris A, Rose DW, Rosenfeld MG (2003) *Proc Natl Acad Sci U SA* 100:3245-3250.

7. Kioussi C, et al. (2002) *Cell* 111:673-685.

8. Ikeda S, Kishida S, Yamamoto H, Murai H, Koyama S, Kikuchi A (1998) *EMBO J* 17:1371-1384.

9. Itoh K, Krupnik VE, Sokol, SY (1998) *Curr Biol* 8:591-594.

10. Sakanaka C, Weiss JB, Williams, LT (1998) *Proc Natl Acad Sci USA* 95:3020-3023.

11. Dessimoz J, Bonnard C, Huelsken J, Grapin-Botton, A (2005) *Curr Biol* 15:1677-1683.

12. Murtaugh LC, Law AC, Dor Y, Melton DA (2005) *Development* 132:4663-4674.

13. Papadopoulou S, Edlund H (2005) *Diabetes* 54:2844-2851.

14. Heiser PW, Lau J, Taketo MM, Herrera PL, Hebrok M (2006) *Development* 133:2023-2032.

15. Heller RS, Dichmann DS, Jensen J, Miller C, Wong G, Madsen OD, Serup P (2002) *Dev Dyn* 225:260-270.

16. Willert K, Brown JD, Danenberg E, Duncan AW, Weissman IL, Reya T, Yates JR, Nusse R (2003) *Nature* 423:448-452.

17. Sander M, Sussel L, Conners J, Scheel D, Kalamaras J, Dela Cruz F, Schwitzgebel V, Hayes-Jordan A, German, M (2000) *Development* 127:5533-5540.

18. Miyazaki J, Araki K, Yamato E, Ikegami H, Asano T, Shibasaki Y, Oka Y, Yamamura K (1990) *Endocrinology* 127:126-132.

19. Karnik SK, Hughes CM, Gu X, Rozenblatt-Rosen O, McLean GW, Xiong Y, Meyerson M, Kim SK (2005) *Proc Natl Acad Sci U S A* 102:14659-14664.

20. Rane SG, Dubus P, Mettus RV, Galbreath EJ, Boden G, Reddy EP, Barbacid, M (1999) *Nat Genet* 22:44-52.

21. Georgia S, Bhushan A (2004) *J Clin Invest* 114:963-968.

22. Kushner JA, Ciemerych MA, Sicinska E, Wartschow LM, Teta M, Long SY, Sicinski P, White MF (2005) *Mol Cell Biol* 25:3752-3762.

23. Pelengaris S, Khan M, Evan GI (2002) *Cell* 109:321-334.

24. Herrera PL *Development* (2000) 127:2317-2322.

25. Heit JJ, Apelqvist ÅA, Gu X, Winslow MM, Neilson JR, Crabtree GR, Kim SK (2006) *Nature* 443: 345-349.

26. Harada N, Tamai Y, Ishikawa T, Sauer B, Takaku K, Oshima M, Taketo MM (1999) *EMBO J* 18:5931-5942.

27. Hsu W, Shakya R, Costantini F (2001) *J Cell Biol* 155:1055-1064.

28. Holland AM, Hale MA, Kagami H, Hammer RE, MacDonald RJ (2002) *Proc Natl Acad Sci USA* 99:12236-12241.

29. Smart NG, Apelqvist ÅA, Gu X, Harmon EB, Topper NJ, MacDonald RJ, Kim, SK (2006) *PLoS Biology* 4: e39

30. Gu G, Dubauskaite J, Melton DA (2002) *Development* 129:2447-2457.

31. Jonsson J, Carlsson L, Edlund T, Edlund H (1994) *Nature* 371:606-609.

32. Offield MF, Jetton TL, Labosky PA, Ray M, Stein RW, Magnuson MA, Hogan BL, Wright CV (1996) *Development* 122:983-995.

33. Heller RS, Klein T, Ling Z, Heimberg H, Katoh M, Madsen OD, Serup P (2003) Gene Expr. 11:141-147.

34. Pedersen AH, Heller RS (2005) *Biochem Biophys Res Commun* 333:961-968.

35. Laybutt DR, Weir GC, Kaneto H, Lebet J, Palmiter RD, Sharma A, Bonner-Weir S (2002) *Diabetes* 51:1793-1804.

36. Briata P, Ilengo C, Corte G, Moroni C, Rosenfeld MG, Chen CY, Gherzi R (2003) *Mol Cell* 12:1201-1211.

37. Hardikar AA, Marcus-Samuels B, Geras-Raaka E, Raaka BM, Gershengorn MC (2003) *Proc Natl Acad Sci USA* 100:7117-7122.

38. Aarskog D, Ose L, Pande H, Eide N (1983) *Am J Med Genet* 15:29-38.

39. Gage PJ, Suh H, Camper SA (1999) *Development* 126:4643-4651.

40. Kitamura K, Miura H, Miyagawa-Tomita S, Yanazawa M, Katoh-Fukui Y, Suzuki R, Ohuchi H, Suehiro A, Motegi Y, Nakahara Y, Kondo S, Yokoyama M (1999) *Development* 126:5749-5758.

41. Lin CR, Kioussi C, O'Connell S, Briata P, Szeto D, Liu F, Izpisua-Belmonte JC, Rosenfeld MG (1999) *Nature* 401:279-282.

42. Liu C, Liu W, Lu MF, Brown NA, Martin JF (2001) *Development* 128:2039-2048.

43. Fujino T, et al. (2003) *Proc Natl Acad Sci USA* 100:229-234.

44. Harmon EB, Apelqvist AA, Smart NG, Gu X, Osborne DH, Kim SK (2004) *Development* 131:6163-6174.

45. Kim SK, Hebrok M, Li E, Oh SP, Schrewe H, Harmon EB, Lee JS, Melton DA (2000) *Genes Dev* 14:1866-1871.

46. Bruning JC, Winnay J, Bonner-Weir S, Taylor SI, Accili D, Kahn CR (1997) *Cell* 88:561-572.

47. Ahlgren U, Jonsson J, Edlund H (1996) *Development* 122:1409-1416.

48. Chen H, Carlson EC, Pellet L, Moritz JT, Epstein PN (2001) *Diabetes* 50:2040-2046.

FIGURE LEGENDS

Figure 1. Purified Wnt3a induces expression of *Pitx2*, *cyclin D2* and other cell cycle regulators in β cells and promotes cell expansion. (**A**) Expression of Ki67 in Nkx6.1₊ cells of purified WT P4 islets stimulated with Wnt3a, vehicle or Wnt3a + Fz8-CRD. (**B**) Growth of MIN6 cells stimulated with vehicle only, Wnt3a, or Wnt3a + Fz8-CRD and counted at 24, 48, and 72 hours. Each condition was performed in triplicate. (**C**) MIN6 cells stimulated with Wnt3a or vehicle were assayed for BrdU incorporation by immunofluorescence analysis. Results are shown as the percentage of BrdU₊ cells out of all DAPI₊ cells. (**D**) Real-time RT-PCR analysis of *Pitx2*, *cyclin D2*, *cyclin D1*, and *cdk4* cDNA from purified P8 islets treated with vehicle only, purified Wnt3a, or Wnt3a + Fz8-CRD. (**E**) Real-time RT-PCR analysis of *Pitx2*, *cyclin D2*, *cyclin D1*, and *cdk4* cDNA from MIN6 cells treated with vehicle only, purified Wnt3a, or Wnt3a + Fz8-CRD. (A-C) Presented as the average ± s.e.m.. All RT-PCR results were normalized to b-actin and are the average value from triplicate experiments. P values are indicated in the panels.

Figure 2. Chromatin immunoprecipitation (ChIP) demonstrates that Pitx2 associates with specific elements in the *cyclin D2* promoter upon Wnt3a stimulation. (**A**) Position of DNA regions flanked by primer pairs (PP) used for PCR to assess Pitx2 association with elements within the *cyclin D2* promoter. Consensus bicoid binding sequences at the directed positions are marked (red boxes) (**B**) Anti-ChIP performed on 8 hour-Wnt3a-stimulated islet cultures derived from WT P8 mice reveals Pitx2 binding to the *cyclin D2* promoter at sites –908 to –525 upstream of the transcriptional start site. (**C**) Anti-Pitx2 ChIP performed on MIN6 cells treated with Wnt3a for 3 hrs and subsequently analyzed using PCR shows a similar binding pattern to the *cyclin D2* promoter.

Figure 3. Conditional expression of activated ß-catenin in RIP-Cre, ß-cat*active* islets. (**A, B**). Elevated ß-catenin expression and increased number of proliferating Ki67+ cells in RIP-Cre, ßcat*active* islets compared to controls (**C**) Quantification of insulin+, Ki67+ cells in control and RIPCre, ß-cat*active* islets. (**D-E**) Immunostaining reveals insulin expression is maintained in proliferating Ki67+ cells in RIP-Cre, ß-cat*active* islets. (**F**) Quantification of pancreatic ß-cell mass in control and RIP-Cre, ß-cat*active* mice. (**G-H**) Immunostaining reveals increased numbers of cyclin D2-expressing insulin+ cells in RIP-Cre, ß-cat*active* islets. (**I**) Real-time PCR quantification of *cyclin D2* mRNA levels in isolated control and RIP-Cre, ß-cat*active* islets. All data is statistically significant $P < 0.005$. (**J**) Serum insulin levels in fed control and RIP-Cre, ß-cat*active* mice. (**K**) Assessment of insulin secretion in response to increased glucose as performed on cultured islets. *P* values were not significant (NS). (**L**) Intraperitoneal glucose tolerance tests of control and RIP-Cre, ß-cat*active* mice after overnight fasting. In panels J-L, values represent mean ± S.E.M. *P* values are indicated where appropriate.

Figure 4. Dox-dependent expression of Axin, Pitx2 and Cyclin D2 in *Pdx1-tTA*/TRE-Axin islets. Immunohistochemical detection of Myc-tagged Axin expression in islets from (**A**) *Pdx1*-tTA/TRE-Axin P4 mice express Myc-tagged Axin (arrows), which is absent in (**B**) WT and (**C**) *Pdx1*-tTA/TRE-Axin (+ Doxycycline) control mice at P4. Original magnification 63x. Immunofluroescent detection of Nkx6.1 (green), Pitx2 (red), and merge (yellow) in the islets of P4 WT and *Pdx1*-tTA/TRE-Axin mice and *Pdx1*-tTA/TRE-Axin mice on Doxycycline from the time of conception (**D-I**). White arrowheads indicate Nkx6.1+/Pitx2+ nuclei (**H,I**). Percentage of Nkx6.1+ that are Pitx2+ in *Pdx1*-tTA/TRE-Axin and control mice (**J**). Immunofluorescent detection of Nkx6.1

(green) and Cyclin D2 (red) in the islets of P4 WT and *Pdx1*-tTA/TRE-Axin mice and

Pdx1-tTA/TRE-Axin mice on Doxycycle (**K-S**). Percentage of Nkx6.1+ that are Cyclin

D2+ in *Pdx1*-tTA/TRE-Axin and control mice (**T**). Data are presented as the average ±

S.E.M. *P* values are indicated in the figures. Data are from at least 5 mice per genotype.

Original magnification 100X.

Figure 5. Conditional Axin expression in Pdx1+ progenitors impairs b **cell**

development.

Immunofluorescent detection of insulin+ (green) and glucagon+ (red) cells in (**A**) WT and

(**B**) *Pdx1*-tTA/TRE-Axin islets (no Doxycycle), and in (**C**) WT and (**D**) *Pdx1*-

tTA/TRE-Axin islets administered Doxycyline from the time of conception. The relative

(**E**) insulin+ area and (**F**) glucagon area per islet compared in WT and *Pdx1*-tTA/TRE-

Axin mice, and in WT and *Pdx1*-tTA/TRE-Axin mice administered Doxycycline from

the time of conception. (E) The P value for insulin+ area between *Pdx1*-tTA/TRE-Axin

islets and control islets is !0.02. (F) The P value for glucagon+ area among all genotypes

in not significant (NS). (**G**) Morphometric analysis of insulin+ area as a percentage of

total pancreas area from P28 WT and *Pdx1*-tTA/TRE-Axin mice. (**H**) Total insulin

(ng)/pancreas (mg) in P28 *Pdx1*-tTA/TRE-Axin and WT mice. All data are from at least

3 litters, with 4-8 mice per genotype. Data are presented as the average ± s.e.m.. (A-D)

Original magnification 100X.

FIGURE LEGENDS, SUPPLEMENTARY INFORMATION (SI)

SI Figure 1. Co-expression of Nkx6.1 and Ki67 in nuclei of islet ß-cells following

indicated exposures to vehicle, purified Wnt3a or Wnt3a + Fz8-CRD. Co-localization of

Nkx6.1 (green) and Ki67 (blue) is indicated in nuclei by white arrowheads and the merged color (teal).

SI Figure 2. RT-PCR quantification of mRNA levels for *Pitx2* and *CyclinD2* in human islets

cultured with the indicated factors.

SI Figure 3. (A-B) Localization of ß-catenin in islets from control (A) and RIP-Cre cat$_{active}$ (B) mice by immunohistochemistry. ß-catenin (green), DAPI (blue) and insulin (red) were detected by immunofluorescence microscopy. White arrowheads in panel B highlight nuclei with prominent nuclear ß-catenin signal. **(C-F)** Pancreatic insulin levels and insulin secretion of islets from RIP-Cre β-cat$_{active}$ and control mice. Insulin levels were calculated on a per islet basis (**C**) as well as per islet DNA content (**D**) to normalize cell number between islets. Assessment of insulin secretion in response to step increase of arginine (**E**) or KCl (**F**) at the indicated concentrations.

Suppl. Figure 4. Western immunoblot to detect Myc-labelled Axin (black arrowhead) in islet protein isolated from mice of the indicated genotypes (**A**). Immunofluorescent detection of BrdU incorporation in Nkx6.1$_+$ cells in WT (**B**) and *Pdx1*-tTA/TRE-Axin (**C**) E16.5 embryos. The relative number Nkx6.1$_+$ (**D**), and Nkx6.1$_+$BrdU$_+$ (**E**) cell nuclei per pancreas in E16.5 WT and *Pdx1*-tTA/TRE-Axin embryos or in *Pdx1*-tTA/TRE-Axin embryos on Doxycycline from the time of conception. Data are presented as the average ± s.e.m.. P values are indicated in the figures. Data are from at least 5 mice per genotype. Original magnification 100x.

SI Figure 5. Intraperitoneal glucose challenge of P28 mice after a 16 hour overnight fast: Black line, open circle: *Pdx1*-tTA/TRE-Axin mice; Red line, Pdx1-tTA littermates; Blue

line, TRE-Axin littermates; Black line, closed circle, WT mice. Indicated P values are for

data from *Pdx1*-tTA/TRE-Axin and *Pdx1*-tTA mice. All data are from at least 3 litters,

with 4-8 mice per genotype. Data are presented as the average ± s.e.m.

SUPPORTING MATERIALS AND METHODS

Immunohistochemistry

All tissue was fixed in 4% paraformaldehyde (Electron Microscopy Sciences).

Immunohistochemistry was performed using paraffin-embedded tissue and

immunofluorescence studies were performed on either paraffin- or cryo-preserved tissue,

depending on antibody requirements. Antigen retrieval (Vector Laboratories) was used

on all tissue and horse or goat serum (Invitrogen) was used for antibody blocking.

Primary antibodies included: human (mouse) anti-c-Myc AB-1 (1:40, Calbiochem),

chicken anti-mouse insulin (1:500, Chemicon International), guinea pig antimouse

glucagon (1:200, Linco Research, Inc.), rabbit anti-mouse Nkx6.1 (1:200, S. K. Kim

Laboratory), rabbit anti-mouse CyclinD2 M-20 (1:100, Santa Cruz Biotechnology, Inc.),

goat antimouse Pitx2 C-16, (1:50, Santa Cruz Biotechnology, Inc.), mouse-b-catenin

(1:100, BD Transduction Labs) and mouse anti-Ki67 (1:100, Novocastra, Newcastle,

United Kingdom). Guinea pig anti-mouse Nkx6.1 (1:1000) was a generous gift from M.

Sander (U.C. Irvine, CA). Alexa-Fluor antibodies 488 (1:200), 555 (1:500), and 633

(1:200) (Molecular Probes) were used for immunohistology studies. Immunoperoxidase

detection for c-Myc was performed using biotin (1:200) and Vectastain Elite ABC,

Avidin/Biotin Blocking, and DAB kits (Vector Laboratories). Mouse-anti-BrdU

(Amersham Biosciences) was used according to the manufacturer's protocol. Images

were captured using a Leica SP2 AOBS confocal microscope (provided by the Cell

Sciences Imaging Facility, Stanford University Medical Center). Light images were captured using a Zeiss Axioplan 2 microscope and Zeiss Axiovision software. Cell counting, point-counting morphometry, and b-cell quantification were performed using standard morphometric techniques (44, 45) unless otherwise noted. For counting of insulin+ or glucagon+ cells in P4 and P28 mice, cell number was quantified based on antibody+ staining per islet. The area of insulin+ or glucagon+ cells was determined using Volocity (Improvision) software analysis and reported as relative area. At least 30 islets per pancreas were counted and at least 4 mice were examined per genotype. For P28 pancreas analysis, total pancreatic tissue area was also quantified using Volocity software, permitting comparison of the ratio of insulin+ cells per total pancreas area. For this analysis, whole pancreata were serially sectioned to generate 7 micron-thick tissue sections and 25 representative sections per pancreas were used. At least 4 mice were examined per genotype. For quantification of cells expressing Nkx6.1, Pitx2, Cyclin D2, or BrdU cells were point-counted; pancreas tissue was obtained from at least 4 mice per genotype. All data are presented as the average ± s.e.m.. Twotailed T tests were conducted to determine statistical significance.

BrdU incorporation studies

For BrdU studies in neonatal mice, 0.2ml of BrdU, prepared at 1.25mg/ml, was injected I.P. 2 hours before harvest. Pancreas tissue was isolated and prepared as described above.

Glucose tolerance tests, islet and insulin analysis

Mice were fasted for 14-16 hours, and baseline blood glucose levels (dL/ml) were measured from tail-vein blood. Mice were challenged with 2mg/kg glucose and glucose tolerance tests were conducted as previously described (45, 46). Pancreas tissue from

mice was collected and homogenized in acid alcohol (47) and normalized to pancreas weight. Insulin content was determined using the Mercodia Ultrasensitive Mouse Insulin ELISA kit (Alpco Diagnostics). Human islets were procured from NDRI (National Disease Research Interchange) with 90% islet purity, and 85% viability. Human islets were cultured on 48 well-plate with 200 islets per well in CMRL-1066 medium (modified for islet cell culture from Cellgro/Mediatech, Herndorn, VA) supplemented with 10% FBS, L-glutamine 2mM, Penicillin(100units/ml)-streptomycin(100ug/ml), HEPES(1mM), Fongizone (0.25ug/ml). Islet insulin secretion, insulin levels and DNA levels were measured as previously described (48). Briefly, in a microplate, five islets were handpicked into each well with modified Krebs-Ringer bicarbonate buffer (KRBB) containing 3 mM glucose. After washes, islets were incubated consecutively in indicated low and high levels of glucose or arginine KRBB for 1 hour. Islet total insulin was extracted with acid ethanol. Insulin level was measured with a mouse insulin enzymelinked immunosorbent assay kit (ALPCO Diagnostics, Windham, NH). Islet DNA was quantified with picogreen (Molecular Probes).

In vitro MIN6 cell and islet proliferation assays

MIN6 cells were plated onto 10cm dishes (1×10^6 cells/dish) for cell counting or onto chamber slides (Lab-Tek; 10,000 cells/well) for BrdU analysis, rested in MIN6 media (High-glucose DMEMGlutamax, Pennicilin/Streptomycin, HEPES (Invtirogen-GIBCO) and 15% fetal calf serum (Hyclone) overnight, and then pulsed with Wnt3a (final concentration 100ng/ml which is equal to 2.4 nM), vehicle only, or Wnt3a plus Fz8-CRD (final concentration 200ng/ml which is equal to 3.3 nM), for 8 hours. Isolated pancreatic islets were exposed to the same concentrations of Wnt or Fz8-CRD. Cells were collected

at 24, 48, and 72 hours for counting assays; each condition was performed in triplicate. For the BrdU incorporation assay, MIN6 cells or islets were pulsed with BrdU (final concentration of 0.6mg/ml) at 6 hours post-stimulation and collected fixed with 4% PFA at 8 hours. Cells were stained with anti-BrdU (as described above). For cell analysis, >15,000 cells per condition were counted based on DAPI incorporation. The percentage of BrdU+ spots per total number of DAPI+ spots per image was determined using Volocity software. Results are the average of 10 images per experimental condition and described in terms of arbitrary area units.

Chromatin immunoprecipitation assay

ChIP assays were performed on pancreatic islets and MIN6 cells using a kit from Upstate Biotech. Briefly, DNA was crosslinked to protein with formaldehyde. Cellular lysates were obtained by scraping followed by pulsed ultrasonication to shear cellular DNA. We performed overnight immunoprecipitations with an anti-Pitx2 antibody (10mg/IP Santa Cruz Biotechnology). On the next day the crosslinks were reversed, and bound DNA was purified by phenol:chloroform extraction. We performed PCR using primers specific for cyclin D1, cyclin D2, and cdk4 proximal promoter sequences. Primer sequences are listed below:

Cyclin D2-1F: CACACCGTGAAACATTACAG

Cyclin D2-1R: CAGTTGGTTTGGTTTTGTTT

Cyclin D2-2F: TCTCTCTCAAACTTCCCAAA

Cyclin D2-2R: CACGTGGATGATATTCCTTT

Cyclin D2-3F: ATGAGTATCTGCCTTGGGTA

Cyclin D2-3R: AGGTTTTCTTTCCTCCTCTG

Cyclin D2-4F: ATGTCCAAAGGAGAAAAACA

Cyclin D2-4R: CCATTCCATTAGAAAAGCAC

Cyclin D1-1F:CCAAGAAAAATAAACCGTTG

Cyclin D1-1R: GAATAGTTCGCCTAGCTTGA

Cyclin D1-2F: GGTGGCCATTATTTCATCTA

Cyclin D1-2R: GAATAGTTCGCCTAGCTTGA

Cdk4-1F:ACCCTGTCATCTGTTTATGC

Cdk4-1R: AGGTGTTAGTGGGAGATCCT

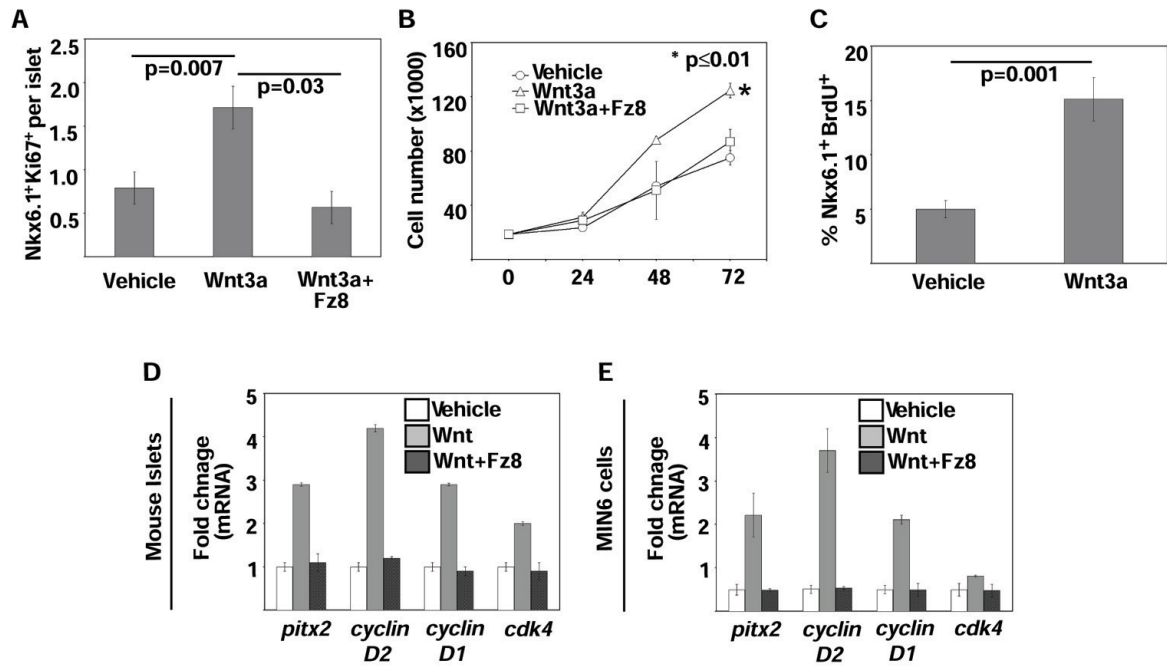Cdk4-2F:AAACAAAAACATCGCATACC, Cdk4-2R:
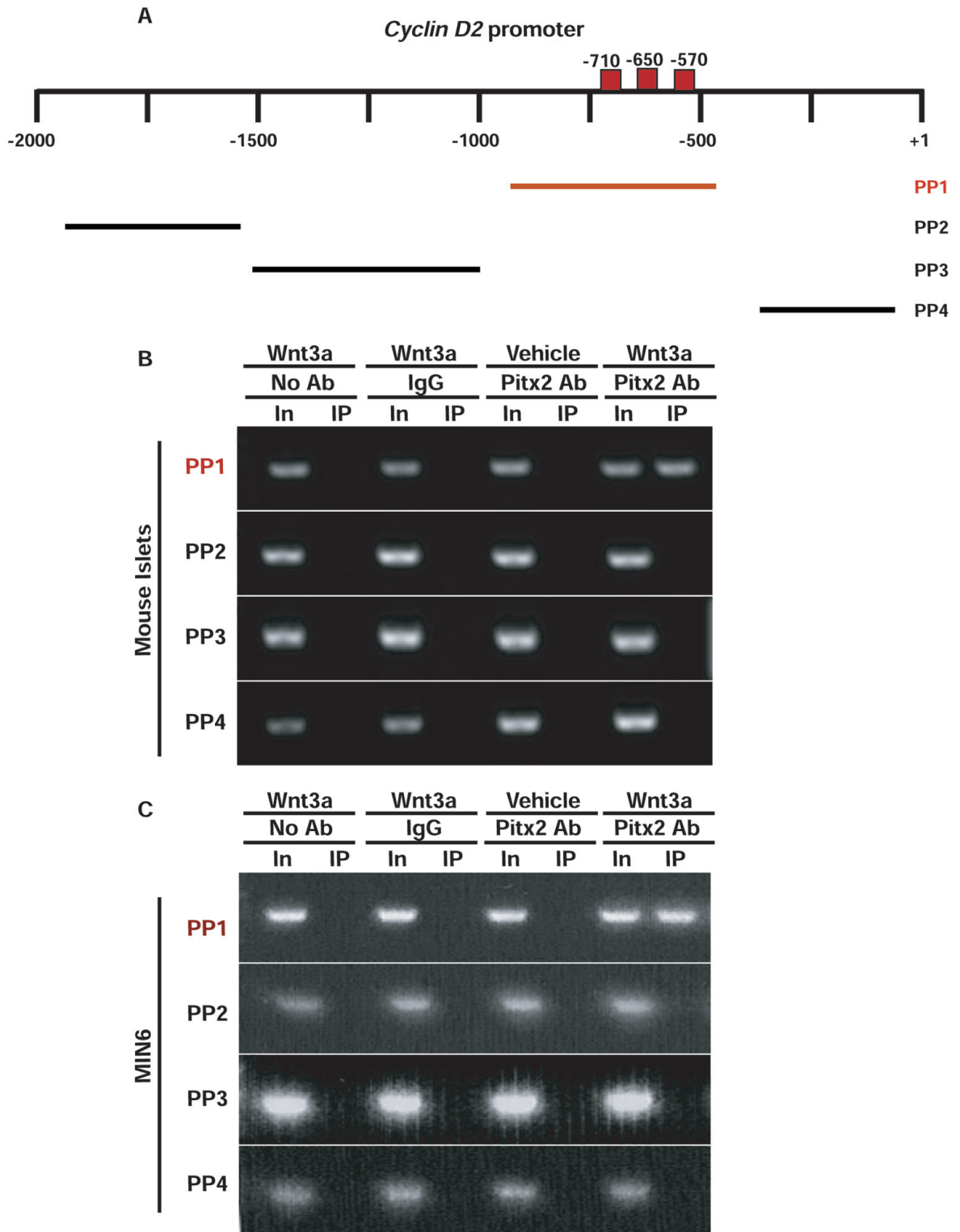
GTTCTGGACACGTGATCTTC.

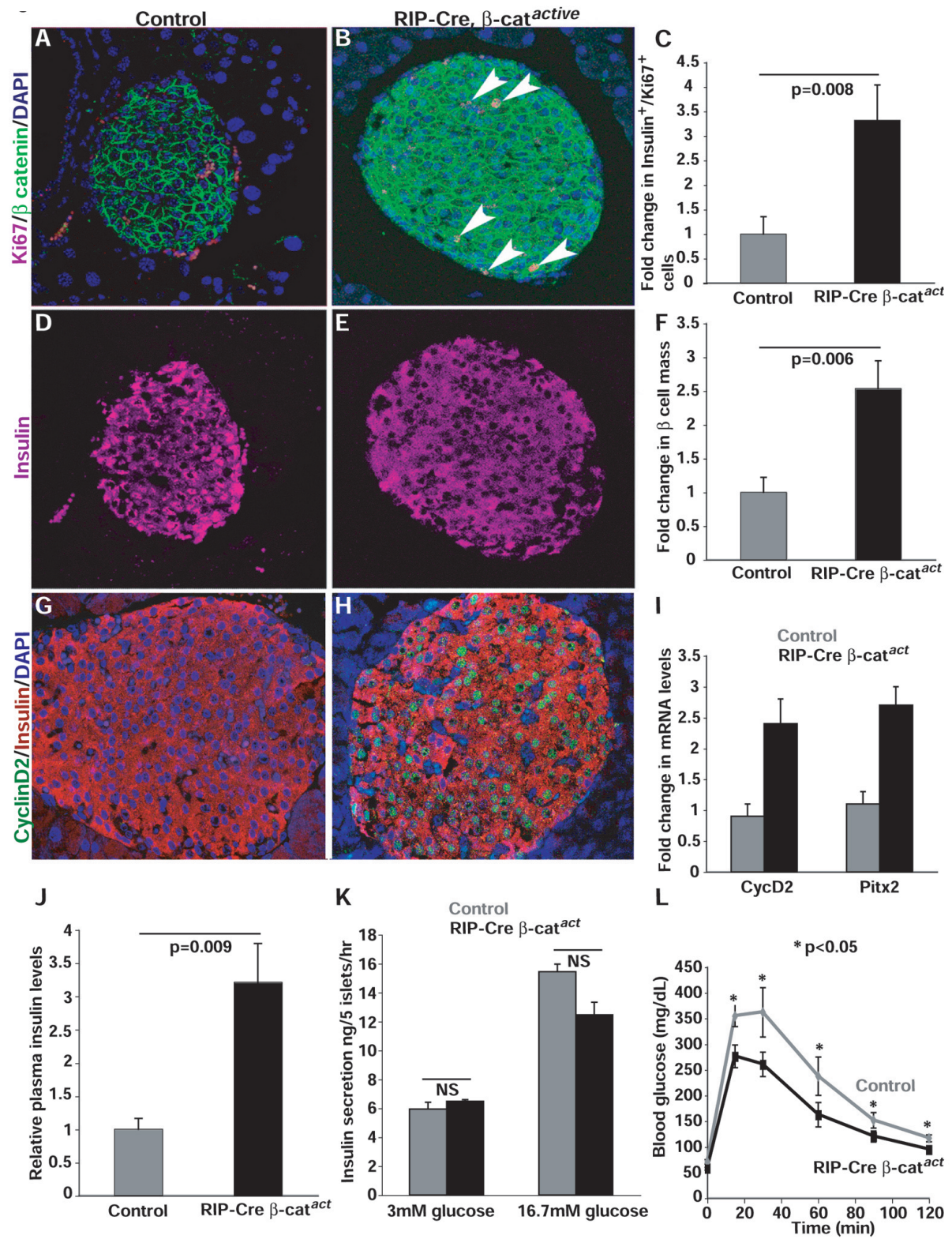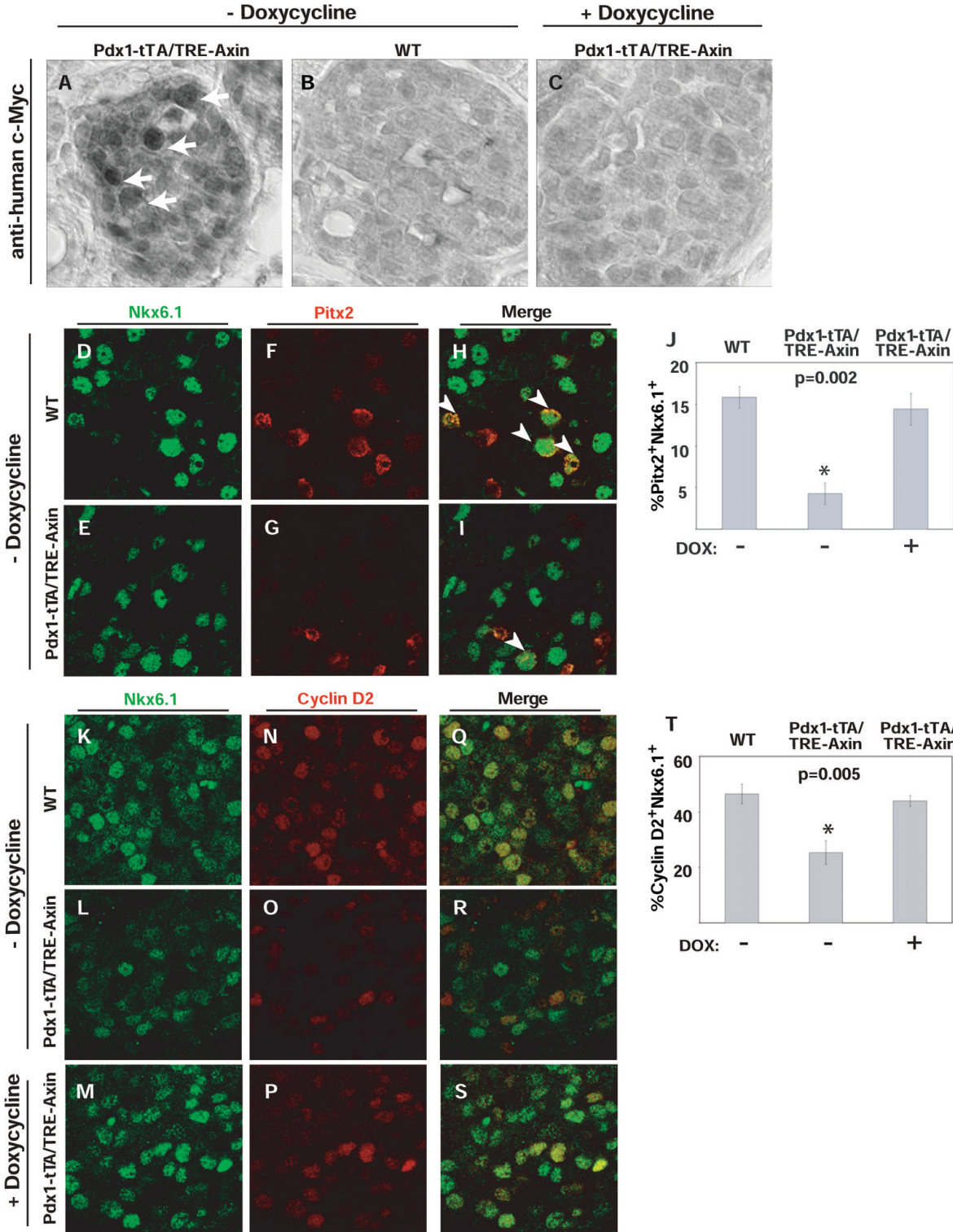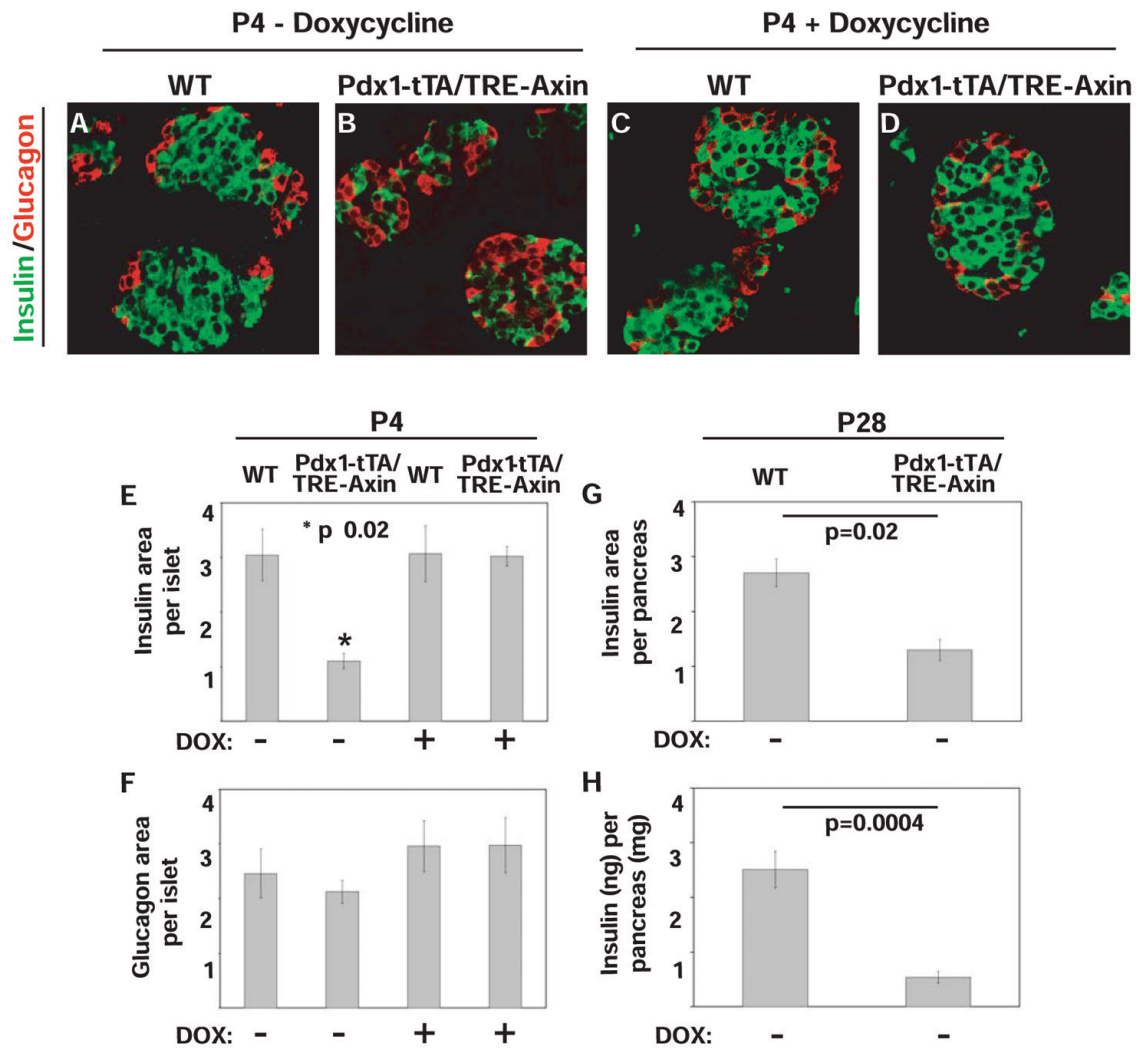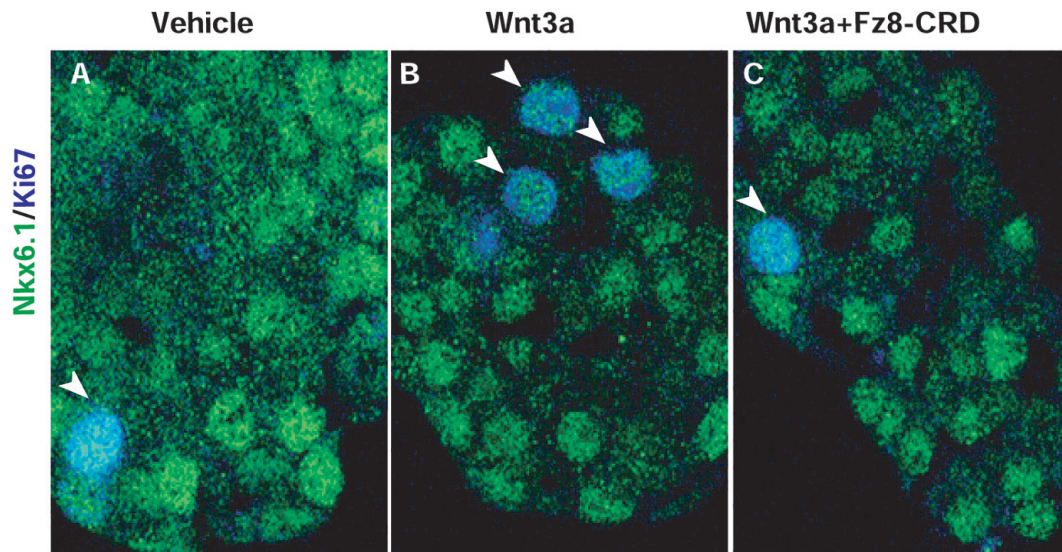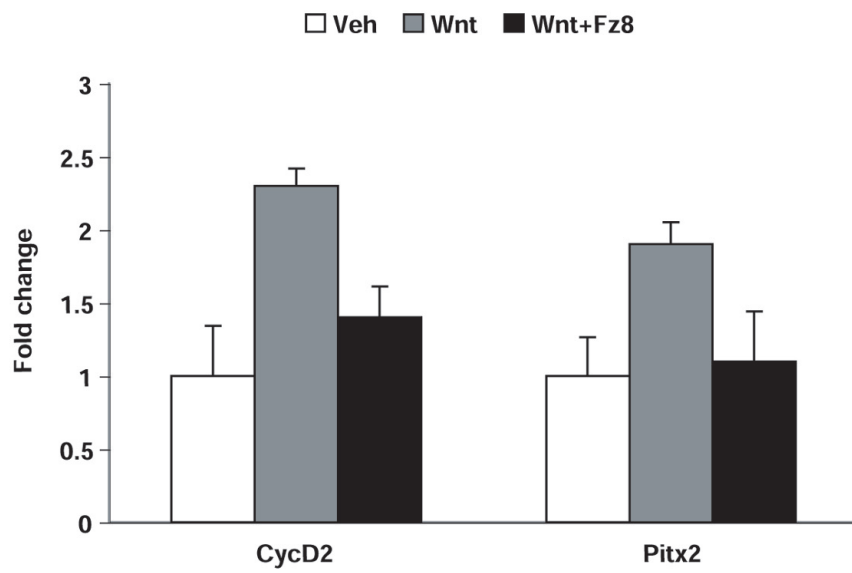Figure 1

Figure 2

Figure 3

Figure 4

Figure 5

Supplemental Figure 1

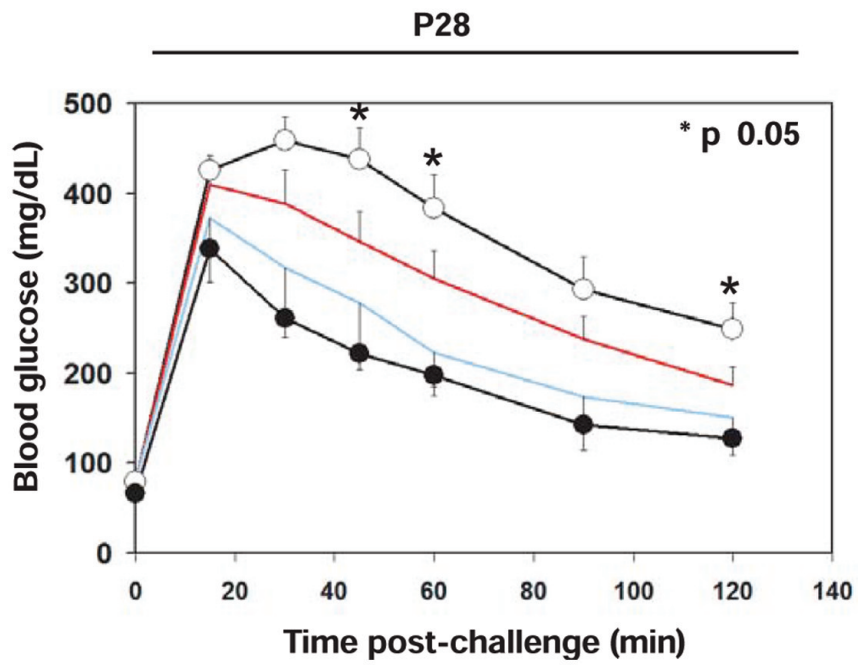Supplemental Figure 2

Supplemental Figure 3

Control

RIP-Cre, β-cat^active

β-catenin/Insulin/DAPI
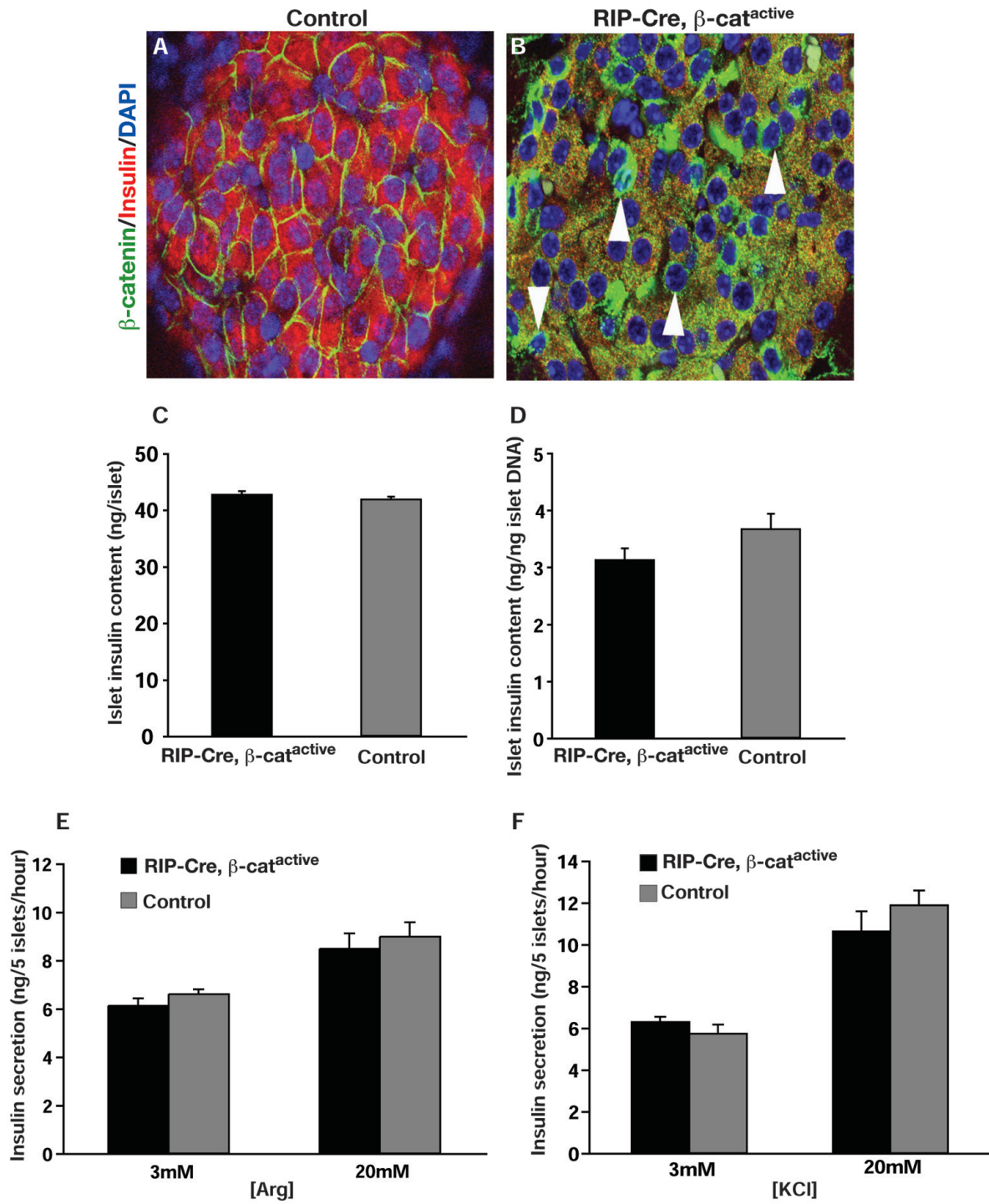
Supplemental Figure 4
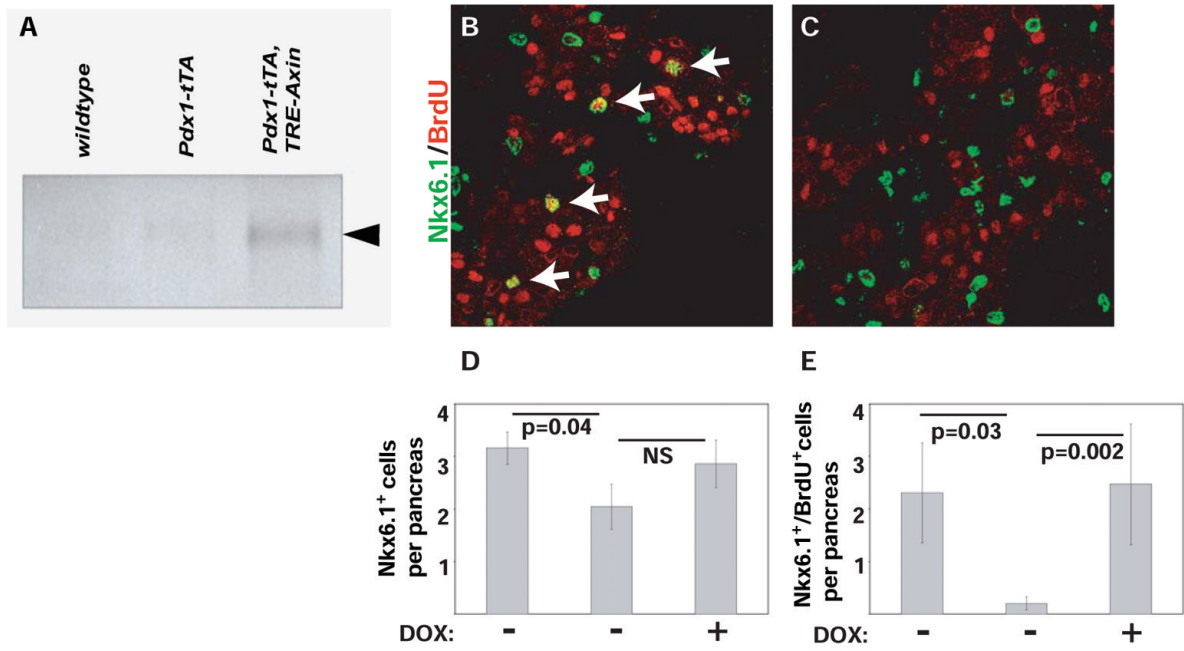
Supplemental Figure 5

P28

* p 0.05

Chapter 4

Stabilization of β-catenin induces pancreas tumor formation

Abstract

Recent studies have shown that β-catenin signaling within the canonical Wnt pathway plays a critical role during pancreas development. However, the pathway is normally down-regulated in the adult organ. Here, we report that constitutive stabilization of β-catenin using Cre/loxP technology to remove the third exon of the β-catenin gene results in the formation of large pancreatic tumors at a high frequency in adult mice. These tumors closely resemble human solid pseudopapillary pancreatic tumors (SPT), a rare neoplasm with low malignant potential. Moreover, immunohistochemical evidence of β-catenin dysregulation has been found in a cohort of human SPT samples. Taken together, these findings suggest that aberrant β-catenin signaling may contribute to the formation of human SPT.

Rationale

In Chapter 2 of this thesis, we demonstrated that constitutive activation of β-catenin increases pancreatic acinar cell proliferation in PdxCre^{late} β-cat^{active} mice, resulting in gross enlargement of the pancreas(Heiser et al., 2006). Despite this enhanced proliferative rate, these mice do not develop lesions and gross pancreas morphology is not distorted. However, Cre-recombinase is not expressed within the ductal compartment of PdxCre^{late} mice, a niche that has long been suspected to harbor stem cells capable of pancreatic regeneration or tumorigenesis. While the PdxCre^{early} mouse strain does target the ductal compartment, its early and robust expression during development results in near complete ablation of the pancreas and neonatal lethality in β-cat^{active} mice. As a result, analysis of the adult pancreas is not possible in these mice.

Moreover, several groups have reported evidence of increased β-catenin signaling pathway activity in human SPT based upon strong nuclear accumulation of β-catenin within the nucleus (Min Kim et al., 2006; Nishimori et al., 2006). In addition, activating mutations in the third exon of β-catenin have been found in some human SPT's (Min Kim et al., 2006). However, it was unclear whether these mutations were the proximate cause of the SPT lesions.

Therefore we crossed the *β-cat^active* mice into the *p48 Cre* strain which was previously shown to target all three pancreatic cell lineages: islet, acinar, and duct (Kawaguchi et al., 2002).

Materials and Methods

Mice

Noon of the day when vaginal plugs are detected is treated as e0.5 day post coitum. Mice carrying the floxed exon 3 allele of β-catenin (*β-cat^active*)(Harada et al., 1999) were crossed with strains expressing Cre-recombinase under the control of the *p48* promoter (Kawaguchi et al., 2002) and maintained in a mixed background. In all experiments presented in this work, the floxed exon 3 allele of β-catenin was maintained as a heterozygote to insure that the level of β-catenin signaling pathway activation was consistent. Thus, the *β-cat^active* nomenclature used refers to mice containing one wild type and one floxed exon 3 allele of β-catenin. To verify the expression pattern of Cre-recombinase, a *Z/AP* reporter line was used (Lobe et al., 1999).

Tissue preparation, immunohistochemistry, and microscopy

Embryonic tissues were fixed and paraffin wax imbedded as previously described(Kawahira et al., 2003). Hematoxylin/eosin staining, immunohistochemical and

immunofluorescence analysis were performed as previously described (Kim et al., 1997b).

The following primary antibodies were used at the indicated dilution: guinea pig insulin, diluted 1:400 (Linco, 4011-01), rabbit glucagon, 1:400 (Linco; 4030-01f) , mouse placental alkaline phosphatase, diluted 1:200 (Sigma), mouse E-cadherin 1:100 (BD; 610181), mouse β-catenin, 1:100 (BD; 610154), rabbit Pdx-1 1:1,000 (kindly provided by Dr. Michael German), FITC-conjugated DBA Lectin 1:1,000 (Sigma).

The following secondary antibodies were used for immunofluorescence: anti rabbit Alexa 555; 1:200 (Molecular Probes; A-21428), anti rabbit Alexa 488 1:200 (Molecular Probes; A -11034), anti guinea pig Cy3, 1:200 (Jackson; 706-165-148), anti guinea pig alexa 633, 1:200 (Molecular Probes A-21105), anti mouse Alexa 488, 1:200 (Molecular Probes; A-11029). For immunohistochemistry, a biotinylated anti-goat (Vector; BA-9500) was used at a dilution of 1:200. Staining for diaminobenzidine (DAB) was performed with the ABC Elite immuoperoxidase system (Vector).

Immunofluorescently stained slides were mounted with Vectashield hard mount media containing the nuclear stain, DAPI (Vector). Immunohistochemically stained slides were mounted with Permount reagent. Bright field images were acquired using a Zeiss Axio Imager D1 scope; fluorescent images were captured using a Leica DMIRE2 SP2 confocal microscope.

Morphometric quantification of Pdx1$^+$ cell number

For e12.5, the whole pancreas was sectioned and aliquoted as described previously(Kawahira et al., 2003) in order to obtain representative results. In order to quantitate the number of Pdx1+ cells present in 7 control, 5 *PdxCre^{early} β-cat^{active}*, and 5

p48Cre β-cat^{active} intact e12.5 embryos were paraffin imbedded, cut into 6μm sagittal

sections, and aliquotted onto slides. Following immunofluorescence staining for E-

cadherin (to mark the epithelium) and Pdx1, the number of Pdx1+ cells within the

pancreatic epithelium was counted on 1 section every 96μm until the entire pancreatic

bud was evaluated.

Results and Discussion

Cell autonomous inhibition of Pdx1 expression in p48 Cre mice

The Z/AP reporter mouse was used to characterize the expression pattern of Cre

recombinase within the *p48Cre* mouse strain. In this strain, cells that lack Cre-

recombinase activity are marked by β-galactosidase expression. Conversely, cells that do

contain Cre-recombinase activity are marked by expression of alkaline phosphatase

(Lobe et al., 1999).

Based upon our analysis, cells expressing *Cre* recombinase are present at e10.5 in the

p48Cre mouse. However, the number of cells expressing Cre within the early epithelium

of the *p48 Cre* mouse is significantly less than in the PdxCre^{early} mouse strain at the same

point (data not shown). Previously, we showed that Pdx1 expression is lost within a a

majority of cells in the e12.5 epithelium of the PdxCre^{early} β-cat^{active} mouse (Heiser et al.,

2006). Therefore, we analyzed p48Cre β-cat^{active} mice at e12.5 in order to determine

whether a similar effect was induced by β-catenin activation in this context. As expected,

76% of epithelial cells within the PdxCre^{early} β-cat^{active} mice exhibit elevated cellular

levels of β-catenin (Fig. 1B, green), while β-catenin remains localized to the plasma

membrane in the pancreatic epithelium of control animals (Fig. 1A, green). In contrast,

only 12% of cells within the pancreatic epithelium of the p48Cre β-cat^{active} exhibit

elevated cellular levels of β-catenin (Fig. 1C, green). Interestingly, cells that have

elevated levels of β-catenin in both the PdxCre^{early} β-cat^{active} and p48Cre β-cat^{active} mouse

strains do not express Pdx1 (Fig. 1B,C). Quantitation of the number of Pdx1+ cells

within the pancreatic epithelium (as marked by E-cadherin staining, data not shown)

reveals a significant reduction in Pdx1$^+$ cells in the PdxCre^{early} β-cat^{active} when compared

to control animals that correlates well with the number of cells that have been targeted by

this mouse strain (Fig. 1D). While the p48Cre β-cat^{active} mouse, exhibits a trend that

suggests a mild reduction in the number of Pdx1$^+$ cells, it is not statistically significant

when compared to control (Fig. 1D). This is undoubtedly due to the low number of cells

within the early pancreatic epithelium that are targeted by the p48Cre mouse strain.

In addition, adjacent cells within the epithelium of these mice that have normal

membrane localization of β-catenin, retain Pdx1 expression. This suggests that activation

of β-catenin within the early pancreatic epithelium induces a cell autonomous loss of

Pdx1 expression (Fig 1B,C).

Stabilization of β-catenin causes an increase in pancreas mass in p48Cre β-catenin

mice.

At birth, the gross pancreatic morphology of p48 β-cat^{active} (Fig. 2B) appears similar

to control (Fig. 2A); pancreatic mass is also equivalent at this time point (Fig. 2E, graph

inset). Interestingly, our earlier study found that the pancreas fails to form in PdxCre^{early}

β-cat^{active} mice (Heiser et al., 2006), a phenotype that is likely caused, in part, by the loss

of Pdx1 expression (Fig. 1B). Therefore, it appears that activation of β-catenin within the

comparatively small number of cells of the early pancreatic epithelium in the p48Cre β-

cat^{active} is not sufficient to disrupt pancreas formation. Alternatively, cells that express

p48 in the early pancreatic epithelium may respond differently to the activation of β-catenin.

While pancreas morphology and mass normal at P0, one month old p48Cre β-cat^{active} exhibit a grossly enlarged pancreas (Fig. 2D) that is four times greater in mass than control (Fig. 2E). Pancreas mass continues to increase with age in the p48Cre β-cat^{active} (Fig. 2E).

We have previously shown that β-catenin activation within pancreatic acinar cells in the PdxCre^{late} β-cat^{active} mouse results in increased proliferation and similar pancreas enlargement(Heiser et al., 2006). Based upon the strong Cre-activity within adult exocrine pancreatic cells in the p48Cre mouse strain (data not shown), the pancreas mass phenotype observed in the p48Cre β-catenin mouse is consistent with our previous experimentation.

p48Cre β-cat^{active} mice exhibit ductal associated lesions at P0

Tissue from adult p48Cre Z/AP mice was analyzed in order to determine the extent of Cre activity within the exocrine, endocrine, and ductal compartments of the pancreas. Cre-mediated recombination in the Z/AP results in the expression of alkaline phosphatase. Alkaline phosphatase staining was detected within the majority of acinar cells (data not shown) and a subset of endocrine (data not shown) and ductal cells (Fig 3A), as published previously(Kawaguchi et al., 2002).

At P0, prominent ductal associated lesions are visible throughout the pancreas of the p48Cre β-cat^{active} mice (Fig. 3C). These lesions are not seen in control mice (Fig. 3B) or in PdxCre^{late} β-cat^{active}, which do not have any Cre activity in pancreatic ducts(Heiser et al., 2006). High levels of nuclearly localized β-catenin are seen within these ductal

associated lesions (Fig. 3E), while β-catenin is seen exclusively at the plasma membrane in control animals (Fig. 3D). Despite their proximity to ductal structures, cells within the lesion that have elevated levels of β-catenin do not express the ductal marker mucin. Formal proof of the ductal origin of these cells is lacking, due to the absence of cell lineage tracing experiments. However, the location of these cells is supportive of their ductal origin.

p48Cre βcat^{active} develop large pancreatic tumors at a high frequency

Pancreatic tumors are not observed in PdxCre^{late} β-cat^{active} mice despite the dramatic increase in pancreatic mass (Heiser et al., 2006). However, large, well encapsulated tumors are detectable at the gross morphological level in p48Cre β-cat^{active} mass by three months of age (Fig. 4A). These tumors are slow-growing and non-metastatic; moreover, affected animals continue to eat and groom normally. By 12 months, nearly half of all mice exhibit large tumors, which are most often found in the ventral pancreas (Fig. 4B).

In cross section at the gross and histological levels, areas of necrosis (Fig. 4C, yellow), cystic structures (Fig. 4C, E *), and solid, pseudopapillary regions (Fig. 4C, E #) are visible. Some pancreas, including acinar and islet structures, remains attached to the outer shell of the tumor (Fig. 4E, arrows).

The Wnt target genes, Axin2 and Cyclin D2, are significantly upregulated in the pancreases of p48Cre β-cat^{active} mice when compared to control (Fig 4. D,F), indicating that stabilization of β-catenin has resulted in robust activation of the canonical Wnt signaling pathway. Tumors isolated from p48Cre β-cat^{active} demonstrated an even greater increase in both Axin2 and Cyclin D2 expression (Fig 4. D,F).

Tumors in p48Cre β-cat^active mice are morphologically similar to human solid

pseudopapillary tumors of the pancreas.

Solid pseudopapillary tumors (SPT) of the pancreas are rare neoplasms that seldom

have associated malignancy. Based upon published reports, upregulation of β-catenin is

often seen in these lesions (Min Kim et al., 2006; Nishimori et al., 2006). Therefore, we

directly compared the morphology of a collection of human SPT tissue and the tumors

observed in p48Cre β-cat^active mice.

We found that the mouse tumors recapitulated many of the microscopic features that

characterize solid pseudopapillary tumors in humans. All of the mouse tumors were well

circumscribed with a distinct fibrous capsule (Fig. 5 A,B) and exhibited extensive

necrosis (Fig. 5 C,D red arrow) and haemorrhage (Fig. 5 C,D black arrow) centrally with

preserved tissue typically being found beneath the fibrous capsule (Figure 5A,B). The

tumor cells in the subcapsular region were arranged in solid sheets, while a

pseudopapillary pattern was visible in some cases with several layers of tumour cells

adhering to thin fibrovascular cores. However, in most of the mouse tumours the

pseudopapillae were less well formed than in human SPT (Figure 5 E, F black arrows).

The intervening spaces were filled with haemorrhage or necrotic debris. No glandular

spaces were present. Focal calcifications were observed in one mouse tumor, a feature

that is sometimes seen in human SPT (Figure 5 C,F green arrow).

As in human SPT's (Fig. 5 G,H) the mouse tumor cells were small, polygonal and

monomorphic with a moderate amount of clear or pale eosinophilic cytoplasm. In

contrast to many human cases of SPT, no eosinophilic hyaline cytoplasmic inclusions or

cholesterol clefts were identified in the mouse tumors, although foamy macrophages were

often present. Like human SPT, the mouse tumour cell nuclei were round to ovoid with dispersed, finely granular chromatin and inconspicuous nucleoli (Fig. 5 G,H). No nuclear grooves were seen in the mouse tumors. Mitotic figures were also rare. The results of this morphological comparison are summarized in Table 1.

Tumors in p48Cre β-cat^{active} mice have marker expression that is similar to human SPT

Human SPT demonstrated expression of markers consistent with the published literature: The majority of human SPT's (11/13) had clear and dramatic upregulation of β-catenin (Fig. 6 A,B). 13 expressed alpha1 anti-trypsin (Fig. 6, E, F), NSE, vimentin and cyclin D1 (Fig. 6 I, J). No human tumors expressed chromogranin, AE1/AE3, estrogen receptor. Only 1 of 13 expressed significant levels of synaptophysin, a marker of pancreatic islets (representative negative staining shown in Fig.6 M,N). Eleven of 13 human tumors expressed CD10, 10 of 13 expressed significant levels of progesterone receptor and 12 of 13 expressed CD56 (N-CAM).

Six murine tumors from p48Cre β-cat^{active} mice were examined for the same markers. All 6 showed no staining for synaptophysin (Fig. 6, O,P), chromogranin, NSE, AE1/AE3, ER or PR, but expressed alpha1 anti-trypsin (Fig. 6, G,H) and cyclin D1 (Fig. 6, K,L). Clear upregulation of β-catenin was seen in all 6 murine tumors (Fig.6 C,D). Reliable staining for the detection of Vimentin, CD10 and CD56 (N-CAM) was not successful in murine tissues. The results of the marker comparison are summarized in Table 2.

Based upon our analysis, it appears that the tumors found in p48Cre β-cat^{active} mice recapitulate many of the aspects of the human SPT lesion. Activating mutations that map to the third exon of β-catenin have been identified in human SPT patients (Min Kim et

al., 2006). However, this study proves that such mutations can act as the direct cause of this type of pancreatic tumor.

It is also interesting to note that PdxCre^late β-cat^active (Heiser et al., 2006) mice do not develop tumors, despite exhibiting a dramatic gain in pancreas mass that is equivalent to the phenotype seen in the p48 Cre β-cat^active mice. Because the p48Cre β-cat^active mice drive activation of the β-catenin signaling pathway in ductal cells, a compartment not targeted in the PdxCre^late β-cat^active, it appears likely that the pancreatic ducts harbor the cell type responsible for these tumors. Definitive proof could come through the use of a pancreatic duct specific –Cre line, a strain that has not yet been made.

References

Harada, N., Tamai, Y., Ishikawa, T., Sauer, B., Takaku, K., Oshima, M. and Taketo, M. M. (1999). Intestinal polyposis in mice with a dominant stable mutation of the beta-catenin gene. *Embo J* 18, 5931-42.

Heiser, P. W., Lau, J., Taketo, M. M., Herrera, P. L. and Hebrok, M. (2006). Stabilization of beta-catenin impacts pancreas growth. *Development* 133, 2023-32.

Kawaguchi, Y., Cooper, B., Gannon, M., Ray, M., MacDonald, R. J. and Wright, C. V. (2002). The role of the transcriptional regulator Ptf1a in converting intestinal to pancreatic progenitors. *Nat Genet* 32, 128-34.

Kawahira, H., Ma, N. H., Tzanakakis, E. S., McMahon, A. P., Chuang, P. T. and Hebrok, M. (2003). Combined activities of hedgehog signaling inhibitors regulate pancreas development. *Development* 130, 4871-9.

Kim, S. K., Hebrok, M. and Melton, D. A. (1997b). Notochord to endoderm signaling is required for pancreas development. *Development* 124, 4243-4252.

Lobe, C. G., Koop, K. E., Kreppner, W., Lomeli, H., Gertsenstein, M. and Nagy, A. (1999). Z/AP, a double reporter for cre-mediated recombination. *Dev Biol* 208, 281-92.

Min Kim, S., Sun, C. D., Park, K. C., Kim, H. G., Lee, W. J. and Choi, S. H. (2006). Accumulation of beta-catenin protein, mutations in exon-3 of the beta-catenin gene and a loss of heterozygosity of 5q22 in solid pseudopapillary tumor of the pancreas. *J Surg Oncol* 94, 418-25.

Nishimori, I., Kohsaki, T., Tochika, N., Takeuchi, T., Minakuchi, T., Okabayashi, T., Kobayashi, M., Hanazaki, K. and Onishi, S. (2006). Non-cystic solid-pseudopapillary tumor of the pancreas showing nuclear accumulation and activating gene mutation of beta-catenin. *Pathol Int* 56, 707-11.

Figure Legends

Figure 1: Cell autonomous loss of Pdx1 expression in p48 Cre β-cat^{active} mice. The

majority of cells in the pancreatic epithelium of PdxCre^{early} β-cat^{active} mice at e10.5

exhibit elevated levels of cytoplasmic and nuclear β-catenin (B, green) when compared to

control mice (A, green). Only a subset of cells within the pancreatic epithelium of the

p48Cre β-cat^{active} exhibit elevated levels of β-catenin at e10.5 (C, green). All cells with

elevated levels of β-catenin in the PdxCre^{early} β-cat^{active} and p48Cre β-cat^{active} mice lose

Pdx1 expression (B,C red), while adjacent cells with normal β-catenin levels retain Pdx1

expression that appears equivalent to control (A, red). The number of Pdx1+ progenitor

cells within the pancreatic epithelium at e12.5 is significantly reduced in the *PdxCre^{early}*

β-cat^{active} mutants (orange, n=5) when compared to control (blue, n= 7) and *p48Cre* β-

cat^{active}(red, n=5) mutants (C). Error bars indicate standard deviation. Confidence

intervals were determined using the student's t-test; # = not significant, ** = p<0.01.

Figure 2: Stabilization of β-catenin causes an increase in pancreas mass in p48Cre β-

cat^{active} mice. The gross morphology of pancreata from a control (A) and p48Cre β-

cat^{active} (B) is equivalent at P0. By 1 month of age, pancreata from p48Cre β-cat^{active} are

grossly enlarged (D) when compared to control (C). Quantitative measurements revealed

an approximately 4 fold increase in pancreatic mass at 6 months of age.(E, n≥7 for each

time point analyzed, control: blue, p48Cre β-cat^{active} red). Confidence intervals were

calculated using student's t-test. P values: #, not significant; **, p<0.01. Error bars

represent standard error of the mean.

Figure 3: p48Cre β-cat^{active} mice exhibit ductal associated lesions at P0. Cre recombinase activity (marked by alkaline phosphatase, red) is detected in the interlobar ducts (red)of p48Cre Z/AP mice (A). At birth, prominent ductal lesions are seen in the pancreata of p48Cre β-cat^{active} mice (C) that are not observed in the pancreata of control littermates (B). Strong nuclear accumulation of β-catenin (green) is seen in these ductal associated (duct labeled by mucin in red) lesions (E), while in control animals, β-catenin remains localized to the plasma membrane in pancreatic ducts (D, ducts labeled by mucin in red). Cells that have nuclear localized β-catenin do not coexpress mucin.

Figure 4: p48Cre βcat^{active} mice develop large pancreatic tumors at a high frequency. Gross morphology of typical tumor seen in the pancreas of p48 Cre β-cat^{active} (A, right) compared to a pancreas from a littermate control (A, left). Gross morphology of a cross section of the murine tumor reveals pseudopapillary regions (C, labeled by #) and cystic structures (C, labeled by *). Histological examination of the murine tumor (x10 magnifcation) show the anaplastic, pseudopapillary regions (E, labeled by #), cystic structures (E, labeled by *) and the pancreatic remnant surrounding the tumor (E, labeled by arrow). Tumors are first detectable in p48Cre β-cat^{active} mice at 3 months of age. By 12 months of age, nearly 50% of p48Cre β-cat^{active} mice exhibit tumors (B; n≥8 for each time point examined). Expression of the Wnt target genes, Axin 2 (D) and CyclinD1 (F) are significantly upregulated in the p48Cre β-cat pancreas when compared to control pancreas at 9 months of age by RT-PCR. Tumors found in p48 β-cat^{active} mice exhibit a further increase in overexpression of Axin 2 (D) and CyclinD1 (F).

Figure 5: Tumors in p48Cre β-cat^active mice are morphologically similar to human solid pseudopapillary tumors of the pancreas. Slides were stained with hematoxylin and eosin to provide contrast. Low power view (x50) of human SPT (A) and murine tumor (B) Black arrows indicate tumor capsule (A,B). Low power view (x50) of human SPT (C) and murine tumor (D) with black arrows indicating areas of haemorrhage (C,D), red arrows indicating areas of necrosis (C,D), and green arrow to indicate a site of calcification (C). Human SPT (E) and murine tumor (F) with black arrows indicating pseudopapillae (E,F) and green arrow showing calcification (F) similar to that indicated in (C). High power view (x100) of human SPT (G) and murine tumors (H).

Figure 6: Tumors in p48Cre β-cat^active mice have marker expression that is similar to human SPT.. Normal human pancreas showing membranous β-catenin staining (A) and pancreas from p48Cre β-cat^active mice exhibiting nuclear accumulation of β-catenin (C). Both human SPT's and the murine tumors show marked cytoplasmic and nuclear staining for β-catenin (B,D). Alpha1 anti-trypsin was expressed in human SPT (F) and murine tumors (H) with a globular pattern but was not expressed in normal human (E) or p48Cre β-cat^active pancreas (H). CyclinD1 was expressed at high levels in human SPT (J) and murine tumors (L). Elevated levels of CyclinD1were also detected in the exocrine tissue of the p48Cre β-cat^active pancreas (K). Cyclin D1 was not detected in normal human pancreas tissue (I), Neither human SPT's (N), nor murine tumors (P) express synaptophysin. Synaptophysin is detectable in both normal human pancreatic islets (M)

and the islets of p48Cre β-cat^{active} mice (O). All images were aquired at high

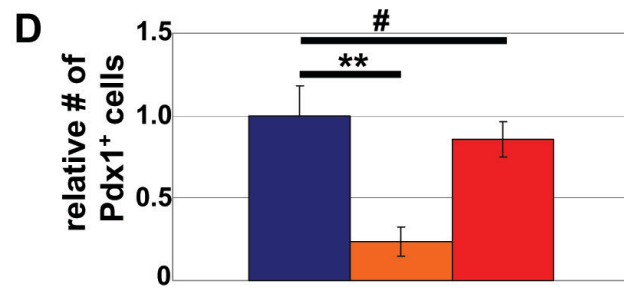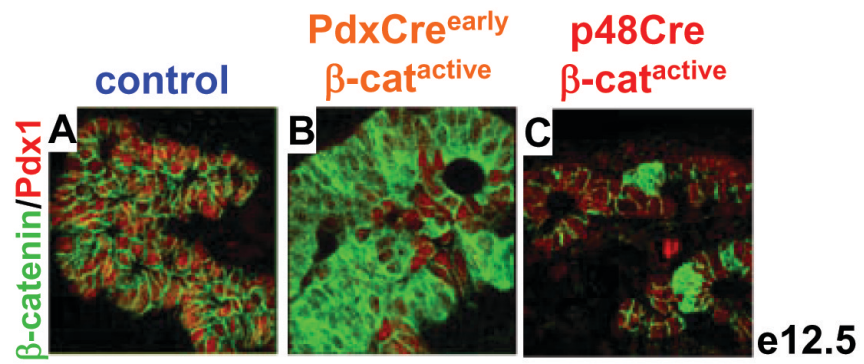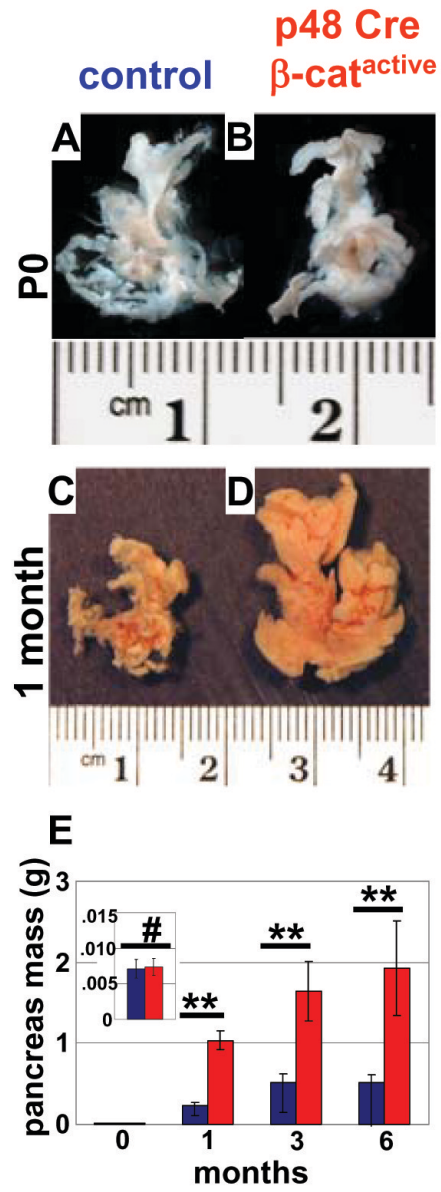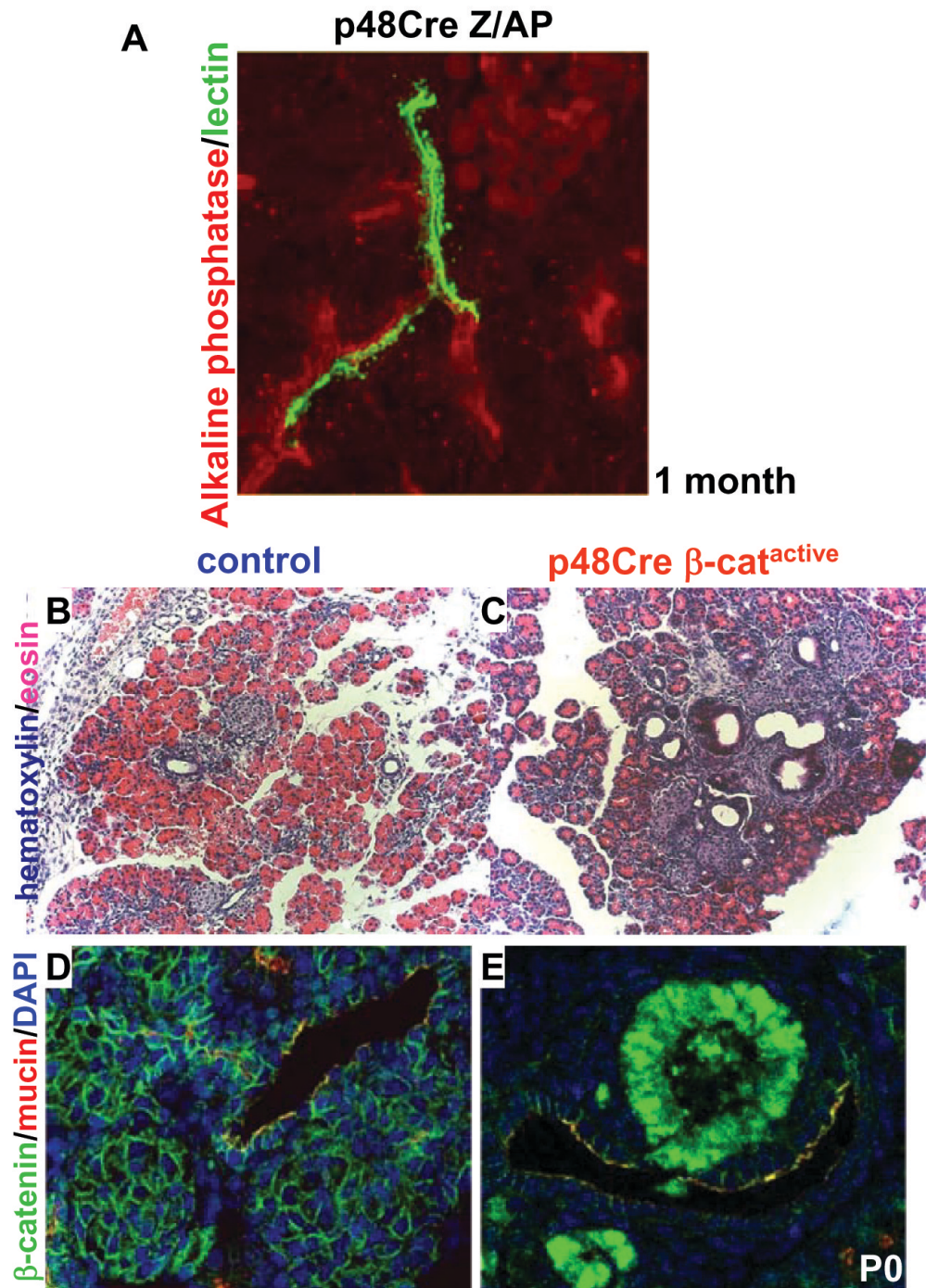magnification (x400); tissues were counterstained with hematoxylin to improve contrast.

Figure 1

β-catenin/Pdx1

control   PdxCre^{early} β-cat^{active} p48Cre β-cat^{active}

A   B   C

β-catenin/Pdx1   e12.5

D relative # of Pdx1$^+$ cells

#

**

Figure 2

Figure 3

A

p48Cre Z/AP

Alkaline phosphatase/lectin

1 month

control   p48Cre β-cat^active

B   C

hematoxylin/eosin

D   E

β-catenin/mucin/DAPI   P0

118

Figure 4

119

Figure 5

human

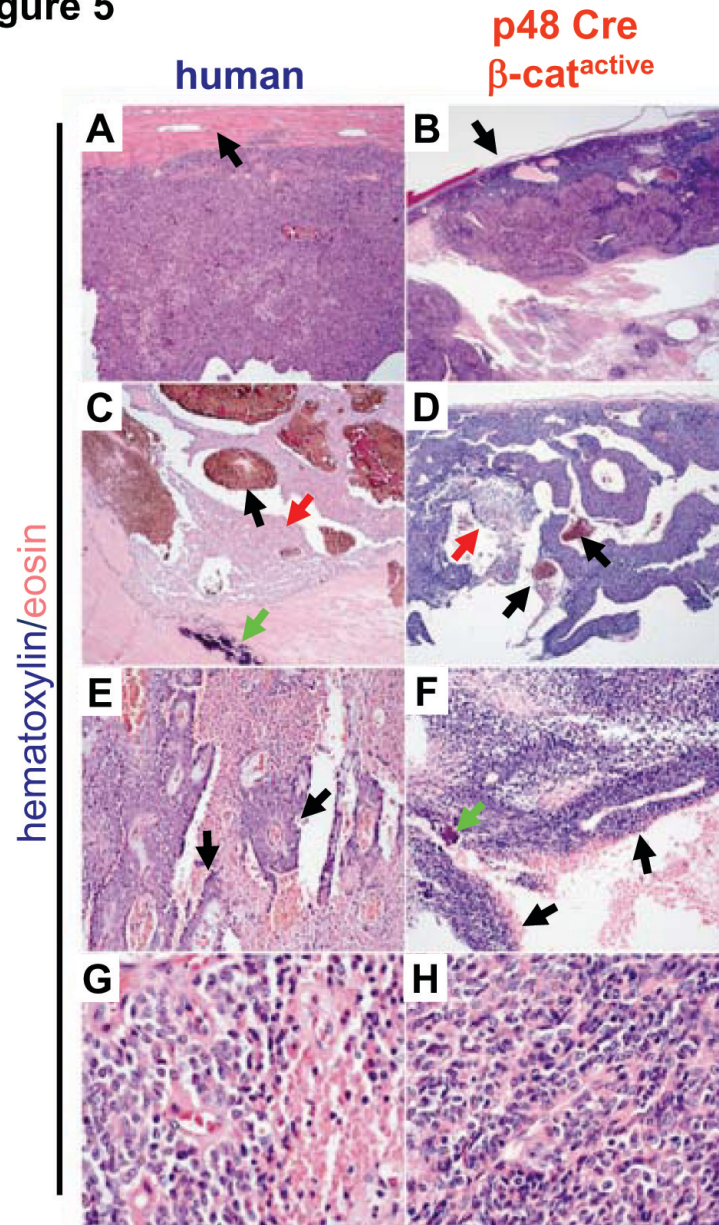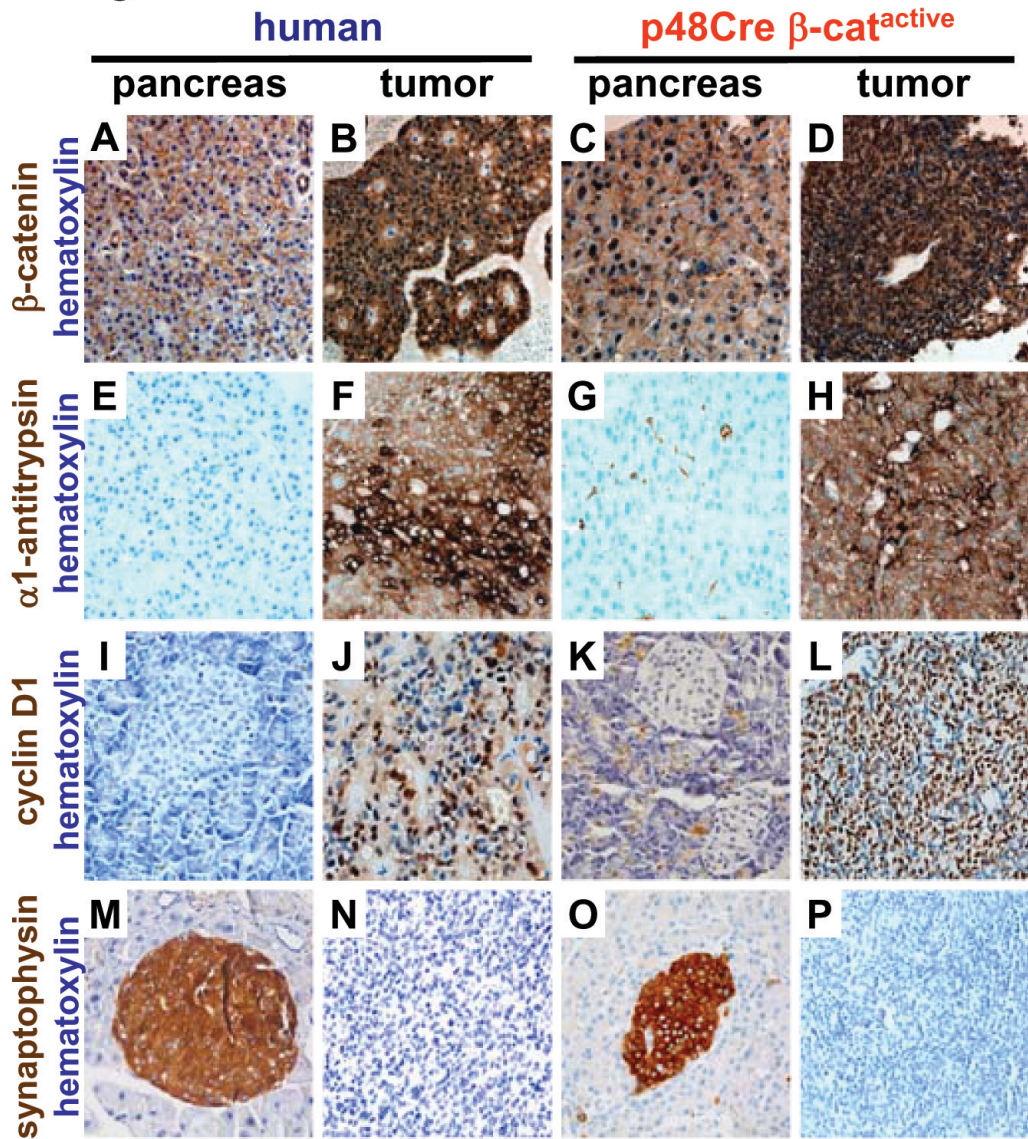**p48 Cre**
β-cat^{active}

hematoxylin/eosin

120
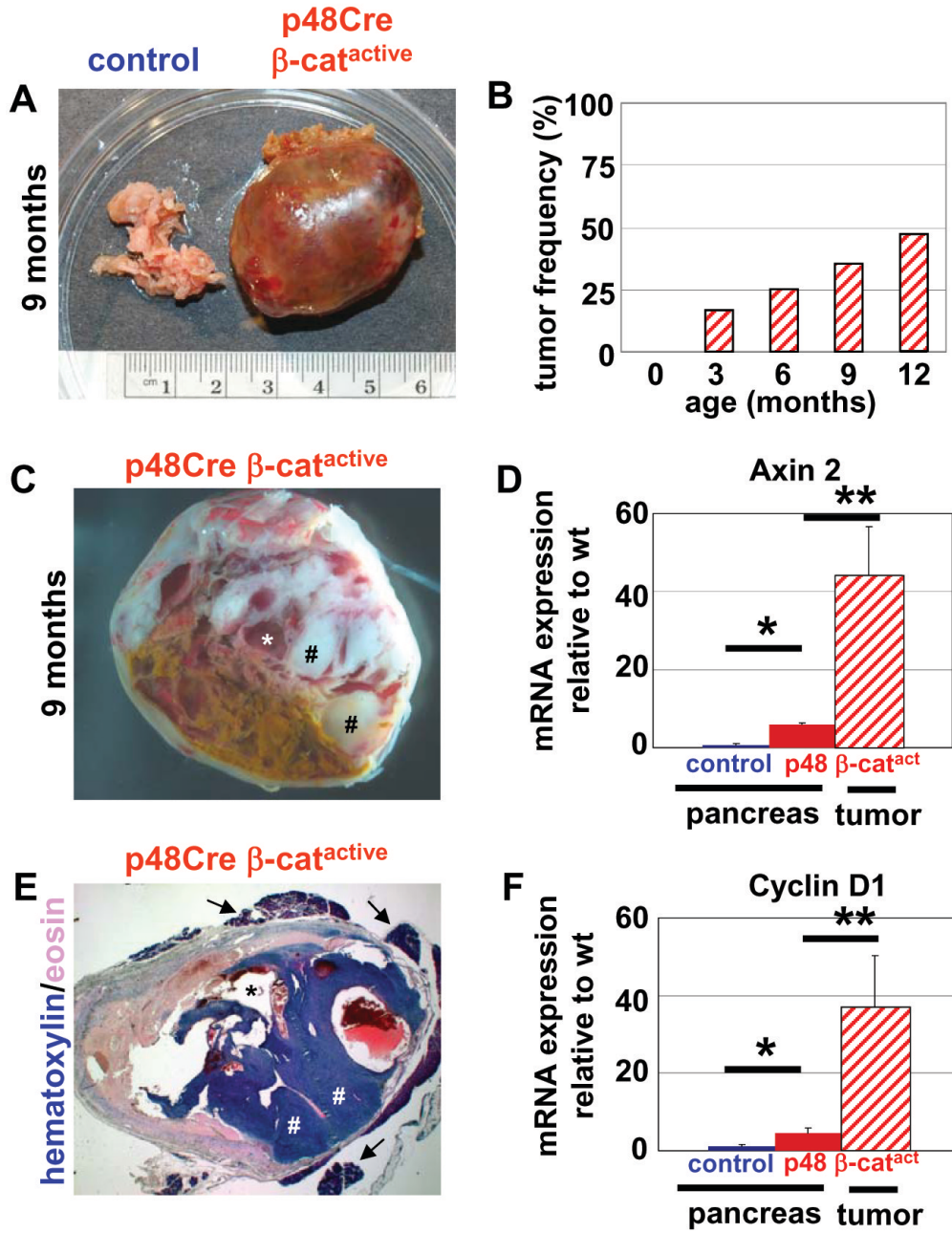
Figure 6

Table 1

Comparison of morphological features of murine tumors (p48Cre β−cat^active) to human solid pseudopapillary tumors.

	Human	**Mouse**
Well circumscribed	Yes	Yes
Extensive necrosis, hemorrhage and cystic degeneration	Yes	Yes
Solid sheets peripherally and central pseudopapillae	Yes	Yes
Glandular spaces	Yes	No
Small polygonal monomorphic cells	Yes	Yes
Clear or pale cytoplasm	Yes	Yes
Eosinophillic hyaline cytoplasmic inclusions	Yes	No
Cholesterol clefts	Yes	No
Foamy macrophages	Yes	Yes
Nuclei round to ovoid with dispersed finely granular chromatin	Yes	Yes
Inconspicuous nucleoli	Yes	Yes
Nuclear grooves	Yes	No
Scanty mitotic figures	Yes	Yes

Table 2

Comparison of immunohistochemical features of murine tumors (p48Cre β−cat^active) to human solid pseudopapillary tumors.

	Human	**Mouse**
β-catenin	nuclear / cytoplasmic	nuclear / cytoplasmic
Synaptophysin	negative	negative
α_1-antitrypsin	Focal with globular pattern	Focal with globular pattern
AE1/AE3	negative	negative
Chromogranin	negative	negative
NSE	positive	Focal weak positive
ER	negative	negative
PR	60% positive	negative
Cyclin D1	positive	positive
Vimentin	positive	NP
CD10	80% positive	NP
CD56	90% positive	NP

Chapter 5

Concluding remarks

Serendipity plays a large role in any scientific endeavor, and this one has been no different. When I began to undertake the analysis of the β-cat^{active} mice, I was fortunate to have a large assortment of transgenic pancreas Cre mice with complementary expression domains to choose from. By using the PdxCre^{early} strain, I was able to ask questions about what was occurring at the earliest stages of organ specification. The mosaic and delayed expression of the PdxCre^{late} provides an opportunity to determine the effect of the activating mutation during the early stages of organogenesis and epithelial branching. In addition, the p48 Cre has the added benefit of targeting the pancreatic ducts, and potentially a heretofore unappreciated pancreatic stem cell that may lie at the heart of pancreatic cancer initiation. Finally, the RIP-Cre mouse allows for β-cell specific targeting to assay β-cell development and adult function. The major findings of this work are summarized in Figure 1.

The experimentation described in this dissertation has demonstrated that tight regulation of the timing and dosage of the β-catenin signaling pathway is essential for normal pancreas development. Moroever, the β-catenin signaling pathway can act to block differentiation, enhance proliferation, or initiate tumorigenesis depending entirely on the biological context and cellular niche of its activation.

In addition, we have shown that β-catenin activation in the p48 Cre is sufficient to induce the formation of large pancreatic tumors that resemble human SPT's. Other work in our lab has shown that Wnt signaling can be a contributing factor in the progression of pancreatic adenocarcinoma (Pasca, et al, submitted, Genes and Development). It will be interesting to explore whether the addition of another known oncogenic mutation in a

gene, such as p53 or kRas, to the p48 β-cat^{active} mouse might be enough to convert the

largely benign SPT-like tumors we have observed into something more sinister.

This study also illustrates the need for caution when using transgenic mouse lines.

Small differences in the timing and expression domain of Cre recombinase can have

profound consequences on the outcome and interpretation of experiments.

Figure legends:

Figure 1 displays a schematic illustrating the cellular compartments targeted by the

different mouse Cre strains, and their respective phenotype when crossed to the β-cat^{active}

mouse. White circles indicate no Cre expression. Gray striped circles indicate mosaic

Cre expression. Dark gray circles indicate robust Cre expression.
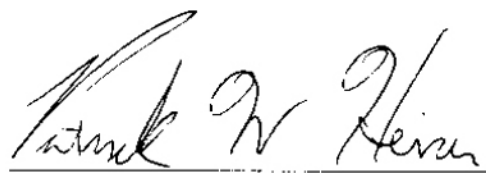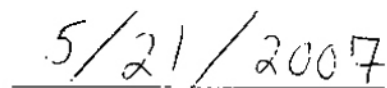
Figure 1
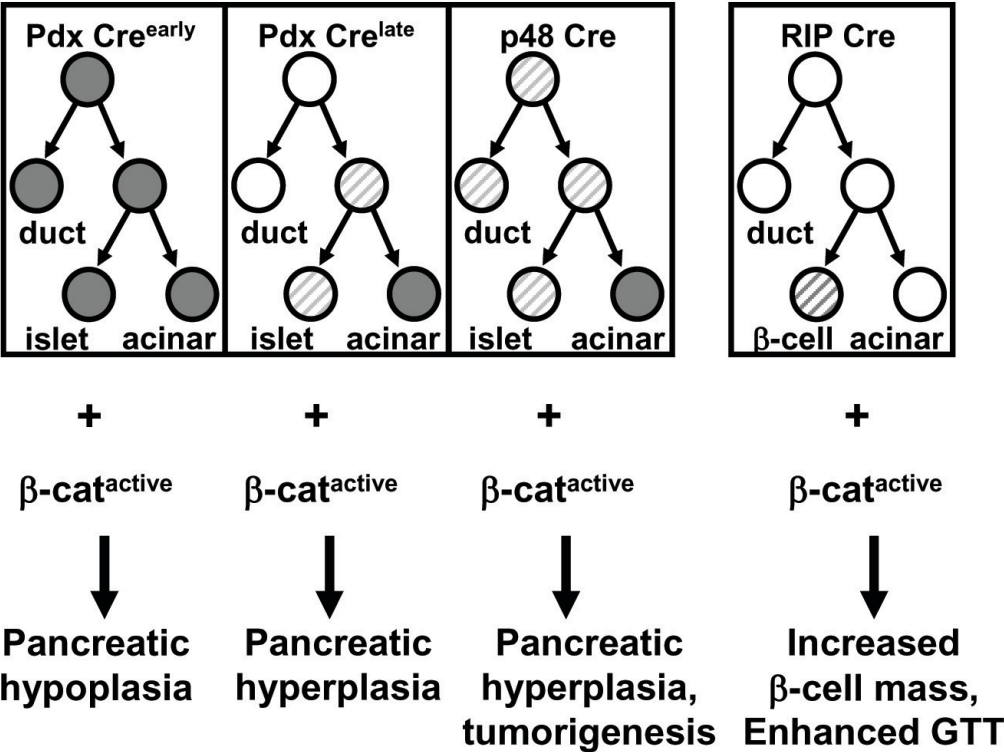
Publishing Agreement

It is the policy of the University to encourage the distribution of all theses and dissertations. Copies of all UCSF theses and dissertations will be routed to the library via the Graduate Division. The library will make all theses and dissertations accessible to the public and will preserve these to the best of their abilities, in perpetuity.

I hereby grant permission to the Graduate Division of the University of California, San Francisco to release copies of my thesis or dissertation to the Campus Library to provide access and preservation, in whole or in part, in perpetuity.

_____   5/21/2007
Author Signature   **Date**

128